WATER FLOW THROUGH COASTAL WETLANDS

Annual Report 2004

Everglades National Park
1443CA5280-01-019
National Park Service
H525003D064

Principal Investigators: Evelyn E. Gaiser and Michael S. Ross
Southeast Environmental Research Center
Florida International University
Miami, FL 33199

Southeast Environmental Research Center
11200 S.W. 8th Street, OE 148 • Miami, FL 33199 • Tel: (305) 348-3095 • Fax: (305) 348-4096 • www.fiu.edu

TABLE OF CONTENTS

I. EXECUTIVE SUMMARY…….....3

II. PARTICIPATING INDIVIDUALS……....4

III. PUBLICATIONS…….……5

IV. STUDY AREA…….…...6

V. RESULTS COMPLETED

A. VEGETATION……..7
B. PERIPHYTON……....……..16
C. PALEOECOLOGY…….….41

I. EXECUTIVE SUMMARY

Coastal ecosystems are threatened by salt-water encroachment resulting from sea-level rise and hydrologic modification of natural drainages. Historically, coastal ecosystems in South Florida were characterized by predictable community zones running parallel to the coastline, which from the coast to the interior included a coastal fringing mangrove forest, a transitional mixed mangrove forest, a scrub/dwarf mangrove forest, and a mixed gramminoid freshwater marsh interspersed with tree islands containing broadleaf hardwoods (hammocks) and natural tidal creeks and estuaries ("transverse glades"). By 1940 and increasingly over the next several decades, a network of canals were built that drained overland flow for urban and agricultural development, which extirpated most tidal creeks and caused rapid salt-water encroachment into areas normally fed by overland freshwater flow.

The goal of "Water Flow through Coastal Wetlands" was to assess changes in the spatial distribution of plant, mollusk and periphyton communities in coastal wetlands and nearshore environments of the Biscayne Bay Coastal Wetlands (BBCW). We are characterizing modern communities at large spatial scales using remotely sensed images and at smaller scales by surveying plant, mollusk and periphyton community structure at 226 plots established in a ~7 km long band of coastal wetland. To relate the structure of these communities to environmental data we measured nutrient availability, water depth, soil depth and composition, and salinity at each site. An added goal of the proposed research was to determine the potential for reconstructing past environments through paleoecology. Sediment cores were taken along transects perpendicular to the coastline, and we determined the rate of migration of community zones from the sediment record.

We have found that habitat zonation in the BBCW has changed substantially in the past 50-100 years due to drainage, in several respects: (1) tidal creeks linking the interior freshwater marsh to the coast have disappeared, (2) the freshwater marsh has been drained and native vegetation displaced to the west by invasive exotic trees and to the east by the expanding dwarf mangrove forest, and (3) all coastal vegetation bands are now restricted to the east of canals that, by running parallel to the coastline, prohibit natural mixing of fresh- and salt-water during the tidal cycle. We found strong linkages between periphyton community composition and vegetation structure, which are driven, in part, by the separation of fresh from marine waters by the L-31E canal, and the strong salinity gradient between the canal and ocean margin. Mollusk assemblages were also correlated with salinity and vegetation type. Models have been developed that accurately predict salinity and vegetation composition from diatom and mollusk community composition, which will be useful in tracking the effects of modified water deliveries on BBCW ecosystems. Sediments throughout the system contained an upper peat surface overlying compact marl. Salinity and habitat inference models were applied to sedimented mollusk assemblages to reconstruct environmental conditions within the BBCW. Although we are still awaiting radiometric estimates of sediment age, sedimentation rates from nearby locations suggest that a pre-drainage interior migration rate of coastal ecotones of 0-0.5 m y^{-1} has accelerated to 3-30 m y^{-1} during the last few decades of drainage.

II. PARTICIPATING INDIVIDUALS

Principal Investigators:
Evelyn E. Gaiser, Ph.D., FIU
Michael S. Ross, Ph.D., FIU

Collaborating Scientists:
Lynne Coultas, Ph.D.,
Krish Jayachandran, Ph.D., FIU

Post-doctoral Associates:
Jay Sah, Ph.D., FIU
Serge Thomas, Ph.D., FIU

Laboratory Managers:
Pablo Ruiz, FIU
Christine Taylor, FIU

Research Technicians:
David Jones, FIU
Raphael Traveiso, FIU
Franco Tobias, FIU
Alejandro Leon, FIU

Graduate Students:
Anna Wachnicka, FIU

Undergraduate Students:
Angelikie Zafiris, FIU

III. PUBLICATIONS AND PRESENTATIONS

Peer-Reviewed Publications:

Gaiser, E. E., A. Wachnicka, P. Ruiz, F. Tobias and M. S. Ross. 2004. Diatom indicators of ecosystem change in coastal wetlands. In S. Bortone (Ed.) Estuarine Indicators. CRC Press, Boca Raton, FL. pp. 127-144.

Ross, M. S., E. E. Gaiser, J. F. Meeder and M. T. Lewin. 2001. Multi-taxon analysis of the "white zone", a common ecotonal feature of South Florida coastal wetlands. In Porter, J. and Porter, K. (eds). The Everglades, Florida Bay, and Coral Reefs of the Florida Keys. CRC Press, Boca Raton, FL, USA. pp. 205-238.

Ross, M. S. , P. L. Ruiz, G. J. Telesnicki, & J. F. Meeder 2001. Estimating above-ground biomass and production in mangrove communities of Biscayne National park, Florida (USA). Wetlands Ecology and Management 9: 27-97.

Tobias, F. and E. Gaiser. In Press. Taxonomy and distribution of taxa in the genus *Gomphonema* from the Florida Everglades, U.S.A. Diatom Research.

Wachnicka, A. and E. Gaiser. In Press. Morphological characterization of *Amphora* and *Seminavis* (Bacillariophyceae) from South Florida, U.S.A. Diatom Research.

Gaiser, E. E., A. Zafiris, P. L. Ruiz, F. A. C. Tobias and M. S. Ross. Submitted. Tracking rates of ecotone migration due to salt-water encroachment using fossil mollusks in coastal south Florida. Hydrobiologia.

Presentations:

Gaiser, E. E., A. Zafiris and M. Ross. 2004. Using paleoecology to calculate rates of migration of coastal vegetation zones due to salt-water encroachment in South Florida. Annual meeting of the Ecological Society of America, Portland, OR.

Zafiris, A., E. E. Gaiser and M. Ross. 2004. Tracking effects of salt-water encroachment on coastal ecotones of South Florida using mollusks. National Conference on Ecosystem Restoration. Orlando, FL.

Ross, M. S. & P. L. Ruiz. 2003. Freeze incidence and mangrove encroachment in Florida coastal marshes. Annual meeting of the the Ecological Society of America, Savannah, GA.

Zafiris, A., E. E. Gaiser and M. Ross. 2003. Tracking effects of salt-water encroachment on coastal ecotones of South Florida using mollusks. Annual meeting of the the Ecological Society of America, Savannah, GA.

Gaiser, E. E., A. Wachnicka, A. Zafiris, P. Ruiz and M. Ross. 2003. Paleoecological determination of effects of saltwater encroachment on community migration in coastal South Florida wetlands. Annual Meeting of the Ecological Society of America, Savannah, GA.

Gaiser, E. E. and M. S. Ross. 2002. Water flow through coastal wetlands. Biscayne Bay Coastal Wetlands Science Meeting. Miami, FL.

Gaiser, E. E. 2002. Using diatoms to create performance measures in Biscayne coastal wetlands. Biscayne Bay Coastal Wetlands Science Meeting. Miami, FL.

IV. STUDY AREA

The southeastern edge of Florida was historically characterized by expansive coastal mangrove wetlands that were dissected by tidal creeks flowing from the freshwater Everglades to the coast. Through an extensive mapping effort, Egler (1952) was able to distinguish distinct vegetation zones lying in bands parallel to the coast, in what he termed the "southeast saline Everglades". Gradients of salinity, water availability, nutrients and susceptibility to drought and fire resulted in a coastward sequence of gramminoid freshwater wetlands (to the interior), followed by dwarf mangrove scrub swamps in intertidal areas bounded by fringing mangrove forest on the coast. Throughout the last several decades, an extensive network of drainage canals has been constructed in South Florida, effectively draining much of the interior and coastal Everglades for urban and agricultural development. By the turn of the 21st century, the wetland bands had been diminished to the periphery of the coastline: freshwater gramminoid marshes had been largely displaced by an enroaching mangrove scrub community and most tidal creeks had disappeared (Ross et al. 2000; Fig. 1a). Alterations in mollusk and periphyton communities due to salt-water encroachment were also apparent (Ross et al., 2001).

The present study focuses on an area of remnant coastal wetlands, parts of which are protected in Biscayne National Park (Fig. 1b). The ~7 km long study area is bounded to the north and south by major east-west drainage canals (Princeton and Mowry, respectively) and bisected north-south by a secondary canal (L-31E). The region is dissected by many smaller east-west ditches which compartmentalize the area longitudinally into 13 hydrologically distinct wetland basins, that range in width from about 0.5 to 2 km. To the west of the L-31E canal, freshwater marshes are now hydrologically isolated from the coast and bounded to the west by agricultural lands, the periphery of which are heavily invaded by exotic trees including *Schinus terebinthifolius* (Brazilian Peppertree) and *Casuarina equisetifolia* (Australian pine). To the east of the L-31E canal, mangrove communities predominate, with strands of upland forest now occupying the remnant tidal creek beds. Though each sub-basin contains a gradation of freshwater to marine communities from the interior to the coast, the distinctiveness of the zones, the abruptness and location of the ecotonal boundaries and their specific composition vary somewhat within the sub-basins.

V. RESULTS COMPLETED – A. VEGETATION

Ross, M. S. and P. L. Ruiz. 2005. Vegetation in the Biscayne Bay Coastal Wetlands. Final Report.

We used a stratified-random design to select study sites within each of the 13 sub-basins. Using aerial photos of the area, each sub-basin was divided into 4-6 units, including, to west of the L-31E canal, a freshwater swamp forest dominated by exotics that have invaded abandoned agricultural land and remnant freshwater gramminoid marsh, and, to the east of the L-31E canal, mangrove forests that can be characterized by canopy height and cover as dwarf, transitional and fringing (along the coastline). Occasionally a sub-basin did not include one or more of these components or another community type was present, in which case the sub-basins were divided accordingly such that each unit was equally represented in sampling. Within each unit a north-south transect was randomly located, and 1-5 sampling stations were evenly distributed along its length. A total of 226 stations were sampled within the 12 km^2 area (Fig. 1b).

At each station, we assessed the vegetation community structure, roughly described the sediments and sampled periphyton and several chemical parameters in surface and/or pore-water. Depth of sediments to the limestone bedrock was measured at five stations with a probe-rod and, using a soil auger, sediments were extracted to measure depths of readily apparent compositional and textural transitions. Using a PVC pipe, five small (3.8 cm^2, 1-2 cm thick) sections of surface soil, commonly occupied by periphyton, were extracted from each location and composited. A portable meter was used to measure pH and conductivity in surface water, if present, or in pore-water that filled the auger hole. Conductivity ($\mu S\ cm^{-1}$) was converted to salinity (ppt) using a model provided from a previous study in a nearby basin where both variables were directly measured.

Vegetation survey

A nested design was used to describe vegetation within a 10 x 10 meter plot at each sampling point. The sampling procedure was as follows:

1. Upon reaching each point, a 10-meter N-S transect was established.

2. For trees (stems >2 meters height), we recorded the species and diameter class (5-cm DBH ranges) of all live and dead individuals within one meter of the line (stems <10 cm DBH), two meters of the line (stems 10-25 cm DBH), and five meters of the line (>25 cm DBH). We recorded the species and diameter class of all dead fallen stems (> 5 cm DBH) whose trunk intersected the line. We estimated live cover by species in a 4- meter-wide band enclosing the center line, using the following cover classes: 1, 0-1%; 2, 1-4%; 3, 4-16%; 4, 16-33%; 5, 33-66%; and 6, >66%. Finally, we recorded the upper and lower height of each species that intercepted or was within 1 meter of a vertical height pole positioned at three locations along the centerline, i.e., 0, 5, and 10 meters from the origin.

3. For shrubs (woody stems between 60 cm and 2 meters in height), we recorded the density of all stems in five 1-m^2 plots established at five locations along the center line, i.e., west of the

line, at 0, 2, 4, 6, and 8 meters from the origin. Stems were counted by species in two size categories: small shrubs (60-100 cm tall) and large shrubs (1-2 m tall).

4. For seedlings (woody stems 0-60 cm in height), we recorded the density of all stems in a 3 x 3 dm subplot in the southeast corner of the 1 m^2 plot described above. Stems were counted by species in two size categories: small seedlings (0-30 cm tall) and large seedlings (30-60 cm tall).

5. For all plants < 2 meters height (herbs, seedlings, shrubs), we estimated cover in the 1 m^2 plots described above, using the same cover classes as described above for tree cover.

Forest types

The vegetation map of the study area is presented in Figure 1. Based on our data and observations, ten primary vegetation units and several hybrid variants were prevalent. Among the primary types, five were mangrove units distinguished on the basis of stature and landscape position (dwarf mangrove forest, transitional mangrove forest, interior mangrove forest, fringe mangrove forest, and mangrove tree island), two were freshwater forests (swamp forest and Australian pine forest), and three were marsh types distinguished on the basis of composition (cattail marsh, sawgrass marsh, and salt marsh). A detailed definition of these types and important variants is included in Table 1.

Current vegetation distribution and landscape dynamics

Except in the first three units south of the C-102 (Blocks 11-13), wetlands east of the L-31E Canal fall exclusively into one of the five mangrove forest types. Mangroves are also common immediately west of the L-31E, especially north of the Military Canal; however, further west than the FPL service road they generally give way to freshwater wetland types. Forests within the mangrove belt are arranged in a regular sequence from coast toward the interior, as follows: Fringe → Interior → Transitional→ Dwarf mangrove forest. This zonation pattern is broken up only by the westward extension of the Interior mangrove forest type along several serpentine, active and inactive tidal creeks. Declining forest stature along the community sequence from Fringe to Dwarf forest is symptomatic of a general decrease in plant productivity, at least as far inland as the L-31E Canal. Whereas the mechanism underlying this dramatic productivity decline with distance from the coast is not entirely understood, it appears to involve a suite of interrelated factors, including phosphorus availability, substrate (marl v. peat), soil aeration, and frequency of tidal wetting (Ross et al. 2001, 2003).

In the northeastern portion of the study area, non-mangrove plant taxa become more important in the coastal landscape. Blocks 12 and 13 include substantial areas of salt marsh vegetation, and Australian pine-dominated forests occupy much of the terrain immediately east of the levee in Blocks 11-13 (Figures 1-3). Compared to the coastal wetlands to the south, (1) these blocks are longer (the coastline here trends to the northeast, diverging further from the L-31E Canal), and (2) the wetlands are broken up by a dense network of N-S trending mosquito ditches, lined with the remains of the original dredged material. In combination, these two factors cause tidal influence to be reduced in these wetlands, especially where the N-S ditches are not

hydrologically connected with larger E-W ditches that do conduct tidal waters. Moreover, the dredged materials provide substrate for exotic and native species adapted to less hydric conditions than occur in the wetlands themselves. The result is a more heterogeneous vegetation mosaic in which brackish water taxa and ruderals play a larger role than in coastal wetlands further south.

Vegetation patterns west of the L-31E are difficult to interpret from Figure 1 because of the limited extent of the map in that sector. *Cladium* marshes prevail in Blocks 1-5 (Figures 1 & 4). These marshes appear to be very productive, and include significant mixtures of tree species with brackish and fresh water affinities, especially *Conocarpus erecta, Myrica cerifera, Laguncularia racemosa,* and *Casuarina equisetifolia*. Red mangrove is common in low areas and along local drainages. North of the Military Canal, sawgrass is less abundant (though still present in small amounts) and woody plants dominate (Figures 1 & 4). Beyond Block 7, other land uses prevail on adjacent parcels west of the study area, and mapped wetlands in this section exhibit more overt signs of disturbance than those to the south (Figure 3).

We have not yet completed our analyses of historical changes in the wetland landscape of Blocks 1-13. As part of the project's Final Report, these will be based on a comparison of Figure 1 with a photo-interpretation of ca 1:24,000 black and white images shot in 1940. However, one portion of this photo series has already been analyzed in conjunction with the L-31E Pilot Project; a vegetation map, developed on the basis of aerial photo CJF 6-29 (Soil Conservation Service, July, 1940), encompasses Blocks 1-7 and adjacent areas to the south and west (Figure 5). The map shows a relatively clear coastal vegetation sequence within the study area, as follows: (1) a narrow (<200 meters wide) tall mangrove forest (probably equivalent to the current Fringe and Interior forest types) fringing the coast throughout, and running up the tidal creeks as much as 1 km, (2) a low mangrove community (likely equivalent to today's Transitional mangrove forest) inside the fringe forest, extending west to and slightly beyond the present position of the L-31E Canal, (3) a zone of mixed graminoid marsh with mangrove shrubs, adjoining the Fringe forest directly in Blocks 5 and 6, (4) buttonwood woodlands, appearing in a discrete band near the western border of the current study area, and (5) freshwater marsh vegetation, interior to the buttonwood zone, but encroaching into the study area in Blocks 3 and 4. The most strikingly changed element today from this 1940 landscape is the mixed graminoid-mangrove community, which in this portion of the study area is replaced by Dwarf mangroves except in a small patch of negligible size in Block 7.

In general, in the last 6 decades, the mangrove forest appears to have gotten taller and crowded out other plant communities east of the L-31E Canal, as a result of drainage, interception of sheet flow by the canal and ditch levees, and sea level rise. Landscape heterogeneity has been reduced, exotic plants have changed the nature of the plant communities, and wildlife habitat has been diminished.

Table 1: Description of forest types found in Biscayne National Park

Forest Type	Forest Description
Fringe Mangrove Forest	Forest dominated by trees generally exceeding 9 meters in stature and in some locations reaching 13-14 m in height. This forest is found adjacent to the shoreline and rarely extends beyond 175 meters from the coast. Like the Interior Mangrove Forest, the canopy is mainly composed of *Avicenia germinans* & *Laguncularia racemosa* while the understory and shrub stratum are predominantly *Rhizophora mangle*. This forest type is analogous to the fringe mangrove community described by Lugo (1980).
Interior Mangrove Forest	Forest dominated by trees between 5-9 meters in stature, however trees may exceed 10 meters in more productive sites. The dominant canopy species are *Avicenia germinans* & *Laguncularia racemosa*. As a rule, *Rhizophora mangle* is the dominant understory macrophyte. *Schinus terebinthifolius* is sometimes found within this forest type as well. This forest type is analogous to the basin mangrove community described by Lugo (1980).
Transitional Mangrove Forest	Forest dominated by trees between 2-5 meters in stature. Dominant canopy species is generally *Laguncularia racemosa*. However, *Avicenia germinans*, *Rhizophora mangle* & *Conocarpus erectus* are commonly found emerging from the canopy. Understory is predominantly *Rhizophora mangle*. *Schinus terebinthifolius* is sometimes found within this forest type.
Dwarf Mangrove Forest	Forest dominated by trees generally < 2 meters in stature. Dominant species *Rhizophora mangle*. *Avicennia gerrminans*, *Laguncularia racemosa*, and *Conocarpus erectus* are present in the understory of this community but are not a major component of the canopy. This forest type is analogous to the scrub mangrove community described by Lugo (1980).
Casuarina – Mangrove Forest	Seasonally flooded non-dital wooded forest generally found on disturbed sites containing a higher abundance of halophylic vs non-halophylic macrophytes. *Casuarina equisetifolia* is a major component of the canopy and at time is the sole canopy species. Canopy heights in this forest can exceed 10 meters but rarely exceed 15 meters.
Cauarina Forest	Forest dominated by *Casuarina equisetifolia*. This community type, which can reach up to 20 meters in height, is generally found on topographic highs like levee roads, spoil mounds, canal banks or in interior freshwater wetlands.
Mangrove Tree Island	Small, slightly elevated sections of vegetation within the dwarf mangrove forest community type that resembles the transitional mangrove forest type in both species composition and canopy height. This community type, as a rule, is found on topographic highs relative to the surrounding marsh and is more productive than the adjacent community type.
Swamp Forest	Seasonally flooded non-dital wooded forest containing both halophylic and non-halophylic macrophytes. Rich herb layer dominated by ferns. Canopy height generally below 10 meters.
Abandon Agriculture	Vegetation complex originating from ornamental nursery stock after several years of field abandonment.
Salt Marsh	Tidally influence interior marsh dominated or co-dominated by *Juncus roemerianuse* or *Distichlis spicata*. *Rhizophora mangle* is generally the dominant shrub species however *Avicennia gerrminans*, *Laguncularia racemosa*, and *Conocarpus erectus* are sometimes present, as well. Shrub canopy height rarely exceeds 2 meters.
Sawgrass – Mangrove Marsh	Seasonally flooded non-dital marsh co-dominated by *Cladium jamaicenses* and *Rhizophora mangle* found exclusively west of the L-31E levee. Species composition is generally rich and includes *Juncus roemerianuse*. This marsh type is similar to the red and white mangrove swamp described by Craighead (1971).
Sawgrass Marsh	*Cladium jamaicenses* dominated freshwater marsh.
Sawgrass – Casuarina Marsh	*Cladium jamaicenses* dominated freshwater marsh with an emergent canopy of *Casuarina equisetifolia* which in place may reach 7 meters in height.
Cattail Marsh	Freshwater marsh dominated by *Typha domingensis*.

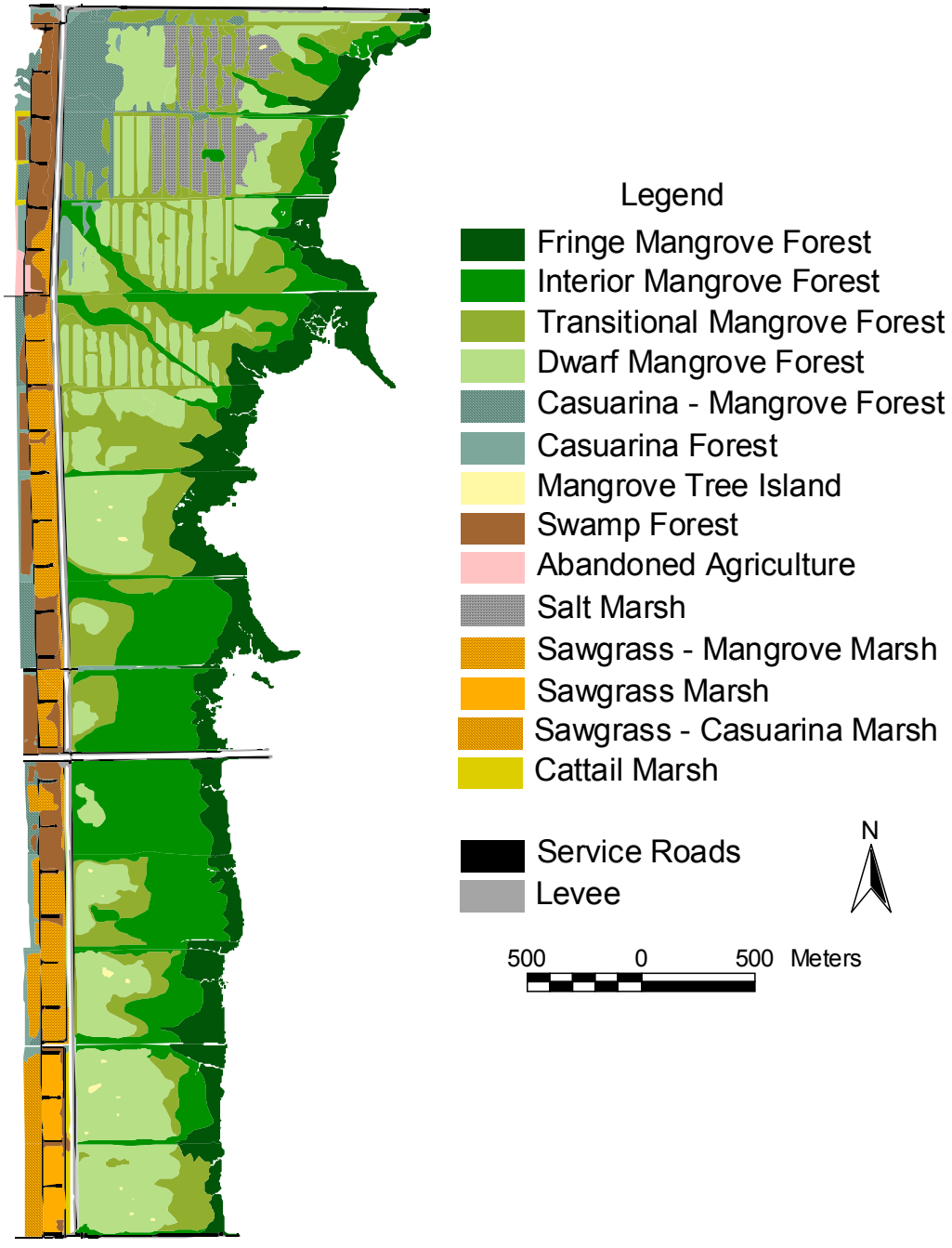

Figure 1: 2002 vegetation map of the coastal wetlands along the western shore of Biscayne Bay between the Mowry and Princeton Canals.

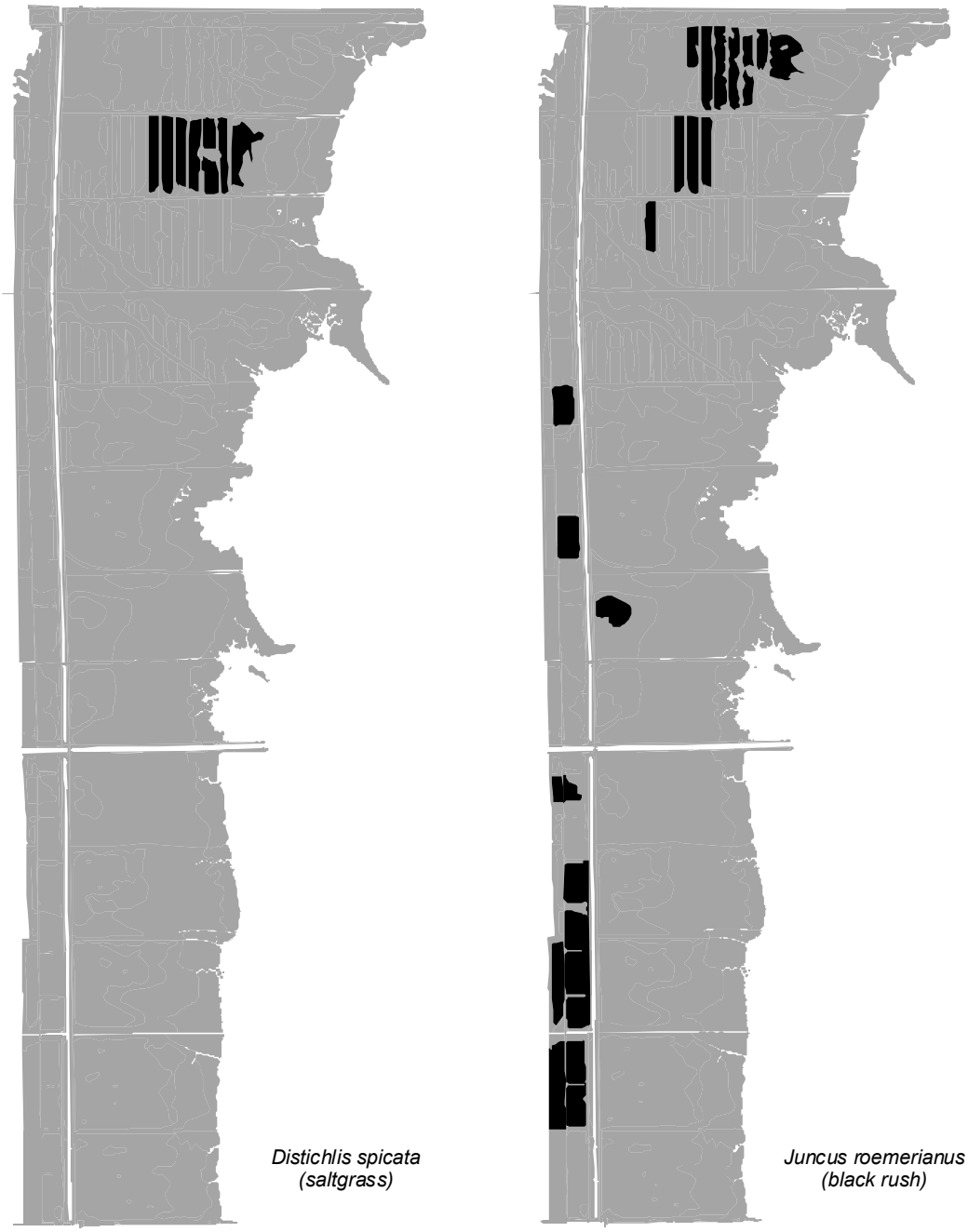

Figure 2: The 2002 distribution of saltgrass and black rush (in black) along the western shore of Biscayne Bay between the Mowry and Princeton canals.

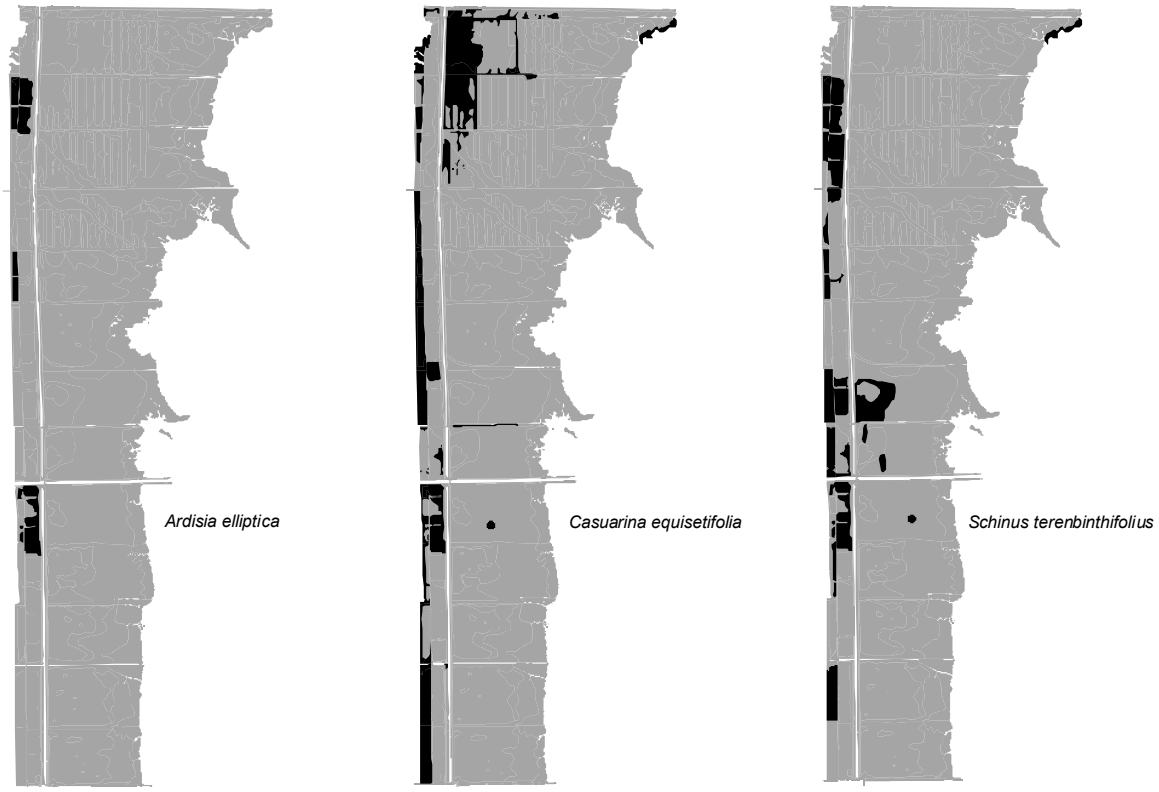

Figure 3 The 2002 distribution of three exotic species (in black) along the western shore of Biscayne Bay between the Mowry and the Princeton Canals.

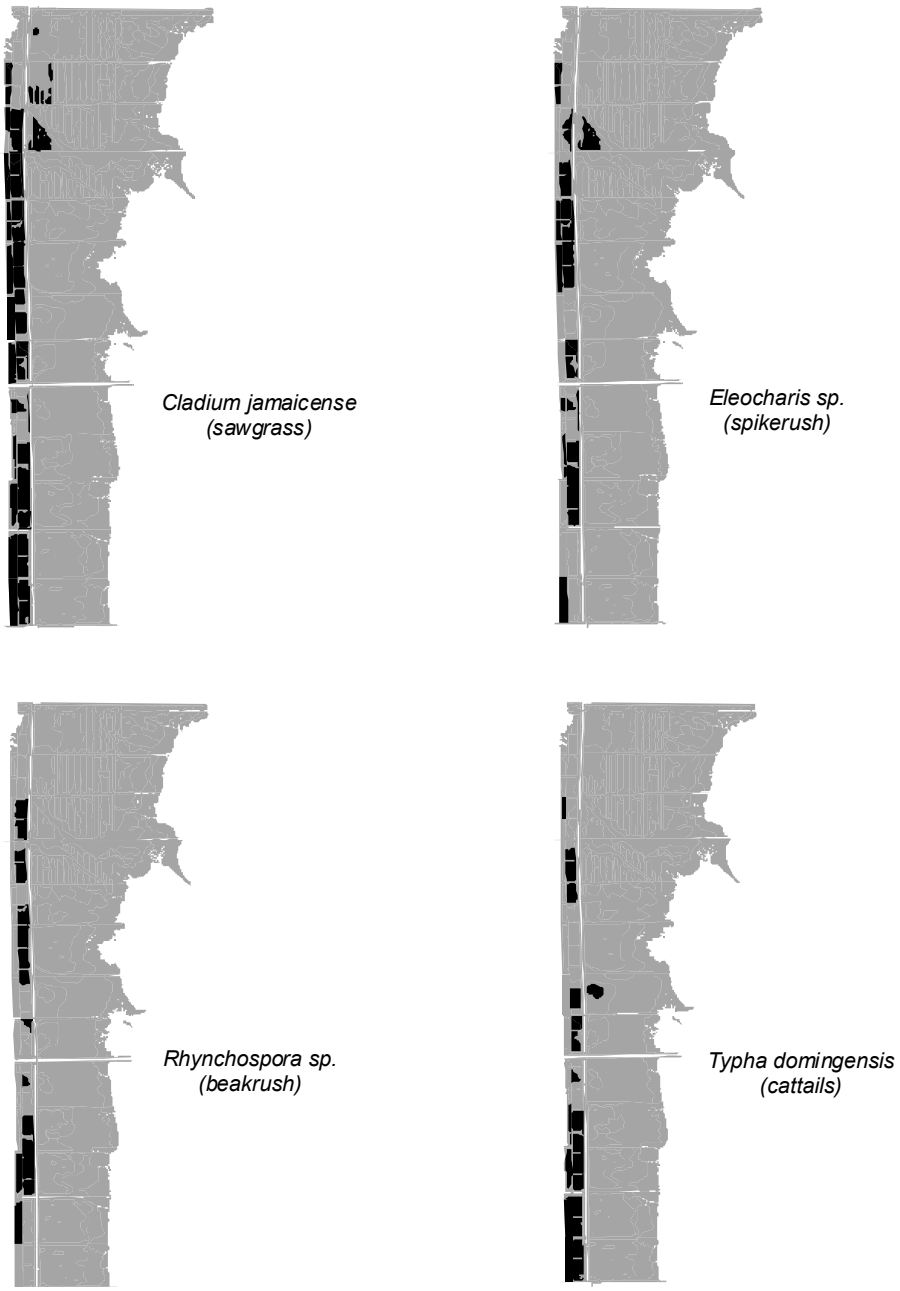

Figure 4: The 2002 distribution of sawgrass, spikerush, beakrush, & cattails (in black) along the western shore of Biscayne Bay between the Mowry and the Princeton Canals.

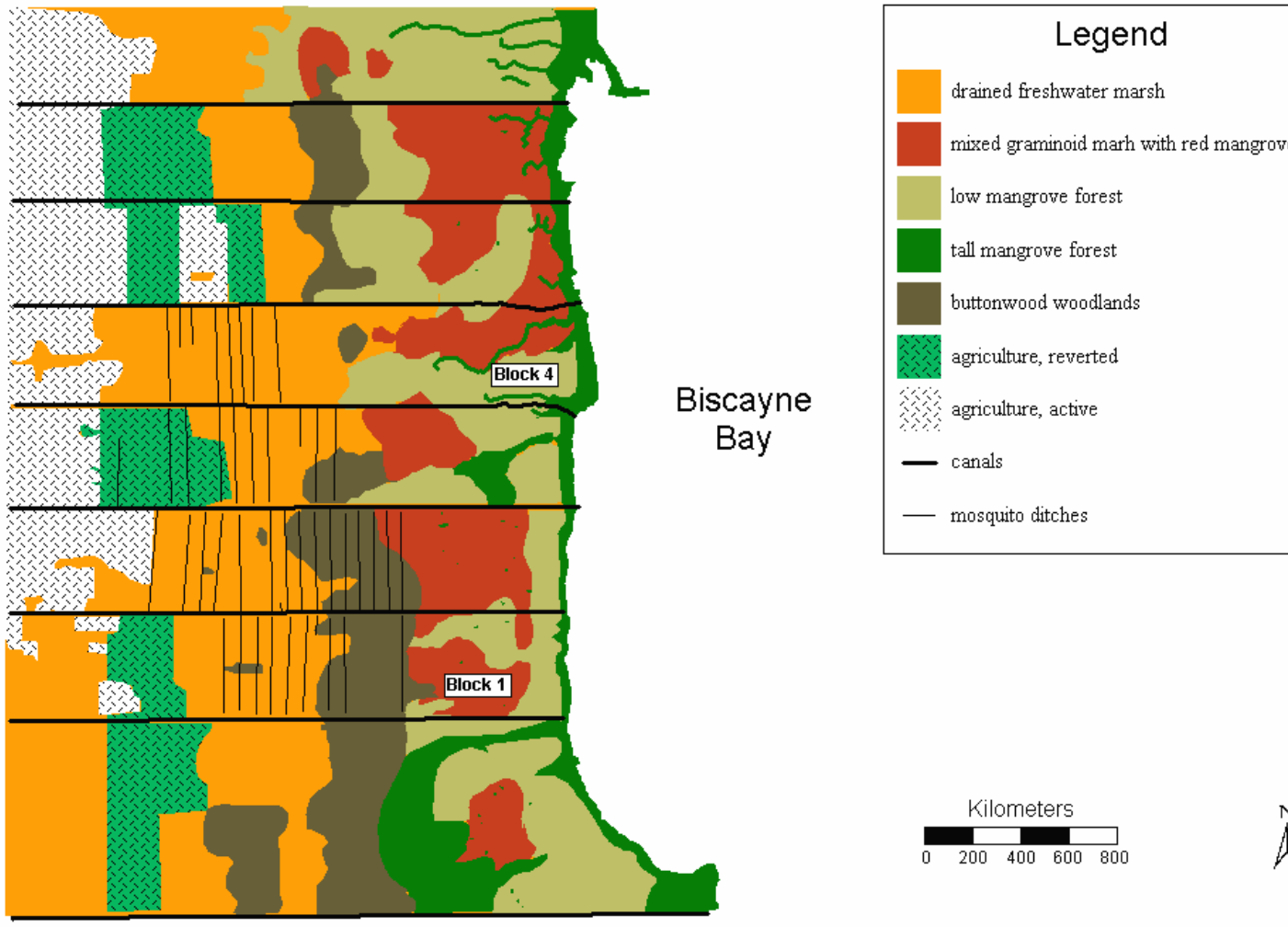

Figure 5: 1940 vegetation map of the coastal wetlands along the shore of Biscayne Bay between Block 7 and Convoy Point.

V. RESULTS COMPLETED – B. PERIPHYTON

Gaiser, E. E., A. Wachnicka, P. L. Ruiz, F. A. C. Tobias and M. S. Ross. 2004. Diatom indicators of ecosystem change in subtropical coastal wetlands. pp. 127-144 In Bortone, S. (ed) Estuarine Indicators. CRC Press.

ABSTRACT

Diatoms are ubiquitous in wet coastal environments, and the composition of their species-rich assemblages varies predictably with the strong biotic and physical gradients that characterize the intersection of freshwater and marine habitats. Compositional turnover occurs at a rate that integrates environmental variability at short-time scales but that allows detection of significant long-term directional change earlier and often more reliably than physical and other biological indicators. Here we present results of a survey of the diatom and related algal flora of benthic periphyton communities that proliferate in coastal wetlands of southeast Florida. The study area contained five broadly-defined vegetation zones that parallel the coastline, including, from the interior to the coast, a (1) freshwater swamp forest, (2) freshwater gramminoid marsh, (3) dwarf mangrove forest, (4) transitional mangrove forest, and (5) fringing mangrove forest. A species--rich assemblage of over 400 diatom and 50 non-diatom micro-algal taxa was distributed in relation to these vegetation types, with primarily salinity and canopy height driving compositional differences among sites. Taxon distributions are described and assemblage-based predictive models are presented that can be applied in long-term monitoring or paleoecological studies to measure rates and ecological effects of sea-level rise and salt-water encroachment.

INTRODUCTION

Coastal ecosystems often support a diverse benthic micro-algal community that, together with associated bacteria, fungi and macroalgae, form prolific periphyton growths on sediments and the grasses and/or wet forest vegetation that inhabit the coastline. Particularly in the subtropics and tropics, coastal periphyton communities form the base of a productive and diverse food web both in the marsh and the adjacent offshore marine environment as tides transport both periphyton products and consumers across the marine-freshwater interface (Admiraal, 1984; Day et al., 1989). Coastal wetlands at this interface present a diversity of environmental conditions because of the strong gradients in salinity, water availability and nutrient supply inherent in this transitional environment. A variety of habitat types result (depending on latitude), including interior freshwater forested marshes, supertidal gramminoid marshes, intertidal estuarine lagoons, hypersaline pools, mangrove swamps and/or grassy salt marshes. Consequently, coastal periphyton communities contain some of the most compositionally diverse algal floras in the world (de Wolf, 1982). Because algae are strongly influenced by their surrounding chemical and structural environment, they provide a useful tool for environmental monitoring in complex coastal systems (Vos and de Wolf, 1993; Sullivan, 1999; Cooper et al., 1999a).

Several anthropogenic influences threaten the existence and viability of coastal systems worldwide, including nutrient enrichment, over-harvesting of consumable resources, landscape modification and saltwater encroachment (National Research Council, 1993). Documentation of detrimental ecological effects of the latter has, in recent decades, been increasing in frequency and extent around the globe (Park et al., 1989), as the rate of salt-water encroachment into

coastal ecosystems increases due to sea-level rise exacerbated by diversion and depletion and/or diversion of coastward overland freshwater flow. The history of coastal ecosystems in South Florida provides an unfortunate example of the magnitude and complexity of effects that decades of canalization and sea-level rise can have on intertidal communities. Rates of salt-water encroachment in coastal South Florida exceed 400 m per decade in some areas (Ross et al., 2000), resulting in the disappearance of vast areas of freshwater marsh and interior migration of mangrove swamps.

Because salinity has an overriding influence on microbial community composition, algae, particularly diatoms, have been used to track rates of salt-water encroachment in both modern monitoring and paleoecological studies (Gasse et al., 1983; Juggins, 1992; Ross et al., 2001). Algal populations respond on time scales of weeks to months to changes in environmental conditions, integrating much of the small-scale temporal variation that is often the source of unwanted "noise" in continuous salinity recording data (Snoeijs, 1999). Transfer functions have been created from the modern distribution of diatoms along salinity gradients (in coastal areas and closed-basin "saline" lakes, e.g., Campeau et al., 1995; Fritz et al., 1999, respectively) that allow salinity to be predicted from diatom community composition with a very high degree of accuracy. However, while many coastal diatom taxa are thought to be widely distributed, application of salinity preferences for diatoms collected in other regions (ie., Baltic Sea, Snoeijs, 1999; Thames River, England, Juggins, 1992; Chesapeake Bay, Cooper, 1995; Mississippi Salt Marsh, Sullivan, 1982) to South Florida would be problematic because there would likely be a low degree of taxonomic overlap with these datasets. Subtropical wetlands in general and specifically the Everglades have been poorly explored taxonomically resulting in incompletely defined ecological and range size distributions. Further, coastal environments of the sub-tropics are dominated by mangrove swamps, and besides studies by Siqueiros-Beltrones and Castrejon (1999, Balandra Lagoon, Baja California), Navarro and Torres (1987, Indian River, Florida), Sullivan (1981, Mississippi salt marsh), Reimer (1996, Bahamas), and Podzorski (1985, Jamaica) there have been few explorations of coastal mangrove diatoms. The composition and range size distribution of mangrove diatoms and associated microflora, and their response to environmental variation, is practically unknown.

The objectives of the present study were to survey the algal flora of periphyton communities in coastal wetlands in the Everglades of southeast Florida. Periphyton mats are a dominant feature in both freshwater and saline Everglades wetlands (Browder et al., 1982; Ross et al., 2001). The specific purposes of this work were to: (1) document the taxonomic composition of algal assemblages, particularly diatoms, in periphyton of the coastal Everglades and (2) determine environmental drivers of assemblage composition, in order to (3) create algae-based inference models that could be used to track trajectories of environmental change. Our goal was to produce a taxonomic guide to aid in identifying sub-tropical coastal diatoms and to create algae-based environmental inference models that can be employed in long-term monitoring and/or paleoecological studies to document ecological response to habitat alteration along the South Florida coastline.

METHODS

Study Site

The southeastern edge of Florida was historically characterized by expansive coastal mangrove wetlands that were dissected by tidal creeks flowing from the freshwater Everglades to the coast. Egler (1952) was able to distinguish distinct vegetation zones lying in bands parallel to the coast, driven by gradients of salinity, water availability, nutrients and susceptibility to drought and fire, including a coastward sequence of gramminoid freshwater wetlands (to the interior), followed by dwarf mangrove scrub swamps in intertidal areas bounded by fringing mangrove forest on the coast. Throughout the last several decades, an extensive network of drainage canals has been constructed in South Florida, effectively draining much of the interior and coastal Everglades for urban and agricultural development. By the turn of the 21st century, the wetland bands had been diminished to the periphery of the coastline: freshwater gramminoid marshes had been largely displaced by an enroaching mangrove scrub community and most tidal creeks had disappeared (Ross et al. 2000; Fig. 1a).

The present study focuses on an area of remnant coastal wetlands, parts of which are protected in Biscayne National Park (Fig. 1b). The ~7 km long study area is bounded to the north and south by major east-west drainage canals (Princeton and Mowry, respectively) and bisected north-south by a secondary canal (L-31E). The region is dissected by many smaller east-west ditches which compartmentalize the area longitudinally into 13 hydrologically distinct wetland basins, that range in width from about 0.5 to 2 km. To the west of the L-31E canal, freshwater marshes are now hydrologically isolated from the coast and bounded to the west by agricultural lands, the periphery of which are heavily invaded by exotic trees including *Schinus terebinthifolius* (Brazilian Peppertree) and *Casuarina equisetifolia* (Australian pine). To the east of the L-31E canal, mangrove communities predominate, with strands of upland forest now occupying the remnant tidal creek beds.

We used a stratified-random design to select study sites within each of the 13 sub-basins. Using aerial photos of the area, each sub-basin was divided into 4-6 units, including, to the west of the L-31E canal, a freshwater swamp forest dominated by exotics that have invaded abandoned agricultural land and remnant freshwater gramminoid marsh, and, to the east of the L-31E canal, mangrove forests that can be characterized by canopy height and cover as dwarf, transitional and fringing (along the coastline). Within each unit a north-south transect was randomly located, and 1-5 sampling stations were evenly distributed along its length. A total of 226 stations were sampled within the 12 km^2 area (Fig. 1b).

Data collection and processing

At each station, we assessed the vegetation community structure, roughly described the sediments and sampled periphyton and several chemical parameters in surface and/or pore-water. Vegetation was assessed using methods of Ross et al. (2001) where species cover and canopy height was estimated separately for upper (~2 meters height) and lower (<2 m) strata in repeated quadrats. Depth of sediments to the limestone bedrock was measured at five stations with a probe-rod and, using a soil auger, sediments were extracted to measure depths of readily apparent compositional and textural transitions. Using a PVC pipe, five small (3.8 cm^2, 1-2 cm thick) sections of surface soil, commonly occupied by periphyton, were extracted from each

location and composited. A portable meter was used to measure pH and conductivity in surface water, if present, or in pore-water that filled the auger hole. Conductivity ($\mu S\ cm^{-1}$) was converted to salinity (ppt) using a model provided from a previous study in a nearby basin where both variables were directly measured (Ross et al., 2001).

In the laboratory, periphyton was picked free of large plant fragments, homogenized, diluted and subsampled for analysis of dry weight (2 days at 100 ºC), ash-free dry weight (AFMD, 1 hr. at 500 ºC), total phosphorus (TP, by automated colorimetry) and soft-algae and diatom composition. Diatoms were cleaned of calcite and organic matter by chemical oxidation and permanently fixed to a glass microslide using Naphrax® mounting medium. At least 500 diatom valves were counted on random, measured transects on a compound light microscope at 1000 X. Non-diatom algae ("soft algae") were analyzed from one station within each unit in sub-basins 1-8 by preparing semi-permanent water mounted slides. At least 500 units (cells, colonies or filaments) were counted and identified on random transects on the slide at 400-1000 X magnification. Abundance estimates were converted to biovolume using critical dimensions (length, width, breadth) of 20 representatives of each morphologically distinct unit and applying volumetric formulas for the closest geometric shape. Diatom and soft algal samples, permanent slides, photos of all taxa, database links and all references used in taxonomic determination, can be accessed through our website at http://serc.fiu.edu/periphyton/index.htm. and are archived in a curated collection in the microscopy laboratory at Florida International University.

Data Analysis

Stations were sorted into five vegetation type categories based on survey data and aerial photographs, including a freshwater swamp forest, freshwater gramminoid marsh, and dwarf, transitional and fringing mangrove forest. The distinctiveness of the categories based on relative cover of species present in more than 5% of the sites was confirmed using analysis of similarity (among community types) employing the Bray-Curtis similarity metric in PRIMER-E/ANOSIM ® software. Plant species significantly influencing the five community types were identified using Dufrene and Legendre's (1997) "Indicator Species Analysis", where taxa having an indicator value (based on relative abundance and frequency among sites) above 40% of perfect indication ($P<0.05$) were considered reliable indicators.

Using the spatial modeling and analysis (V2.0) module in Arcview GIS 3.2 ®, we mapped the distribution of the vegetation community types and other environmental variables (soil depth, canopy height, salinity, and periphyton AFDM and TP content). To interpolate between points, we used the IDW method which weights the value of each point by the distance that point is from the cell being analyzed and then averages the values. The output grid cell size was 10 meters and number of neighbors was 3 points. Means of each parameter were calculated within each vegetation type and compared using a Student's T-test, and correlations among parameters were determined using the Pearson correlation coefficient on log-transformed data, with $P < 0.001$.

Patterns in relative abundances and biovolumes of diatom and non-diatom taxa, respectively, were determined using non-metric multidimensional scaling ordination (NMDS), analysis of similarity and weighted-averaging regression. Species by station data matrices were established and species present in fewer than 1% of samples and having a mean relative abundance (when present) of <0.05% were removed prior to analysis. Assortment of sites in the NMDS ordinations based on the Bray-Curtis similarity metric were related to environmental

variables using vector fitting. The significance of algal community patterns relative to vegetation type (a categorical variable) were determined using analysis of similarity on the same similarity matrix as used for the NMDS. Taxa significantly associated with the five vegetation community types were identified using Dufrene and Legendre's (1997) "Indicator Species Analysis".

We used weighted-averaging regression and calibration to determine the strength of the relationship of species composition to salinity and vegetation type. This approach assumes that species abundance responses can be characterized by an optimum or mode where abundances are greatest and a tolerance that defines the breadth of appearance along a gradient. The value of an environmental variable can then be calculated for a sample from an unknown environment, using the average of the optima of the species present, weighted by their abundances and possibly tolerances. Using the weighted-averaging program C2 (Juggins, 2003), we estimated the salinity and vegetation optimum and tolerance for each species as the average among sites in which the taxon occurred and then tested the prediction power by estimating the salinity and vegetation type from a random set of sites (bootstrapping with replacement) and plotted predictions against observed values. Predicted values for salinity and vegetation type from diatom and soft-algae calibration models were mapped using the same approach as for the environmental variables (described above).

RESULTS

Vegetation

The five major vegetation community types distinguished through interpretation of aerial photographs and used to determine selection of sampling sites were confirmed to be compositionally distinct based on relative cover of 45 of the most abundant of the 84 plant species found in the study area (ANOSIM, all combinations, global $R = 0.48$, $P<0.01$). Compositional differences within freshwater units (upland forest and freshwater marsh) and interior mangrove units (dwarf and transitional) were less ($R = 0.2$ and 0.3, $P<0.05$, respectively) than differences between freshwater and mangrove units (mean $R = 0.4$, $P<0.01$), and the fringing mangrove forest was highly distinguishable from all other units (mean $R = 0.8$, $P<0.001$). Though the coastward sequence of vegetation zones was consistent among sub-basins, there was variation in the breadth of each zone along the 7 km study area (Fig 2a) and we acknowledge that additional distinct community types occur within these units, most notably including a densely vegetated, heavily canopied mangrove forest growing in historic drainages that meander through adjoining units and forests occupying tree islands that punctuate all units of the landscape. Vegetation canopy height was significantly higher in the upland forest and transitional and fringing mangroves than in the freshwater marsh and dwarf mangrove community (Fig. 4a).

Environmental Variation

Compositional differences among units were associated with variation in several environmental parameters. In pore water, while no significant pattern was observed in pH (mean = 7.2), a strong west-east increase in salinity was observed in many of the sub-basins, with the L-31E clearly separating freshwater (salinity < 5 ppt) from marine (5-20 ppt) conditions (Fig. 3a). Soils were significantly deeper in the fringing mangrove forest than other units (126 vs. mean 104 cm,

respectively), and though nearly all cores were characterized by an upper heavily rooted peat, this layer was deepest in the fringing mangroves and gradually became shallower to the interior freshwater marsh (66 vs 12 cm, respectively; Figs. 4b). With implications for linking biotic patterns to environmental variation, several variables were significantly correlated with each other, including soil, peat depth, salinity and pH.

Periphyton biomass and TP content

Algae were organized into periphyton communities of considerable mass throughout the wetland units (Figs. 4c). Periphyton DM was highest in the dwarf mangrove and freshwater marsh units (903 and 575 g m^{-2}, respectively) and lower in the forested units (mean = 266 g m^{-2}). A considerable portion of this mass in all units was comprised of calcite, particularly in the dwarf mangrove and freshwater units, such that when this portion that is not combustible is subtracted from the dry mass (in the AFDM calculation), some of the pattern in periphyton distribution disappears, though AFDM biomass remains significantly higher in the dwarf mangrove forest than other units (Fig. 4c). Likewise, the portion of the periphyton comprised of organic (rather than calcitic) mass was significantly higher in the forested units than in the dwarf mangroves and freshwater marsh. The DM, AFDM and organic carbon content of the periphyton mats were, by nature of their analysis, correlated and also strongly negatively related to canopy height, and less so to peat depth in the sediments.

Very strong trends in the TP content of periphyton mats were evident in the system, with periphyton in the freshwater marsh having significantly lower P than all other units and mats in the transitional and fringing mangrove forest having more than an order of magnitude higher P content than other units (Fig 4d). Patterns of variation in periphyton TP content were positively correlated with peat depth, canopy height and salinity.

Algal community composition

A total of 405 diatom taxa representing 64 genera were collected from periphyton in the study area. Genera represented by the most taxa (number given in parentheses) were *Amphora* (59), *Navicula* (55), *Mastogloia* (51), *Nitzschia* (39), *Fragilaria* (21), *Achnanthes* (16) and *Diploneis* (15). The NMDS ordination (two-dimensions, stress = 0.12) of relative abundance of 133 of the most abundant taxa found clear separation of diatom communities occupying the freshwater units (forest and marsh) from the marine mangrove units. This pattern was verified by the analysis of similarity, which showed that significant separation between freshwater units 1 and 2 vs. marine units 3, 4 and 5 (global $R > 0.6$ for all comparisons, $P<0.001$), but little distinction in comparisons within freshwater and marine units (global $R <0.2$ for all comparisons, $P>0.1$). While the ANOSIM analysis suggested two groups (freshwater vs. marine), the weighted-averaging regression model revealed a more linear gradient from interior to coastal communities (Fig. 2b). A total of 35 indicator taxa were identified, six for the upland forest, five for the freshwater marsh, two for the dwarf mangroves, seven for the transitional mangrove forest and 15 for the fringing mangrove forest (pictured in Figs. 5, 6). When mapped spatially, diatom-based vegetation type predictions appear similar to measured values (Fig. 2b).

The NMDS ordination also revealed significant patterns in diatom composition among sites relative to salinity, canopy height, organic content, peat depth and TP (maximum vector R^2 = 0.34, 0.30, 0.29, 0.24 and 0.23, respectively). Effects of canopy height and TP on diatom

composition were positively correlated and together negatively correlated with the influence of organic content of the periphyton mats. The effect of salinity, the strongest variable influencing composition, was correlated with that of peat depth. Because salinity had an overriding effect on composition, and was only correlated with one other variable, we examined this relationship further using weighted-averaging regression.

Because the frequency distribution of salinity values among sites was bimodal, with sites in the freshwater units confined to the west of the L-31 E canal having much lower values than mangrove sites to the east, the linear model used in the weighted-averaging regression may not provide the best fit to these data. Even so, the model has strong predictive power because most of the taxa incorporated in the model have well-defined salinity optima and narrow tolerances (provided in Appendix I). When mapped spatially, diatom-based salinity predictions appear similar to measured values (Fig 3b).

Fifty-seven additional non-diatom algal taxa were found and identified co-occurring with diatoms in the periphyton communities at the reduced set of sites. The soft-algae flora was taxonomically dominated by coccoid and filamentous cyanophytes (39 and nine taxa, respectively), but also included two coccoid, two desmid and three filamentous chlorophye taxa, one dinoflagellate taxon and one purple-sulfur bacterium (non-algal, but included in counts). Taxa comprising more than 1% of the total biovolume of soft algae included, in decreasing order of abundance, the three filamentous chlorophytes (undetermined branching filaments resembling *Rhizoclonium*; 42%), followed by the blue-green filament *Scytonema* cf. *hofmannii* C.Agardh *ex* Bornet (35%) and three other unidentifiable blue-green filaments (resembling *Schizothrix* spp., 6.5%), 7 *Chroococcus* spp. (5.8%), five *Gloeothece* spp. (3.4%), six *Aphanothece* spp. (2.5%) and the purple-sulfur bacterium (1.3%).

The non-diatom algae responded similarly to measured environmental variables to the diatoms. The NMDS ordination (two-dimensional stress = 0.11) of relative biovolume of 35 of the most abundant taxa separated freshwater forest and marsh sites from marine mangrove units, and this distinction was shown to be significant in the analysis of similarity ($P<0.001$). Several sites were distinctly grouped apart from other sites because they were uniquely dominated by a filamentous chlorophyte resembling *Rhizoclonium*. These included most of the coastal sites in sub-basins 4 and 7. The ANOSIM analysis showed clear separation of algal communities occupying the freshwater units (forest and marsh) from the marine mangrove units. The weighted-averaging regression model for habitat types was strong but less predictive than the diatom-based model (Fig. 2c). Five species were significantly indicative of 3 of the vegetation units, including, for the freshwater forest, two blue-green filaments resembling *Schizothrix calcicola* (Agardh) Gomont and the coccoid blue-green *Gomphosphaeria semenvitis*, for the dwarf mangrove scrub, an unidentified *Gloeothece* sp. and, for the fringing mangroves, an unidentified chlorophyte resembling *Rhizoclonium*. When mapped spatially, algae-based vegetation type predictions appear similar to measured values (Fig 2c).

The NMDS ordination showed the same variables to be important in explaining soft-algal distribution as the diatoms, including salinity, peat depth, canopy height, TP and organic content (maximum vector $R^2 = 0.34$, 0.33, 0.25, 0.21 and 0.20, respectively). Effects of canopy height, TP and peat depth on soft-algal species composition were positively correlated and together negatively correlated with the influence of organic content of the periphyton mats. The effect of salinity, the strongest variable influencing composition, was independent of other variables and we examined this relationship further using weighted-averaging regression. The model to predict salinity from algal species composition is strong. When mapped spatially, the algal-based

predictions are less consistent with actual measured values (in comparison to diatoms; Fig. 3c), although sites to the east and west of the L-31E canal can be clearly distinguished.

DISCUSSION

The fresh-salt-water ecotone lining the coast of southeast Florida coast is migrating rapidly westward. In our 7 km study area, four canals constructed over the last several decades now discharge the majority of overland freshwater flow directly into Biscayne Bay. Comparing the current locations of the five vegetation zones to those observed in the 1940 aerial photograph, several changes are obvious: (1) tidal creeks linking the interior freshwater marsh to the coast have disappeared, so that most freshwater is now delivered in large volumes to point locations where canals terminate, (2) the freshwater marsh has been drained and native vegetation displaced to the west by invasive exotic trees and to the east by the expanding dwarf mangrove forest, and (3) all coastal vegetation bands are now restricted to the east of canals that, by running parallel to the coastline, prohibit natural mixing of fresh- and salt-water during the tidal cycle. Together with sea-level rise (the regional rate is estimated to be 3-4 mm yr^{-1}; Wanless et al., 1994), massive fresh-water drainage has caused a rapid rate of salt-water encroachment that forces mangrove communities to shift landward to the canal boundary which disrupts natural exchange across the coastal ecotone.

Evidence of shifts in the width and location of the vegetation zones can be interpreted from the soil profiles. All of our soil cores contained a substantial marl layer below a surficial peat. In the Everglades, marl soils are generally associated with freshwater marsh communities, particularly wet-prairie meadows (defined as gramminoid marshes that are inundated 6-9 months per year). Peat soils are indicative of deeper water more prolonged flooding, and of mangrove communities along coastlines. We interpret the peat layer in upper soils across the wetland basins to be indicative of: (1) invasion by forest elements into the freshwater marsh due to water diversion from areas west of the L-31E canal, and (2) invasion of mangroves into areas previously occupied by freshwater marsh in areas east of the L-31E. Sedimentation rates from studies in similar communities nearby (1-3 mm/yr^{-1}; Scholl et al., 1969) suggest the contact is coincident with the establishment of the drainage canal network.

The microbial community in the Biscayne Bay coastal wetlands was, in most areas, organized into a cohesive periphyton mat. Organic biomass, measured by AFDM, was high (mean = 190 g m^{-2}) throughout the study area exceeding values found in a nearby mangrove marsh (5-20 g m^{-2}; Ross et al., 2001), where salt-water encroachment has caused a rapid expansion of a broad band of low-productivity (referred to as the "white zone"). The highest values in the shallow freshwater marsh units (mean = 317 g m^{-2}) were comparable to marshes in the interior Everglades, where periphyton biomass can exceed that of emergent plants (Browder et al., 1982). Notably, the percent organic carbon in periphyton mats was highest toward the coast where marl deposition is minimized.

Of the measured environmental variables, only canopy height was correlated with periphyton biomass, with lowest values in heavily canopied fringing forests and highest in open areas of freshwater marsh. It is not unexpected that light availability would control periphyton biomass, although Beanland and Woelkerling (1983) found no effect of canopy on periphyton algal biomass in an *Avicennia* forest in South Australia, and, in our study, biomass was still relatively high in the heavily canopied fringe. Ambient daytime irradiance to the surface of Everglades periphyton mats can exceed 1000 µmol m^{-2} s^{-1}, an intensity which has been shown to

photo-inhibit photosynthesis (Underwood, 2002). Typically periphyton mats have distinct vertical structure, with green productive layers underlying a calcitic, inactive (possibly light-inhibited) surface. In this study, mats in open areas in this study were thick and structured, whereas periphyton in shaded areas was usually comprised of a thin, green film growing attached to roots and leaf litter. This community may be encouraged by the higher TP availability in coastal areas, and contribute to the inverse relationship between periphyton organic content and P availability. It was somewhat remarkable that although P availability (as measured by the TP content of the periphyton mats) varied an order of magnitude in the study area, there was no measurable correlation with periphyton DM or AFDM biomass, though it has been shown to control periphyton biomass in other areas of the Everglades (Gaiser et al., 2004). However, although biomass may be similar to or lower than interior areas, turnover of periphyton in the fringing mangroves may be higher as a result of increased nutrient availability. Other studies have found particularly high algal productivity in fringing mangrove ecosystems and in neighboring seagrass beds (Koch and Madden, 2001). Total algal biomass in one *Rhizophora mangle* forest in Puerto Rico was actually found to exceed the total annual leaf litterfall (Rodriguez and Stoner, 1989), pointing to the impact of benthic periphyton to the food web of mangroves and neighboring lagoons and estuaries.

Periphyton mat biomass was high across the broad range of salinity experienced by this system. This shows that the complicated, intricately connected communities forming highly structured periphyton mats can be created in both freshwater and marine conditions, even though the composition (at all levels, macro and micro-algal, bacterial, fungal, etc…) is likely vastly different owing to the lack of most species to tolerate both purely freshwater and marine conditions.

Indeed, we did find that salinity had an overriding control on algal composition throughout the coastal wetlands. While mats were dominated throughout the system by green algal filaments, *Scytonema* spp. and small coccoid blue-green algae, their morphologies (and, thus, our taxonomic designations) differed along the salinity gradient. The difficulty of assigning names to most of the taxa, alludes to the fact that coastal mangrove micro-algal communities are poorly explored taxonomically. That we could not find many of the taxa collected here listed, described or pictured in studies from similar system suggests either that these studies mis-diagnosed taxa because of the paucity of appropriate taxonomic literature or that there is more regionality to the coastal micro-algal flora than previously thought.

However, at higher levels of taxonomic organization, this flora did resemble that of other microbial mangrove mats collected elsewhere, and, at those levels, responded similarly to salinity variation in the system. Phillips et al. (1994) found that horizontal zonation of algae on pneumatophores of *Avicennia* marina in South Africa was controlled primarily by salinity and wetting frequency, with the green alga *Rhizoclonium* dominating wet areas and providing support for numerous filamentous cyanophyte taxa (notably, *Lygbya confervoides* and *Microcoleus chthonoplastes*, belonging to genera also found in this study). *Rhizoclonium* and other green-algal filaments are often abundant in mangrove periphyton communities, often forming a tertiary layer over the macroalgae that are directly attached to the mangrove roots (Phillips et al., 1994). The macroalgae have been shown to be an important component of mangrove marshes, both in terms of their own productivity and diversity but also through their support of a diverse epiphytic community: it is not uncommon to find upwards of 20 species of macroalgae inhabiting mangrove benthos, providing support for hundreds of microalgal taxa (Collado-Vides, 2000). Although we excluded macroalgae from our detailed analyses, we did

note in field collections that *Bostrichia* was abundant on prop-roots and often coated with a thin green-algal mat (likely *Rhizoclonium* spp.). These *Rhizoclonium*-based communities were particularly important in coastal sites in sub-basins 4 and 7, and is what influenced the separation of these sites in the NMDS ordination.

The filamentous chlorophytes and macroalgae were joined by cyanobacterial filaments, particularly *Scytonema* and *Schizothrix* species which often form the backbone of microbial mats across the full salinity range, from shallow, freshwater calcareous wetlands in the Everglades and Belize (Rejmánková and Komárková, 2000) to intertidal mangroves (Collado-Vides, 2000) to subtidal marine stromatolites (Rasmussen et al., 1993)) and hypersaline lagoons (Hussain and Khoja,1993). These genera both contain species representing the full salinity spectrum, and indeed some of the species (*Scytonema hofmannii*) appear capable themselves of thriving in vastly different salinity regimes. In this study, the *Scytonema* and *Schizothrix* were most abundant in the freshwater marsh where they appeared, upon microscopic examination, to be coated with calcium carbonate crystals, which has been noted elsewhere (Browder et al., 1982). These were displaced by non-calcite precipitating blue-green algae in communities closer to the coast. Similar *Lyngbya* and *Microcoleous*-dominated blue-green algae have been collected from mangrove pneumatophores elsewhere (Hussain and Khoja 1993). While the periphyton matrix appears throughout the system to be macroscopically strung together by filamentous green or blue-green algae, the interstices of this web are often "glued" together by mucilaginous polysachharide produced by abundant and diverse coccoid blue-green algae, which may increase dessication resistance, provide a barrier to fluctuations in salinity, and concentrates nutrients and enzymes that control nutrient cycling.

The most diverse algal component in the periphyton mats studied here was the diatoms. It is common to find a large number of diatom genera in estuaries and near-coast environments because typically genera are confined to either fresh or salt water, and rarely mix except in brackish situations (Snoeijs, 1999). The dominance of *Amphora* and *Mastogloia* in the coastal flora is similar to findings in other parts of Florida and the Caribbean (Montgomery, 1978; Sullivan, 1981; Foged, 1984; Podzorski, 1985; Navarro, 1982; Reimer, 1996). These genera, together with *Navicula*, *Nitzschia*, *Cocconeis*, *Fragilaria* and *Achnanthes*, are probably important in coastal floras circumglobally, at least in the Northern Hemisphere. At lower taxaonomic levels we found several taxa with consistent morphologies that have not appeared elsewhere (or only in the regional literature – Montgomery, 1978; Foged, 1984; Podzorski, 1985; Navarro, 1982) that may be unique to the subtropical/tropical Atlantic coast.

Diatom organized into distinct freshwater and marine assemblages on either side of the L-31 E canal that effectively deterred mixing of tidal and overland freshwater flow. To the east of the canal, the freshwater marsh flora was dominated by *Encyonema evergladianum*, *Brachysira neoexilis*, and *Nitzschia palea* var. *debilis*, which are all common in un-enriched periphyton mats throughout the freshwater Everglades (Slate, 1998; Cooper, 1999b). The freshwater swamp forest contained many of the same taxa as the freshwater marsh, but was the preferred habitat for *Mastogloia smithii*, *Fragilaria synegrotesca*, and 4 species of *Nitzschia* (*N. semirobusta, N. amphibia f. frauenfeldii, N. amphibia,* and *N. nana*). While these are all common elsewhere in the Everglades (Slate, 1998; Cooper, 1999b) the predominance of *Nitzschia* taxa in the forest relative to the marsh is notable, and may reflect a higher stress tolerance for members of this genus (i.e., disturbance and low light intensities).

To the east of the L-31 E canal, the mangrove system was dominated by pennate benthic taxa. Mangrove-inhabiting taxa appear to be capable of withstanding a broad range of salinity

and frequent desiccation. Taxa in the genus *Amphora*, *Achnanthes* and *Triblionella* became gradually more dominant toward the coast, indicating an affinity for higher salinities. These taxa appeared to assort better along the salinity gradient than by the vegetation type categories, likely because of the effect tidal transport from the coastline to the canal levee. Transport was also probably responsible for the presence of notably marine planktonic taxa, such as *Cyclotella striata*, *Catacombas gaillonii*, *Biddulphia* spp. and *Terpsinoë musica*, in benthic samples.

APPLICATIONS

The algal flora of coastal South Florida is not only prolific in terms of biomass and richness, but is highly correlated with salinity and vegetation type -- two factors that will be influenced most by continued salt-water encroachment. Models provided here allow salinity to be predicted from diatom composition with an error of <10% of the actual value. Considering the high degree of variation in continuous salinity recordings, diatoms offer not only a means of monitoring salinity more accurately in the modern environment but also provide a tool for reconstructing past salinity from fossil assemblages. Further, diatom composition offers a tool for hindcasting an ecological variable (vegetation type) from past communities. The predictive power of these models can be strengthened by those of Ross et al. (2001) who created a diatom-based transfer function that predicts distance from the coast in a neighboring South Florida wetland with 100 m resolution. The use of diatoms in coastal environments should receive increased attention in coming years as the realization of their tight linkages to the strong zonation typical of coastal environments is recognized in different regions. While long-term preservation of diatoms in sediments of coastal mangrove systems is sometimes poor (Ross et al., 2001), locations slightly displaced offshore appear to offer better preserved records that have been useful in salinity reconstructions (Huvane et al., 2001). This work strongly advocates the use of diatoms in tracking habitat shifts in response to restoration at the freshwater-marine coastal interface.

LITERATURE CITED

Admiraal, W. 1984. The ecology of estuarine sediment-inhabiting diatoms. Prog. Phycol. Res., 3: 269-322.

Beanland, W. R. and W. Woelkerling. 1983. *Avicennia* canopy effects on mangrove algal communities in Spencer Gulf, South Australia. Aq. Bot., 17: 309-313.

Browder, J. A. et al., 1982. Biomass and primary production of microphytes and macrophytes in periphyton habitats of the southern Everglades. Rep. No. T-662. South Florida Research Center, Homestead, Florida.

Campeau, S., A. Hequette and R. Pienitz. 1995. The distribution of modern diatom assemblages in coastal sedimentary environments of the Canadian Beufort Sea: An accurate tool for monitoring coastal changes. Proceedings of the 1995 Canadian Coastal Conference 1: 105-116. The Canadian Coastal Science and Engineering Association. Dartmouth, Nova Scotia.

Collado-Vides, L. 2000. A review of algae associated with Mexican mangrove forests. In M. Munawar et al., (eds) Aquatic Ecosystems of Mexico: Status and Scope. Ecovision World Monograph Series. Backhuys Publishers, Leiden, The Netherlands. pp. 353-365.

Cooper, S.R. 1995. Chesapeake Bay watershed historical land use: Impact on water quality and diatom communities. Ecol. Appl., 5:703-723.

Cooper, S. R. 1999a. Estuarine paleoenvironmental reconstruction using diatoms. In Stoermer, E. F. and J. P. Smol (eds). The Diatoms: applications for the environmental and earth sciences. Cambridge Press, pp. 352-373.

Cooper, S. R. et al. 1999b. Calibration of diatoms along a nutrient gradient in Florida Everglades Water Conservation Area-2A, USA. J. Paleolimn. 22:413-437.

Day, J. W. et al. 1989. Estuarine Ecology. John Wiley. New York, NY.

Dufrene, M. and P. Legendre. 1997. Species assemblages and indicator species: the need for a flexible asymmetrical approach. Ecol. Monogr., 67: 345-366.

Egler, F. E. 1952. Southeast saline Everglades vegetation, Florida, and its management. Veg. Acta Geobot., 3: 213-265.

Foged, N. 1984. Freshwater and littoral diatoms from Cuba. *Bibl. Diatomologica*, 5: 1-243.

Fritz, S. C. et al. 1999. Diatoms as indicators of hydrologic and climatic change in saline lakes. In Stoermer, E. F. and J. P. Smol (eds). The Diatoms: applications for the environmental and earth sciences. Cambridge Press. pp. 41-72.

Gaiser, E. et al. 2004. Phosphorus in periphyton mats provides the best metric for detecting low-level P enrichment in an oligotrophic wetland. Water Res. 38: 507-516.

Gasse, F., J. F. Talling and P. Kilham. 1983. Diatom assemblages of East Africa: classification, distribution and ecology. Rev. d'Hydrobiol. Trop. O.R.S.T.O.M., 16: 3-34.

Hussain, M. and T. Khoja 1993. Intertidal and subtidal blue-green algal mats of open and mangrove areas in the Farasan Archipelago (Saudi-Arabia), Red Sea. Botanica Marina 36: 377-388.

Huvane, J. K. and S. R. Cooper. Diatoms as indicators of environmental change in sediment cores from northeastern Florida Bay. In B. R. Wardlaw (ed.) Paleoecological studies of South Florida. Bulletins of American Paleontology, 361: 145-158.

Juggins, S. 1992. Diatoms in the Thames estuary, England. Ecology, paleoecology, and salinity transfer function. Bibliotheca Diatomologica, 25: 1-216.

Juggins. S. 2003. C2 User guide. Software for ecological and palaeoecological data analysis and visualisation. University of Newcastle, Newcastle upon Tyne, UK. 69pp.
Koch, M. S. and C. J. Madden. 2001. Patterns of primary production and nutrient availability in a Bahamas lagoon with fringing mangroves. Marine Ecol. Prog. Series, 219: 109-119.
Montgomery, R. T. 1978. Environmental and ecological studies of diatom communities associated with the coral reefs of the Florida keys. Ph.D. dissertation. Florida State University. Tallahassee, FL.
National Research Council 1993. Managing wastewater in coastal urban areas. Washington DC: National Academy Press.
Navarro, J.N. 1982. Marine diatoms associated with Mangrove Prop Roots in the Indian River, Florida, U.S.A. *Bibliotheca Phycologica*, 61: 1-151.
Navarro, N. and R. Torres. 1987. Distribution and community structure of marine diatoms associated with mangrove prop roots in the Indian River, Florida, U.S.A. Nova Hedwigia, 45: 101-112.
Park, R. A. et al. 1989. Costal wetlands in the twenty-first century: profound alterations due to rising sea level. Pp. 71-80 in Wetlands: Concerns and Successes. Proceedings of the American Water Resources Association, Tampa, FL.
Phillips, A. et al. 1994. Horizontal zonation of epiphytic algae associated with Avicennia marina (Forssk) Vierh pneumatophores at Beachwood Mangroves Nature Reserve, Durban, South Africa. Botanica Marina, 37: 567-576.
Podzorski, A.C. 1985. An illustrated and annotated check-list of diatoms from the Black River waterways, St. Elisabeth, Jamaica. *Biblioteca Diatomologica*, 7: 1-177.
Rasmussen, K. A., I. F. MacIntyre and L. Prufert. 1993. Modern stromatolite reefs fringing a brackish coastline, Chetumal Bay, Belize. Geology 21: 199-202.
Reimer, C. W. 1996. Diatoms from some surface waters on Great Abaco Island in the Bahamas (Little Bahama Bank). Beiheft zu Nova Hedwigia, 112: 343-354.
Rejmánková, E. and J. Komárková. 2000. A function of cyanobacterial mats in phosphorus – limited tropical wetlands. Hydrobiologia, 431: 135-153.
Rodriguez, C. and A. W. Stoner. 1989. The epiphyte community of mangrove roots in a tropical estuary: distribution and biomass. Aquat. Bot. 36: 117-126.
Ross, M. S. et al. 2000. The Southeast Saline Everglades revisited: a half-century of coastal vegetation change. J. Veg. Sci., 11: 101-112.
Ross, M. S. et al. 2001. Multi-taxon analysis of the "white zone," a common ecotonal feature of South Florida coastal wetlands. In J. Porter and Porter, K. (eds) The Everglades, Florida Bay and Coral Reefs of the Florida Keys: An Ecosystem Sourcebook. CRC Press. Boca Raton. pp. 205-238.
Scholl, D. W., F. C. Craighead and M. Stuiver. 1969. Florida submergence curve revisited: Its relation to coastal sedimentation rates. Science, 163: 562-564.
Siqueiros-Beltrones, D. A. and E. S. Castrejón. 1999. Structure of benthic diatom assemblages from a mangrove environment in a Mexican subtropical lagoon. Biotropica, 31: 48-70.
Snoeijs, P. 1999. Diatoms and environmental change in brackish waters. In E. F. Stoermer and J. P. Smol (eds). The Diatoms: applications for the environmental and earth sciences. Cambridge Press. pp. 298-333.
Sullivan, M. J. 1981. Effects of canopy removal and nitrogen enrichment on *Distichlis spicata* – edaphic diatom complex. Estuarine, Coastal and Shelf Science, 13: 119-129.

Sullivan, M. J. 1982. Distribution of edaphic diatoms in a Mississippi salt marsh: A canonical correlation analysis. J. Phycol., 18: 130-133.
Sullivan, M. J. 1999. Applied diatom studies in estuaries and shallow coastal environments. In E. F. Stoermer and J. P. Smol (eds) The Diatoms: applications for the environmental and earth sciences. Cambridge Press. pp. 334-351.
Underwood, G. J. C. 2002. Adaptations of tropical marine microphytobenthic assemblages along a gradient of light and nutrient availability in Suva Lagoon, Fiji. European J. Phycol., 37: 449-462.
Vos, P. and de Wolf, H. 1993. Diatoms as a tool for reconstructing sedimentary environments in coastal wetlands; methodological aspects. Hydrobiol. 269/270: 297-296.
Wanless, H. R., R. W. Parkinson and L. P. Tedesco. 1994. Sea level control on stability of Everglades wetlands. In S. M. Davis and J. C. Ogden (eds) Everglades: The Ecosystem and Its Restoration. St. Lucie Press. Delray Beach, FL. pp. 199-223.

Appendix I. Number of occurrences, maximum relative abundances and weighted-averaging (WA) salinity optima and tolerances (ppt) of the 132 most common diatom taxa in the southeast Florida coastal wetland study area. Taxa are listed in order of estimated WA salinity optima.

Taxon	No. Occ.	Max. abund.	Salinity optimum	Salinity tolerance
Achnanthidium minutissimum (Kütz.) Czar.	8	0.29	1.80	0.20
Nitzschia nana Grun. in V. H.	11	0.14	1.83	0.72
Navicula subrostellata Hust.	5	0.07	1.84	0.21
Encyonopsis microcephala (Grun.) Kr.	18	0.43	1.84	0.85
Nitzschia amphibia f. *frauenfeldii* (Grun.) L Bert.	6	0.13	1.84	0.28
Pinnularia maior (Kütz.) Rab.	9	0.02	1.95	0.35
Encyonema carina L-Bert. & Kr.	5	0.04	1.96	0.23
Brachysira neoexilis L-Bert. (Typ2)	16	0.09	2.04	0.66
Nitzschia palea var. *debilis* (Kütz.) Grun. in Cl. & Grun.	23	0.18	2.06	1.24
Nitzschia amphibia Grun.	13	0.06	2.08	1.08
Nitzschia semirobusta L-Bert.	18	0.25	2.19	0.86
Navicula cryptotenella L-Bert.	17	0.32	2.25	1.84
Encyonema evergladianum Kr.	33	0.57	2.25	1.51
Encyonema neomesianum Kr.	14	0.20	2.26	1.09
Encyonema silesiacum (Bl.) Mann	13	0.07	2.32	1.47
Diploneis ovalis (Hilse in Rab.) Cl.	28	0.10	2.39	1.44
Gomphonema intricatum var. *vibrio* (Ehr.) Cl.	5	0.01	2.44	1.44
Mastogloia smithii Thw. *ex* Sm.	38	0.65	2.44	1.53
Diploneis vacilans (Schm.) Cl.	5	0.05	2.62	1.78
Brachysira neoexilis L-Bert. (Typ1)	9	0.04	2.69	1.77
Navicula veneta Kütz.	18	0.09	2.89	2.36
Brachysira neoexilis L-Bert. (Typ3)	7	0.06	2.92	1.52
Navicella pusilla Kr.	29	0.39	3.00	1.88
Nitzschia palea (Kütz.) Sm.	14	0.04	3.11	2.31
Caponea caribbea Podz.	14	0.02	3.40	2.47
Fragilaria synegrotesca L-Bert.	29	0.16	3.41	2.68
Rhopalodia operculata (Ag.) Håkansson	6	0.21	3.66	2.24
Rhopalodia gibba (Ehr.) Müller	9	0.04	3.68	2.89
Nitzschia bergii Cl.-Eul.	4	0.11	3.72	2.23
Amphora sulcata A. Schm.	20	0.57	3.87	2.61
Nitzschia intermedia Hantzsch *ex* Cl. & Grun.	4	0.02	3.89	2.30
Nitzshia dissipata (Kütz.) Grun.	8	0.05	3.94	3.00
Selaphora stroemii (Hust.) Mann	5	0.01	4.15	3.17
Mastogloia smithii var. lacustris Grun.	13	0.02	4.20	2.75
Diploneis litoralis (Donkin) Cl.	9	0.03	4.36	3.06
Diploneis oblongella (Naeg.) Cl.-Eul.	39	0.35	4.58	2.90
Diploneis parma Cl.	14	0.02	5.22	3.53
Nitzschia sigmoidea (Nitzsch) Sm.	5	0.01	5.34	3.23
Nitzschia serpentiraphe L-Bert.	4	0.07	5.89	2.83
Navicula erifuga L-Bert.	16	0.02	5.98	3.85

Kolbesia amoena (Hust.) Kingston	10	0.04	6.14	3.61
Gomphonema vibrioides Reich. & L-Bert.	8	0.01	6.31	3.68
Navicula podzorski L-Bert.	11	0.06	6.46	3.49
Rhopalodia musculus (Kütz.) Müller	5	0.03	7.07	2.89
Nitzschia gracilis Hantzsch	14	0.03	7.20	3.66
Caloneis sp. 02L31E	4	0.02	7.31	3.04
Navicula sp. 03L31E	23	0.34	8.17	3.03
Fragilaria fasciculata (Ag.) L-Bert.	18	0.27	8.85	3.98
Nitzschia graciliformis L-Bert. & Simonsen	5	0.01	9.15	4.41
Seminavis strigosa (Hust.) Danielidis & Economou-Amilli	14	0.17	9.45	4.15
Fragilaria capensis Grun.	4	0.02	10.37	2.25
Mastogloia braunii Grun.	15	0.05	10.55	3.60
Fragilaria femelica (Kütz.) L-Bert.	31	0.36	11.60	2.51
Amphora sp. 22L31E	8	0.10	11.79	1.57
Nitzschia microcephala Grun. in Cl. & Möller	27	0.05	11.97	3.20
Navicula tenelloides Hust.	12	0.07	12.41	3.27
Nitzschia sigma (Kütz.) Sm.	4	0.09	12.74	2.85
Navicula cryptocephala Kütz.	5	0.05	13.07	3.92
Rhopalodia gibberula (Ehr.) Müller	25	0.69	13.09	3.88
Nitzschia scallpeliformis (Grun.) Grun. in Cl. & Grun.	4	0.09	13.13	3.79
Amphora subacutiuscula Sch.	23	0.30	13.26	2.44
Brachysira aponina Kütz.	12	0.11	13.54	3.78
Amphora cymbifera Greg.	7	0.03	13.73	2.00
Mastogloia halophila John	20	0.27	13.89	2.80
Cyclotella meneghiniana Kütz.	12	0.10	14.38	3.88
Proszkinia bulnheimii Grun. Karayeva	4	0.08	14.43	1.47
Nitzschia frustulum (Kütz.) Grun.	12	0.16	14.44	3.82
Amphora eulensteinii Grun.	9	0.05	14.60	2.16
Amphora coffeaeformis Kütz.	15	0.18	14.61	2.02
Entomoneis sp.02L31E	11	0.01	14.69	1.92
Denticula subtilis Grun.	20	0.21	15.18	3.03
Grammatophora oceanica (Ehr.) Grun.	6	0.01	15.30	1.61
Amphora acutiuscula Kütz.	10	0.04	15.31	1.31
Amphora coffeaeformis var. *borealis* (Kütz.) Cl.	4	0.01	15.51	1.40
Amphora coffeaeformis var. *aponina* (Kütz.) Arch. & Sch.	27	0.36	15.55	1.98
Mastogloia reimeri John	11	0.06	15.69	2.96
Cocconeis placentula var. *lineata* (Ehr.) V. H.	9	0.16	15.75	1.77
Bacillaria paradoxa Gmelin	8	0.06	16.02	0.70
Mastogloia erythraea var. *grunowii* Foged	7	0.02	16.06	0.88
Planothidium rostratum (Østrup) Round & Bukhtiyarova	4	0.05	16.34	3.07
Cocconeis scutellum var. *ornata* Grun.	6	0.04	16.48	0.39
Amphora normani Hust.	9	0.09	16.54	0.94
Rhopalodia constricta (Sm.) Kr.	8	0.03	16.59	1.24
Rhopalodia acuminata Kr.	22	0.49	16.60	2.11
Cocconeis placentula Ehr.	10	0.24	16.84	0.96
Mastogloia recta var. *pumila* Hust.	4	0.04	16.85	0.54

Melosira sp. 01L31E	10	0.02	17.02	2.69
Navicula recens L-Bert.	8	0.05	17.02	2.50
Mastogloia angusta Hust.	17	0.17	17.06	2.38
Cocconeis scutellum Ehr.	4	0.13	17.12	0.55
Mastogloia ovalis Schm.	6	0.06	17.24	0.26
Achnanthes nitidiformis L- Bert.	5	0.02	17.28	0.51
Amphora sp. 02L31E	8	0.04	17.30	0.57
Hyalosynedra leavigata (Grun.) Will. & Round	16	0.41	17.31	1.48
Cyclotella distinguenda Hust.	22	0.21	17.38	1.12
Mastogloia braunii f. *minuta* Voigt	10	0.02	17.45	2.41
Licmophora normaniana (Grev.) Wahrer	11	0.03	17.50	0.80
Mastogloia crucicula (Grun) Cl.	5	0.05	17.57	0.54
Rhabdonema adriaticum Kütz.	5	0.21	17.57	0.68
Navicula palestinae (Gerloff)	17	0.37	17.61	1.70
Seminavis sp. 02L31E	4	0.00	17.62	1.22
Mastogloia pumila (Grun.) Cl.	4	0.01	17.67	0.99
Amphora sp. 39L31E	9	0.03	17.74	0.80
Cocconeis placentula var. *euglipta* (Ehr.) Grun.	5	0.08	17.90	0.91
Mastogloia pusilla Grun.	6	0.03	18.23	0.81
Mastogloia sp. 04L31E	5	0.08	18.29	0.88
Diploneis gruendleri (Schm.) Cl.	6	0.02	18.33	0.73
Tryblionella granulata (Grun. in Cl. & Möller) Mann	6	0.05	18.38	0.92
Mastogloia biocellata Navarino & Muftah	7	0.01	18.40	1.27
Mastogloia erythraea Grun.	12	0.06	18.43	2.22
Amphora costata W. Sm.	6	0.13	18.45	0.84
Navicula sp. 01L31E	4	0.11	18.59	0.76
Tryblionella coarctata (Grun. in Cl. & Grun.) Mann	4	0.00	18.66	0.90
Seminavis gracilenta (Grun. ex Schm.) Mann	12	0.02	18.72	1.12
Grammatophora macilenta Sm.	4	0.00	18.74	1.16
Navicula cincta (Ehr.) Ralfs in Pritchard	5	0.07	18.86	0.75
Mastogloia cyclops Voigt	9	0.03	18.93	0.86
Diploneis caffra Giffen	14	0.21	19.07	0.98
Amphora ostrearia var. *lineata* (Bréb. *ex* Kütz.) Cl.	8	0.14	19.11	0.76
Navicula tripunctata (Müller) Bory	5	0.01	19.12	1.21
Amphora veneta Kütz.	4	0.13	19.16	1.04
Planothidium lanceolatum (Bréb.) Round & Bukhtiyarova	4	0.07	19.28	1.08
Melosira nummuloides (Dillwyn) Ag.	4	0.09	19.32	1.29
Nitzschia vitrea Norman	9	0.03	19.38	1.85
Seminavis robusta Danielidis & Mann	12	0.01	19.67	1.01
Navicula pseudocrassirostris (Hust.)	8	0.03	19.73	1.33
Mastogloia nabulosa Voigt	10	0.09	20.00	0.92
Fragilaria tenera (Sm.) L-Bert.	8	0.04	20.25	1.39
Caloneis sp. 01L31E	4	0.00	20.52	1.06
Tryblionella debilis Arnott	7	0.07	20.86	1.33
Mastogloia elegans Levis	13	0.09	20.99	1.03
Amphora sp. 24L31E	6	0.02	21.38	0.66

LIST OF FIGURES

Figure 1. Location of study area in southeast Florida, USA. A) Aerial photograph from 1940 showing recently established east-west canals, north-south drainage ditches and remnant tidal creeks. B) Aerial photograph from 1990 showing additional canals built since 1940, including the L-31E canal, the disappearance of tidal creeks and the distribution of collecting sites among the 13 wetland sub-basins.

Figure 2. Observed distribution of the five major vegetation types within the study area (A) and distribution of vegetation types predicted from diatom community composition (B) and non-diatom algal community composition (C) using weighted-averaging regression. Insets are plots of observed versus inferred vegetation type based on diatom and soft-algae optima and tolerances (R^2 = 0.69, 0.42 and RMSE = 0.77 and 1.2, for diatoms and algae, respectively). Plant species significantly associated with each community type were (1) Freshwater Swamp Forest: *Casuarina equisetifolia* (Australian pine), *Conocarpus erectus* (buttonwood), *Schinus terebinthifolius* (Brazilian pepper), (2) Freshwater marsh: *Cladium jamaicense* (sawgrass), *Juncus rhomerianus* (black rush), *Typha domingensis* (cattail), (3) Dwarf mangrove forest: *Laguncularia racemosa* (white mangrove), *Rhizophora mangle* (red mangrove), (4) Transitional forest: *Avicennia germinans* (black mangrove), (5) Fringing mangrove forest: *Rhizophora mangle, Laguncularia racemosa*, *Avicennia germinans.*

Figure 3. Observed distribution of porewater salinity within the study area (A) and distribution of salinity predicted from diatom community composition (B) and non-diatom algal community composition (C) using weighted-averaging regression. Insets are plots of observed versus inferred salinity based on diatom and soft-algae optima and tolerances (R^2 = 0.91, 0.58 and RMSE = 0.14, 0.34 for diatoms and soft-algae, respectively).

Figure 4. Distribution of (A) vegetation canopy height, (B) soil depth, (C) periphyton ash-free dry mass (AFDM), and (D) periphyton tissue total phosphorus concentration within the study area.

Figure 5. Digital photographs of diatom taxa that were significantly associated with each vegetation community type. From the freshwater forest, (1) *Mastogloia smithii* (a = midvalve focus showing internal partectae and b = surface of valve), (2) *Nitzschia semirobusta*, (3) *Nitzschia amphibia* f. *frauenfeldii*, (4) *Nitzschia amphibia*, (5) *Fragilaria synegrotesca*, (6) *Nitzschia nana*; from the freshwater marsh (7) *Encyonema evergladianum*, (8) *Brachysira neoexilis* (Typ 3), (9) *Brachysira neoexilis* (Typ 2), (10) *Nitzschia palea* var. *debilis*, (11) *Navicula podzorski*; from the dwarf mangrove forest, (12) *Navicula palestinae*, (13) *Mastogloia* reimeri (a = surface of valve and b = midvalve focus showing internal partectae); and from the transitional mangrove forest, (14) *Mastogloia angusta*, (15) *Tryblionella granulata*, (16) *Amphora* cf. *fontinalis*, (17) *Amphora coffeaeformis* var. *aponina*, (18) *Amphora costata*, (19) Rhopalodia acuminata, and (20) *Rhopalodia* gibberula. Scale bar = 10µm; magnification: Figs 1 – 15, 17, 19, 20 (x 1008), Fig. 16 (x 1600), Fig. 18 (x 1250).

Figure 6. Digital photographs of diatoms taxa that were significantly associated with the fringing mangrove forest: (1) *Amphora subacutiuscula*, (2) *Cocconeis placentula*, (3) *Cocconeis*

placentula var. *lineata*, (4) *Cocconeis placentula* var. *euglipta*, (5) *Cocconeis scutellum*, (6) *Cyclotella distinguenda*, (7) *Mastogloia ovalis*, (8) *Mastogloia crucicula* (a = surface of valve and b = mid-valve focus showing internal partectae), (9) *Mastogloia pusilla* (a = surface of valve and b = mid-valve focus showing internal partectae), (10) *Mastogloia nabulosa* (a = surface of valve and b = mid-valve focus showing internal partectae), (11) *Mastogloia erythraea* (a = surface of valve and b = mid-valve focus showing internal partectae), (12) *Diploneis caffra*, (13) *Denticula subtilis*, (14) *Rabdonema adriaticum*, and (15) *Hyalosynedra leavigata*. Scale bar = 10μm; magnification x 1008.

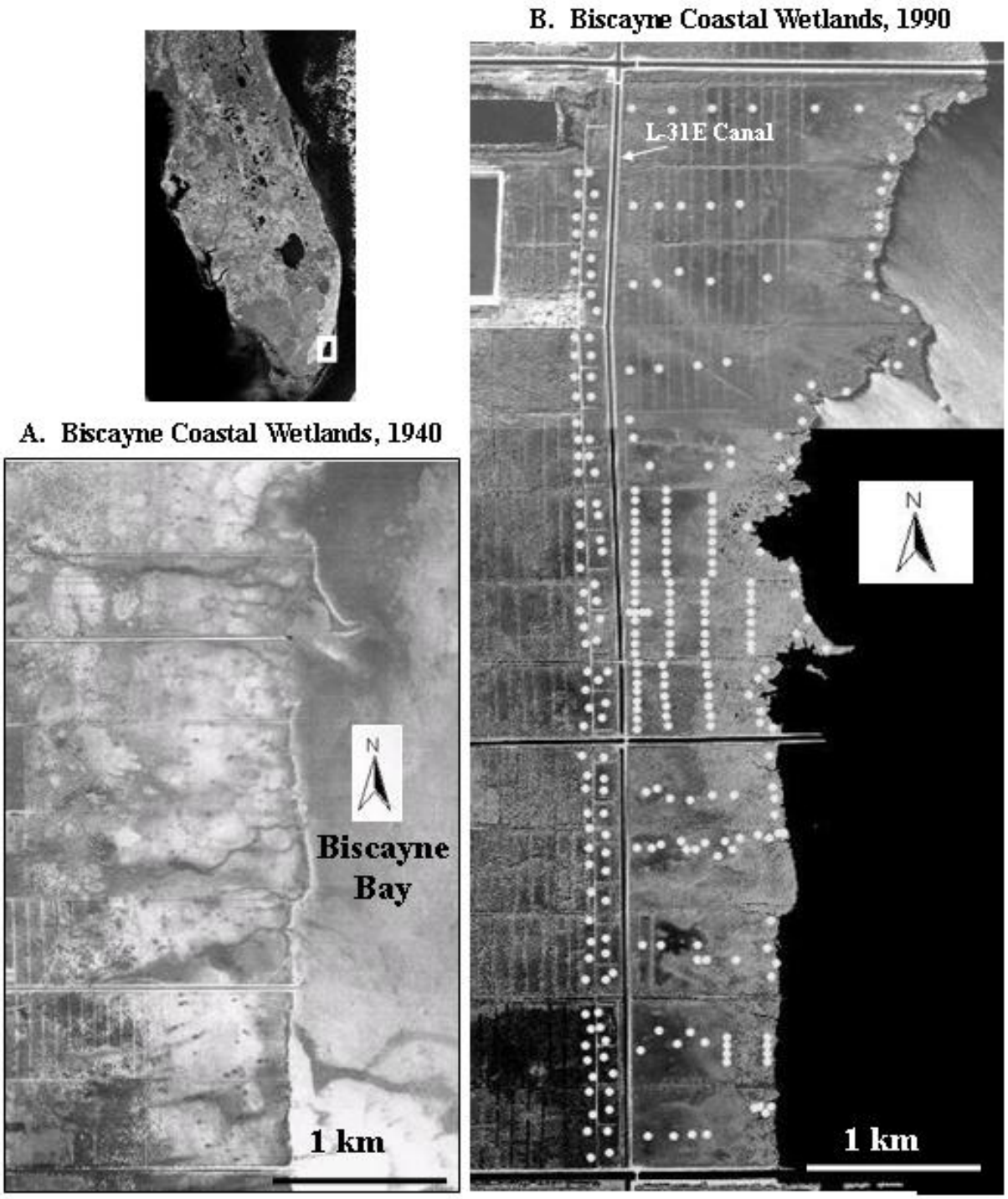
B. Biscayne Coastal Wetlands, 1990
L-31E Canal
N
1 km
A. Biscayne Coastal Wetlands, 1940
N
Biscayne
Bay
1 km

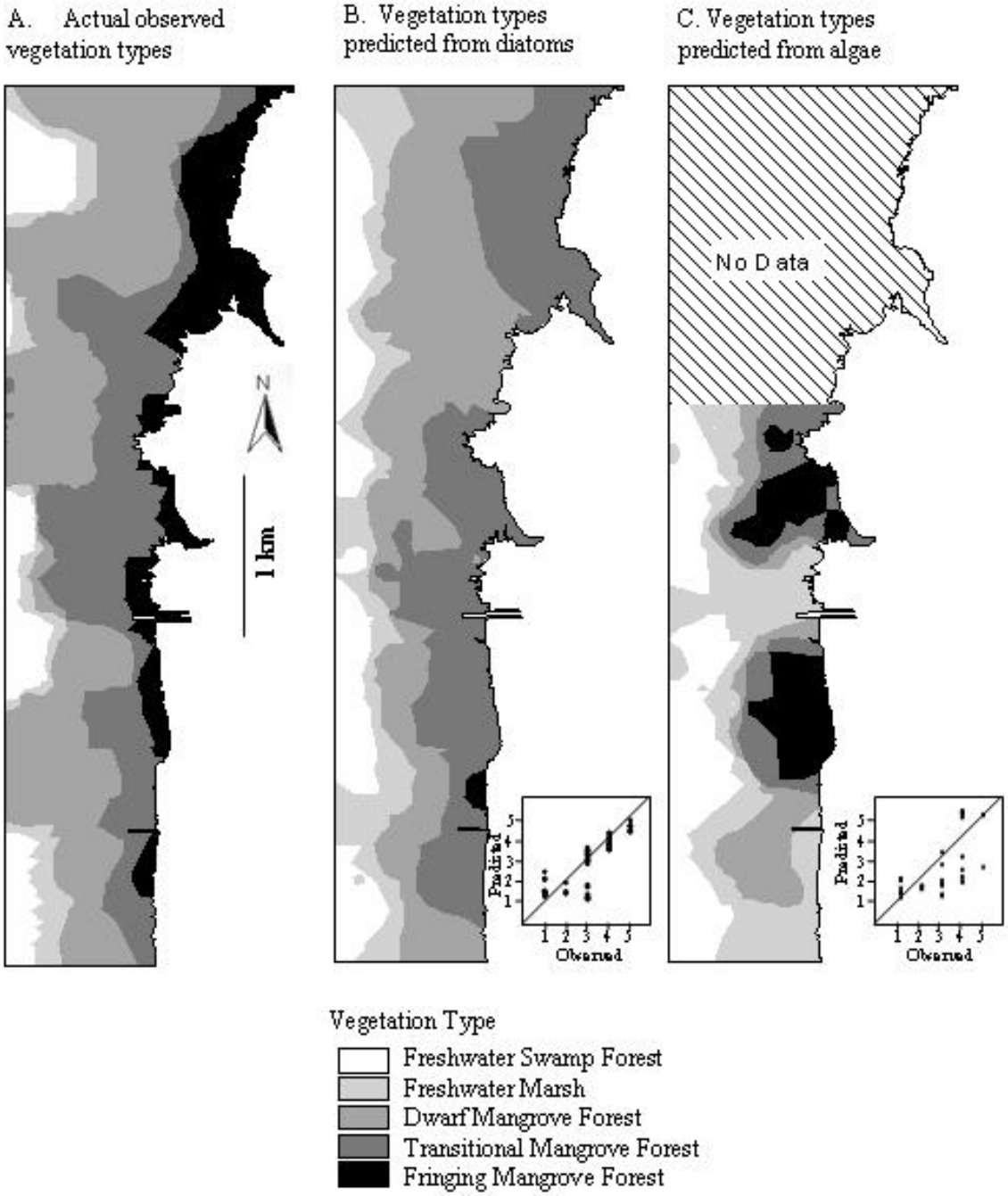
A. Actual observed vegetation types
B. Vegetation types predicted from diatoms
C. Vegetation types predicted from algae
N
1 km
No Data
Predicted
Observed
1 2 3 4 5
Vegetation Type
Freshwater Swamp Forest
Freshwater Marsh
Dwarf Mangrove Forest
Transitional Mangrove Forest
Fringing Mangrove Forest

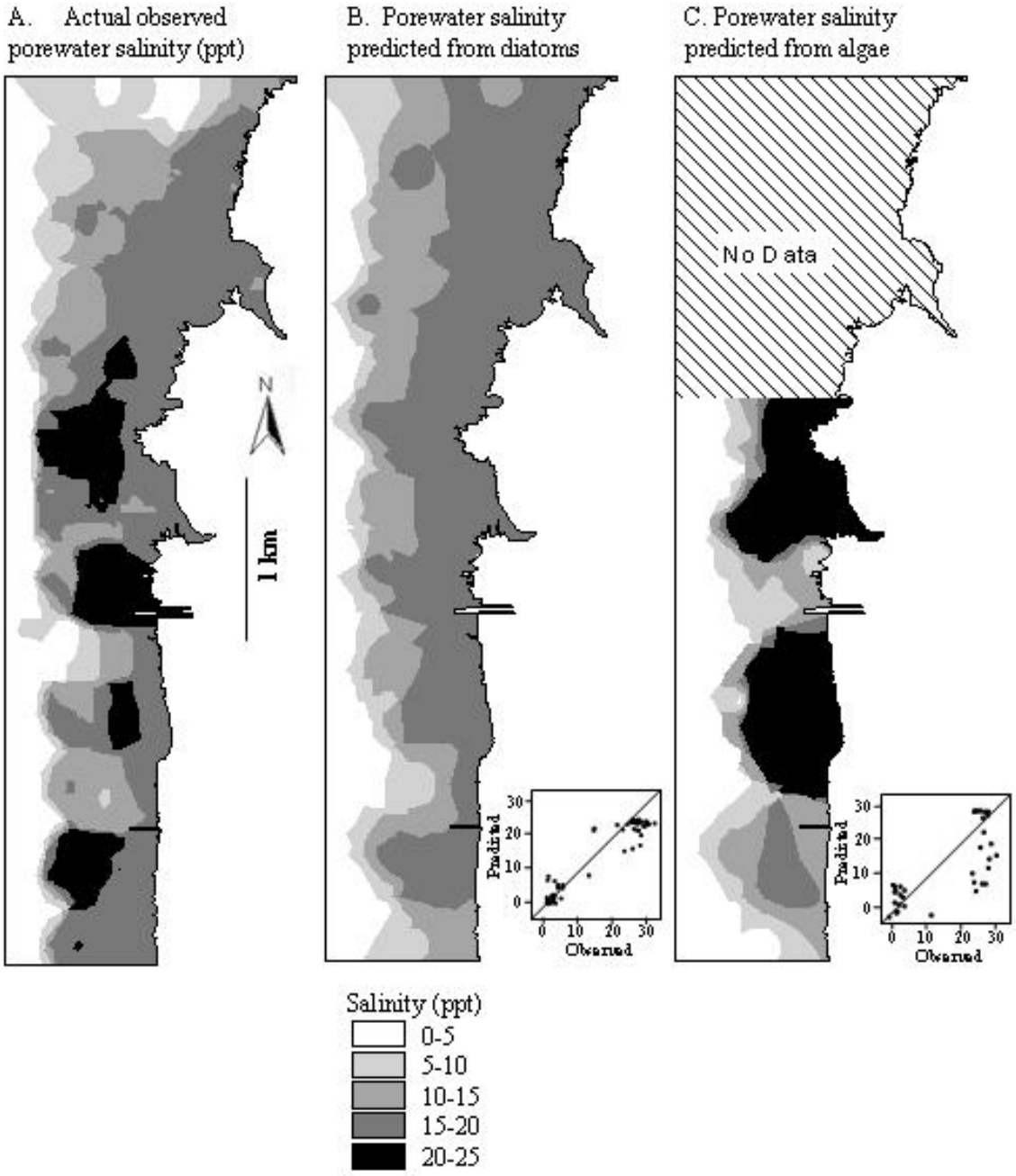
A. Actual observed porewater salinity (ppt)
B. Porewater salinity predicted from diatoms
C. Porewater salinity predicted from algae
No Data
N
1 km
Predicted
Observed
0
10
20
30
Salinity (ppt)
0-5
5-10
10-15
15-20
20-25

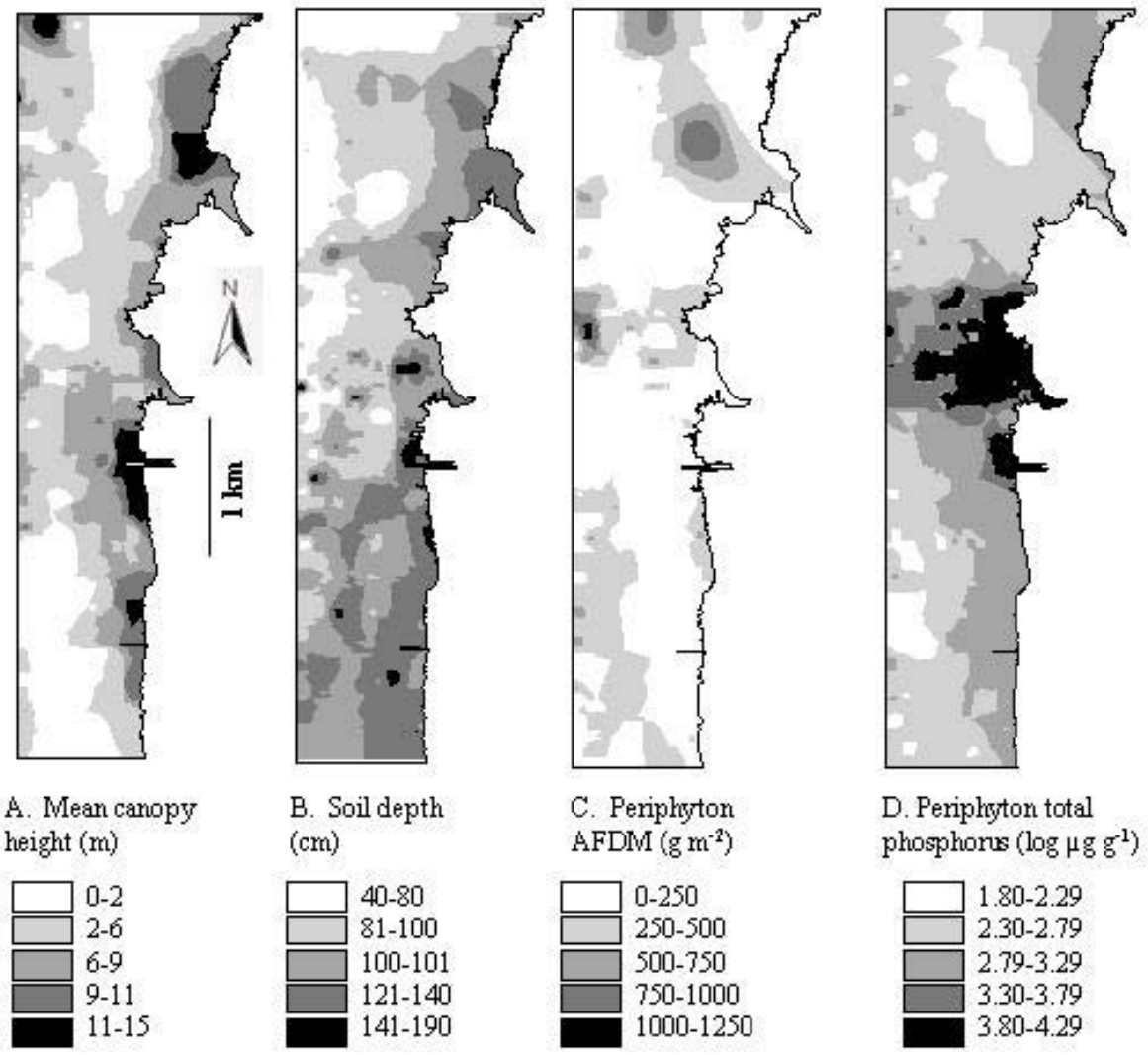
N
1 km
A. Mean canopy height (m)
0-2
2-6
6-9
9-11
11-15
B. Soil depth (cm)
40-80
81-100
100-101
121-140
141-190
C. Periphyton AFDM (g m-2)
0-250
250-500
500-750
750-1000
1000-1250
D. Periphyton total phosphorus (log µg g-1)
1.80-2.29
2.30-2.79
2.79-3.29
3.30-3.79
3.80-4.29

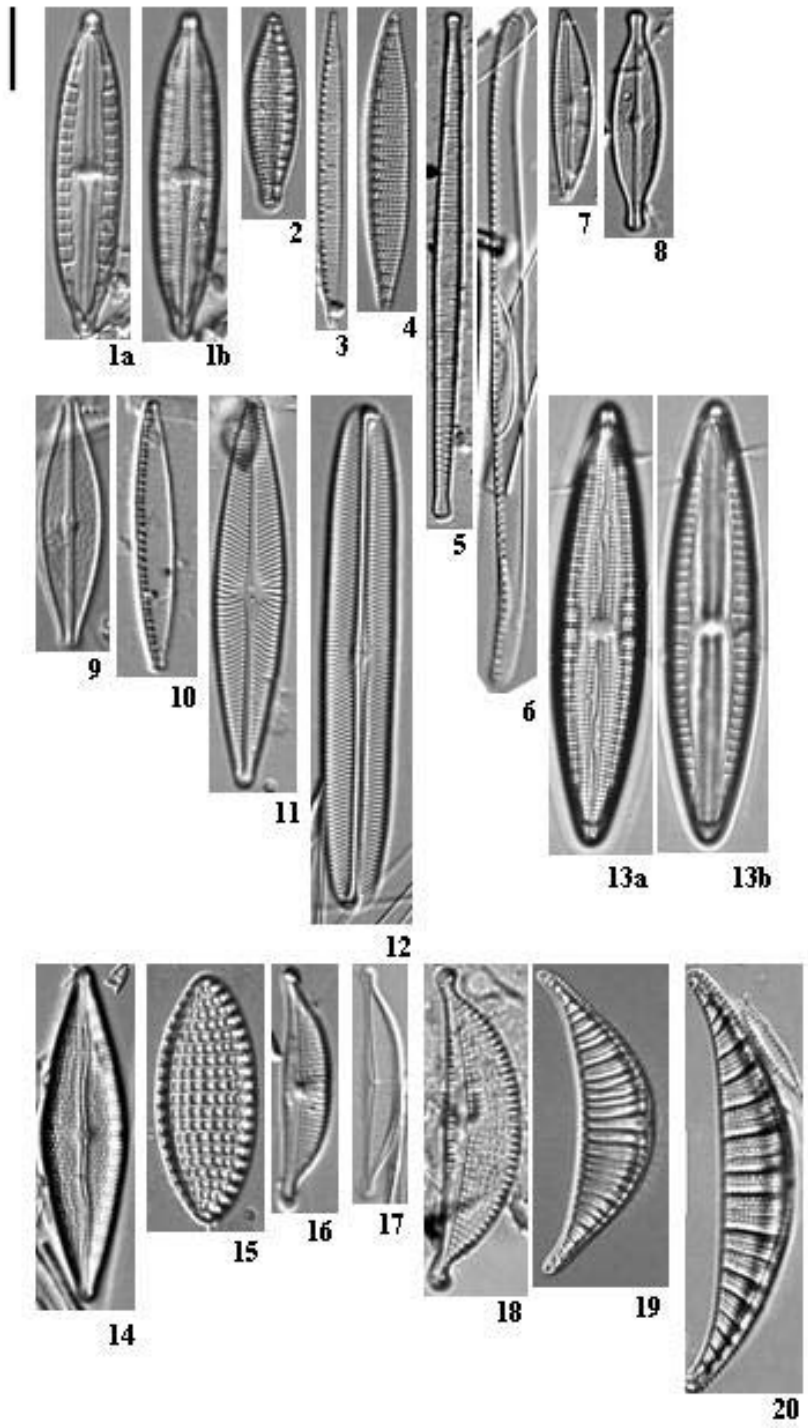
1a
1b
2
3
4
5
6
7
8
9
10
11
12
13a
13b
14
15
16
17
18
19
20

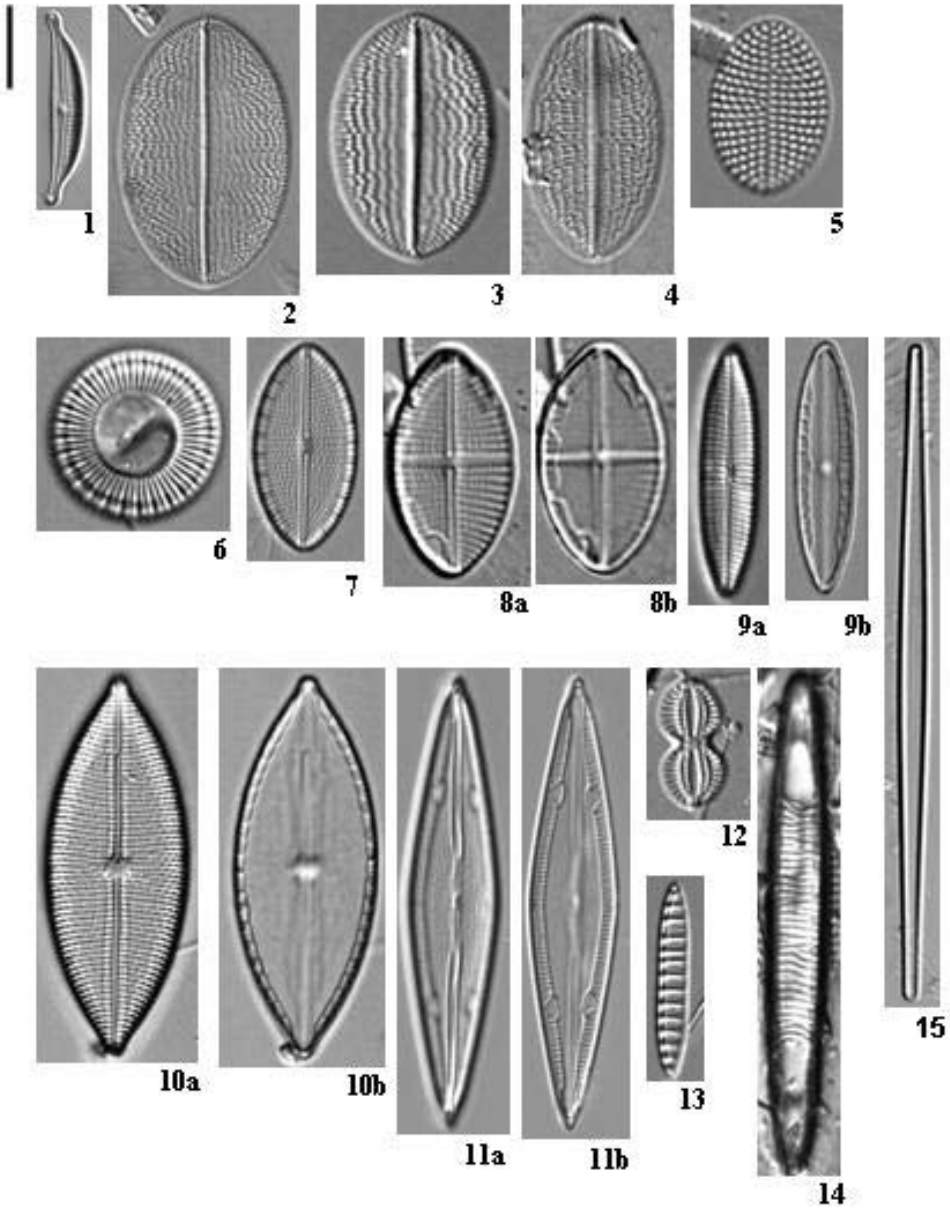
1
2
3
4
5
6
7
8a
8b
9a
9b
10a
10b
11a
11b
12
13
14
15

V. RESULTS COMPLETED – C. PALEOECOLOGY

Gaiser, E. E., A. Zafiris, P. L. Ruiz, F. A. C. Tobias and M. S. Ross. Submitted. Tracking rates of ecotone migration due to salt-water encroachment using fossil mollusks in coastal south Florida. Hydrobiologia.

ABSTRACT

A combination of sea-level rise and diversion of natural tidal drainages has caused rapid salt-water encroachment into South Florida's coastal wetlands. We determined the rate of migration of coastal vegetation zones in response to salt-water encroachment through paleoecological analysis of mollusks in 36 sediment cores taken along transects perpendicular to the coast in a 5.5 km^2 band of coastal wetlands in southeast Florida. Transects intersected ecotones between distinct vegetation zones including, from interior to the coast, freshwater swamp forest, freshwater marsh and dwarf, transitional and fringing mangrove forest. Vegetation composition, soil depth and organic content, porewater salinity and the contemporary mollusk community were sampled from 226 sites to determine vegetation type and salinity preferences for the regional mollusk fauna. Resulting calibration models allowed accurate mollusk-based inference of salinity and vegetation type type from fossil assemblages (0.79 and 0.67, respectively) in chronologically calibrated (^{210}Pb and ^{14}C) sediments. Most sediments were shallow (20-130 cm) and permitted inferences on a coarse temporal scale for three zones; an upper peat layer (zone 1) representing the last 30-70 years, an mixed peat-marl gytta (zone 2) representing the previous ca. 150-250 years and a basal section (zone 3) of Holocene marl deposits with basal dates ranging from 310 to 2990 YBP. Modern peat accretion rates averaged 3.1 mm yr^{-1} while subsurface marl accreted more slowly at 0.08 mm yr^{-1}. Mollusk-inferred pore-water salinity and vegetation type types for zone 1 show a steep gradient with freshwater communities being confined west of a north-south drainage canal constructed in 1960. In contrast, inferences for zone 2 (pre-drainage) suggest that freshwater marshes and associated forest units covered 90 % of the area, with mangrove forests only present along the peripheral coastline. During the entire pre-drainage history, salinity in the entire area was maintained below a mean of 2 ppt and only small pockets of mangrove vegetation type existed to the interior of the shoreline, while the current salinity averages 13.2 ppt and mangroves occupy 95% of the wetland. Over 3 km^2 of freshwater wetland vegetation type have been lost from this basin due to lateral salt-water encroachment rates, calculated from the mollusk-inferred interior migration rate of freshwater vegetation type, of 3.1 m yr^{-1} for the last 70 years (compared to 0.14 m yr^{-1} for the pre-drainage period). This rapid rate of encroachment is facilitated by sea-level rise and freshwater diversion; plans for rehydrating these basins with freshwater will require high-magnitude re-diversion to counteract locally high rates of sea-level rise and a long-term perspective to restoration.

Keywords: Mangroves, sea-level rise, salt-water encroachment, paleoecology, mollusks, Everglades, wetlands

INTRODUCTION

Coastal wetland ecosystems are being reduced in breadth at alarming rates due to losses on their marine margins resulting from sea-level rise and on their interior extent by urban or agricultural expansion (IPCC 1998). Sea level has risen 10 to 25 centimeters in the past 100 years, and it is predicted to rise another 50 centimeters over the next century (Church et al. 2001), linked with the increase in global atmospheric temperature. An estimate by Nicholls et al. (1999) suggests that at this rate sea-level rise could cause the loss of as much as 22% of the world's coastal wetlands by the end of the 21 century. Manipulation of the landscape, particularly of the path of water flow through coastal estuaries, by industrialization and urban expansion of coastal areas has further reduced the extent of natural coastal wetland vegetation type (National Research Council 1993; Park et al. 1989).

Of the many examples of coastal wetland losses due to these two factors, one of the most striking is the wetlands along Florida's Altantic coast, where the rate of sea-level rise is more than double the global average (2-4 mm yr^{-1}, Leatherman et al. 2000) and routes of water flow through adjoining Everglades wetlands have been engineered to an extent that facilitates unprecedented rates of urban expansion. The effects of the latter on coastal wetlands exceed the former, as freshwater draining to the coast has been channelized into a vast network of canals, constructed during the last century to expand agriculture and urban development. Along the southeast Florida coastline, channelization has resulted in the loss of most of the myriad of natural east-west draining creeks that meandered from the Everglades to the coast, hydrating coastal wetlands with freshwater (Meeder et al. 2000). Now, this water is channelized into point-source discharges at the mouths of canals, causing a redistribution of salinity in adjacent Biscayne Bay, being low near the canal outlets (in the wet season when water flood control structures are open) and much higher in interior coastal wetlands (Boyer et al. 1999; Ross et al. 2000).

Salt-water encroachment along the Southeast Florida coast threatens the once extensive estuarine wetland system along the edge of the Atlantic coastline. In the 1940's, prior to the construction of the majority of drainage canals in the southern Everglades, Egler (1952) conducted a vegetation survey in these wetlands that he called the "Southeast Saline Everglades." He was able to distinguish distinct vegetation zones lying in bands parallel to the coast, driven by gradients of salinity, water availability, nutrients and susceptibility to drought, periodic freeze events and fire. He identified a coastward sequence of gramminoid freshwater wetlands (to the interior), followed by dwarf mangrove scrub swamps in intertidal areas bounded by fringing mangrove forest on the coast. Ross et al. (2000) repeated Egler's vegetation survey a half-century later and supplemented interpretations of the magnitude of vegetation change by comparing modern aerial photographs of the area to archived photos available from 1938 and 1940. During the intervening period between these two studies, an extensive network of drainage canals had been constructed to connect the southeast saline Everglades to the larger South Dade Conveyance system to the sea. Completed in the late 1960's, this project allowed more effective drainage of the agricultural and urban lands abutting the coastline. In conjunction with roads and agricultural ditches, operation of the canal system altered fresh water delivery to these wetlands, starving some areas of water while augmenting the supply to others. By the turn of the 21st century, the wetland bands had been diminished to the periphery of the coastline:

freshwater gramminoid marshes had been largely displaced by an enroaching mangrove scrub community and most tidal creeks had disappeared (Ross et al. 2000).

In a related study, Ross et al. (2001) determined the distribution patterns of vegetation, epifauna and periphyton (existing here as benthic mats of primarily cyanobacteria, bacteria and diatoms) along a 4 km transect that ran perpendicular to the coast. The interior-most point along the transect was stationed adjacent to a north-south canal that runs parallel to the coastline and prevents coastward movement of freshwater. Marshes to the west of the canal were dominated by communities typical of Everglades prairies, including sawgrass (*Cladium jamaicense* Crantz) and spikerush (*Eleocharis cellulosa* Torr.). Immediately east of the canal these communities were replaced by a salt-tolerant gramminoid community dominated by *Juncus romoerianus* Scheele and *Distichilis spicata* (L.), which was replaced coastward by a broad zone of very low productivity by sparse dwarf red mangrove (*Rhizophora mangle* L.) and thick benthic periphyton mats. Finally, the coastline was fringed with productive, tall-stature mangroves (including *R. mangle*, *Avicennia germinans* (L.), *Laguncularia racemosa* Gatern. and *Conocarpus erecta* L.). The zone of low productivity sandwiched between the gramminoid marsh and fringing mangroves reflects white on areal photographs and, through comparison with 1940 aerial photographs, this "white zone" has moved interior-ward by 1.5 km, effectively shrinking the freshwater and mixed salt-tolerant graminoid marsh to the interior (Ross et al. 2000).

Ross et al. (2001) also found the distribution of diatoms in periphyton mats and mollusks to be highly correlated with distance from the coastline. A unique community of each existed in the freshwater graminoid marsh, the salt-tolerant graminoid marsh, white zone and fringing forest. Salinity preferences were determined for 154 diatom and 17 mollusk taxa for future monitoring efforts and paleoecological studies (Gaiser et al. 2004). However, diatoms were found to be poorly preserved in subsurface coastal sediments while mollusks were well preserved and abundant in sediments (Ross et al. 2001).

Evidence of rapid rates of salt-water encroachment documented for this region, and the effects on shifting community composition of coastal wetlands has provided a foundation of support for allocation of state and federal funding toward restoration of coastal wetlands, as part of the Comprehensive Everglades Ecosystem Restoration Program (the largest restoration program ever undertaken by the U.S. Federal Government). Restoration largely depends on the magnitude of freshwater that can be re-diverted back into the coastal wetlands, although re-diversion may have diminishing impact as it is counteracted by the opposing effects of sea-level rise. It is, therefore, imperative to understand the magnitude of influence of freshwater diversion on salt-water encroachment in the context of that caused by sea-level rise. Our approach in this study, is thus to determine rates at which ecotones have shifted along the South Florida coastline since channelization efforts began in the early 1900's in contrast to pre-development rates during the ~2000 year history of this wetland basin. We used a paleoecological approach, focusing on mollusks as our major paleoenvironmental proxy, as they have been shown to be excellent indicators of environmental change in coastal ecosystems (Ross et al. 2001; Brewster-Wingard et al. 2001). Specifically, our goals were to (1) determine the current composition mollusk communities in the BBCW and their relationship to coastal zones defined by vegetation community composition, salinity and soil character, (2) interpret the location of these zones

using fossil mollusk communities to determine rates of ecotonal migration due to the combined forces of sea-level rise and freshwater diversion.

METHODS

Study Site

The present study focuses on an area of remnant coastal wetlands in the southeast saline Everglades, parts of which are protected in Biscayne National Park, called the Biscayne Bay Coastal Wetlands (BBCW, Fig. 1). The ~7 km long study area is bounded to the north and south by major east-west drainage canals (Princeton and Mowry, respectively) and bisected north-south by a secondary canal (L-31E). The region is dissected by many smaller east-west ditches which compartmentalize the area longitudinally into 13 hydrologically distinct wetland basins, that range in width from about 0.5 to 2 km. To the west of the L-31E canal, freshwater marshes are now hydrologically isolated from the coast and bounded to the west by agricultural lands, the periphery of which are heavily invaded by exotic trees including *Schinus terebinthifolius* (Brazilian Peppertree) and *Casuarina equisetifolia* (Australian Pine). To the east of the L-31E canal, mangrove communities predominate, with strands of forest vegetation now occupying the remnant tidal creek beds. Though each sub-basin contains a gradation of freshwater to marine communities from the interior to the coast, the distinctiveness of the zones, the abruptness and location of the ecotonal boundaries and their specific composition vary somewhat within the sub-basins.

Modern Survey

To determine the current distribution of mollusks relative to existing patterns of vegetation, soils and salinity in the BBCW, we used a stratified-random design to select study sites within each of the 13 sub-basins (numbered consecutively from south to north). Using aerial photos of the area, each sub-basin was divided into 4-6 units, including, to west of the L-31E canal, a freshwater swamp forest dominated by exotics that have invaded abandoned agricultural land and remnant freshwater gramminoid marsh, and, to the east of the L-31E canal, mangrove forests that can be characterized by canopy height and cover as dwarf, transitional and fringing (along the coastline). Occasionally a sub-basin did not include one or more of these components or another community type was present, in which case the sub-basins were divided accordingly such that each unit was equally represented in sampling. Within each unit a north-south transect was randomly located, and 1-5 sampling stations were evenly distributed along its length. A total of 226 stations were sampled within the 5.5 km^2 area (Fig. 2a) with each site being visited once in the dry season from February to June 2002 and 2003.

A nested design was used to describe vegetation within a 10 x 10 meter plot at each sampling point. The sampling procedure was as follows. Upon reaching each point, a 10-meter N-S transect was established. For trees (stems >2 meters height), we recorded the species and diameter class (5-cm DBH ranges) of all live and dead individuals within one meter of the line (stems <10 cm DBH), two meters of the line (stems 10-25 cm DBH), and five meters of the line (>25 cm DBH). We recorded the species and diameter class of all dead fallen stems (> 5 cm DBH) whose trunk intersected the line. We estimated live cover by species in a 4- meter-wide

band enclosing the center line, using the following cover classes: 1, 0-1%; 2, 1-4%; 3, 4-16%; 4, 16-33%; 5, 33-66%; and 6, >66%. Finally, we recorded the upper and lower height of each species that intercepted or was within 1 meter of a vertical height pole positioned at three locations along the centerline, i.e., 0, 5, and 10 meters from the origin. For shrubs (woody stems between 60 cm and 2 meters in height), we recorded the density of all stems in five 1-m^2 plots established at five locations along the center line, i.e., west of the line, at 0, 2, 4, 6, and 8 meters from the origin. Stems were counted by species in two size categories: small shrubs (60-100 cm tall) and large shrubs (1-2 m tall). For seedlings (woody stems 0-60 cm in height), we recorded the density of all stems in a 3 x 3 dm subplot in the southeast corner of the 1 m^2 plot described above. Stems were counted by species in two size categories: small seedlings (0-30 cm tall) and large seedlings (30-60 cm tall). For all plants < 2 meters height (herbs, seedlings, shrubs), we estimated cover in the 1 m^2 plots described above, using the same cover classes as described above for tree cover.

Within each site, we measured depth of sediments to limestone bedrock with a probe-rod and then used a soil auger to extract sediments to measure and describe depths of compositional and textural transitions (i.e., depth of peat was defined for each core). The color transition and composition of the sediments were described using a Munsell soil index. At each site a portable meter was used to measure conductivity in pore water that collected in the hole created by the sediment sampling. Conductivity ($\mu S\ cm^{-1}$) was later converted to salinity (ppt) using a model from a previous study in a nearby basin where both variables were directly measured (Ross et al., 2001).

From each site, five small sections of benthic periphyton and litter (3.8 cm^2, 1-2 cm thick) were collected using aluminum cores and then combined to form a single sample to determine the distribution of the modern mollusk community. In the laboratory, each sample was gently rinsed with water through a 500 μm sieve and intact mollusks were collected. The mollusks were dried at 80°C for ~3-5 days and then counted and identified to the species level using standard and local literature (Thompson, 2002; Abott, 1954; Abott, 1974). Identifications were later verified by Dr. Rudiger Bieler, Curator of the Field Museum of Natural History, Chicago, IL.

Paleoecological Survey

A series of sediment cores were taken along east-west transects in basins 2, 7, 10 and 13 (Fig. 2b). Several additional sites in other basins that showed interesting textural and compositional patterns were also cored, resulting in 36 coring locations (Fig. 2b). Using a soil auger, sediment cores were extracted in sequential sections until bedrock was encountered. In the field, the sediment sections were arranged in sequence according to depth. The transitions in composition and texture of the sediments were described and measured with a meter stick, proceeding from the surface sediments to the bottom. Sub-samples from each distinct layer were removed, placed in plastic bags, and labeled according to depth range. From 4-6 composite samples were removed from each core. In the laboratory, each subsample was washed and picked for mollusks using the same procedure as for the modern samples.

At a subset of 10 of these sites (Fig. 2b), we removed a pair of intact sediment cores using a 7.6 cm diameter, 2-m long aluminum core tube. The base of the core tube was serrated with a saw

and then driven into the sediments to bedrock by rotating a cross bar at the top of the tube. The serrated edges were bent inward to seal the base of the sediments by driving the tube into bedrock using a pounding block at the top of the tube. The tube containing sediments was then capped and retrieved using a tripod and winch, positioned above the core. Cores were returned upright to the laboratory and maintained in a cold room. The core tube was then split lengthwise on both sides using a rotary saw. Sediments were then also sliced lengthwise using pottery wire pulled down the length of the core. Once exposed, sediments were photographed and detailed notes were taken on stratigraphic observations of color, texture and content. One of each set of cores was then sliced into 1 cm sections; each section was dried in an 80°C for ~3-5 days to be used for radiometric dating. A subsection was analyzed for organic and carbonate content by first combusting at 500ºC for 1 hr, followed by combustion at 1000ºC for 1 hr.

Radiometric dating

To determine the chronology of these 10 cores, we used a combination of ^{210}Pb and ^{14}C radiometric dating for recent (<ca. 100 YBP) and older (>ca. 100 YBP) sediments. The ^{210}Pb analysis was performed in the laboratory of Dr. Daniel Engstrom, St. Croix Watershed Research Station, MN. Lead-210 was measured on dried material from each 1-cm depth interval through its grand-daughter product ^{210}Po, with ^{209}Po added as an internal yield tracer. The polonium isotopes were distilled from 0.2-1.2 g dry sediment at 550° C following pretreatment with concentrated HCl and plated directly onto silver planchets from a 0.5 N HCl solution (modified from Eakins and Morrison 1976). Activity was measured for 1-14 days with ion-implanted detectors and an EG&G Nuclear alpha spectroscopy system. Unsupported ^{210}Pb was calculated by subtracting supported activity from the total activity measured at each level, with supported ^{210}Pb estimated from the asymptotic activity at depth (the mean of the lowermost three samples in the core). Dates and sedimentation rates are determined according to the c.r.s. (constant rate of supply) model (Appleby and Oldfield 1978) with confidence intervals calculated by first-order error analysis of counting uncertainty (Binford 1990).

Organic material from the base of 5 of these cores was selected for ^{14}C analysis by Beta Analytic, Miami, FL. Material was examined under a dissecting microscope, and, if large (>1 mm) plant fragments were found, carbon in these fragments was reduced to graphite and ^{14}C measured by accelerated-mass-spectrometry (AMS). Otherwise, carbon in bulk organic material was synthesized to benzene and ^{14}C measured for an extended period of time on a scintillation spectrometer. Conventional ^{14}C age were calculated after applying ^{13}C/^{12}C corrections and ages reported in units YBP, where present is defined as 2003 when the cores were taken.

Statistical Analysis

Vegetation – To determine the distribution of mollusk communities with respect to vegetation structure, we first sorted stations into five vegetation type categories based on survey data and aerial photographs. The categories were: freshwater swamp forest, freshwater marsh, and dwarf, transitional and fringing mangrove forest. The distinctiveness of the categories based on relative cover of species present in more than 5% of the sites was confirmed using non-metric multidimensional scaling ordination (NMDS) and analysis of similarity (among community types) employing the Bray-Curtis similarity metric (using PCORD and PRIMER/ANOSIM

software). The NMDS ordinations were determined for one to 10 dimensions and final ordination was retained that contained the number of dimensions above which no appreciable loss of stress occurred. Plant species significantly influencing the five community types were identified using Dufrene and Legendre's (1997) Indicator Species Analysis, where taxa having an indicator value (based on relative abundance and frequency among sites) above 40% of perfect indication ($P<0.05$) were considered reliable indicators.

Mapping - Using the spatial modeling and analysis (V2.0) module in Arcview GIS 3.2 ® (ESRI, CA), we mapped the distribution of vegetation community types, soil depth, peat depth and salinity. To interpolate between points, we used the IDW method (McCune and Mefford, 1999), which weights the value of each point by the distance that point is from the cell being analyzed and then averages the values. The output grid cell size was 10 meters and the number of neighbors was 3 points.

Calibration - A transfer function was developed based on the relationships of modern mollusks to vegetation type and salinity to calibrate the mollusk assemblages in the sediment cores. The transfer function was developed using the weighted-averaging regression/calibration program in the software C2 ® (Juggins, 2003). This procedure assumes that the distribution of each species can be characterized by an optimum, defined by where abundances are greatest, and a tolerance, defined by the range of appearance along a gradient. The value of an environmental variable can then be calculated for a sample from an unknown environment, using the average of the optima of the species present, weighted by their abundances and possibly tolerances. Weighted-averaging regression/calibration performed in this manner requires the response gradient to be continuous and linear. While this was directly the case for salinity, we also used this method to predict vegetation community type from mollusk composition, as the community types were always arranged in the indicated sequence (forest-freshwater marsh-dwarf mangroves-transitional mangroves-fringing mangroves) and were suspected to have been so in the past.

Using the weighted-averaging program, we estimated the salinity and vegetation optimum and tolerance for each mollusk species as the average among sites in which the species occurred. Salinity values were log transformed prior to analysis to fit a normal distribution. Because the mollusk species had unequal occurrences, we followed the recommendation of Birks *et al*. (1990) and used the number of occurrences to adjust the tolerance assigned to each species. When tolerances were incorporated into the model, mollusk species with narrow distributions along the gradient were weighted more heavily than species with broadly dispersed or erratic distributions. We used classical regression (Birks *et al*., 1990) to eliminate shrinkage in the range of inferred values, because it resulted in the most evenly distributed residuals. We estimated the salinity and vegetation type at each sites by randomly selecting samples from the same dataset (bootstrapping with replacement) and predicting values based on the remaining sites. The resulting estimates for each station were then plotted against observed values, reporting the R^2 of the relationship and root-mean squared error of prediction (RMSE). Residuals from this model were plotted against observed values to detect trends in estimation precision.

The model was then applied to predict the vegetation type and salinity from the relative abundances of mollusk species present in each bulk sediment subsample. Age-models from dated cores from the same subunit in the nearest basin in the same subunit were used to estimate

the age range for each mollusk sample from undated cores. Then, for presentation purposes, mollusk-based vegetation type and salinity predictions were averaged within each of the three stratigraphic zones present in most cores. Predictions for each of these units were mapped using the same approach as for the environmental variables, as described above.

RESULTS

Modern Survey

Vegetation – Through multivariate community analyses, we were able to confirm the distinctiveness of the five major plant community types suggested through prior analysis of aerial photographs and survey data (see Gaiser et al., 2004). Based on relative cover 45 of the most abundant of the 84 total plant species found in the study area, the ANOSIM comparison found a global R of 0.48 ($P<0.01$) for all combinations suggesting a high degree of compositional distinctiveness among all community types. Compositional differences within freshwater units (freshwater swamp forest and freshwater marsh) and interior mangrove units (dwarf and transitional) were less ($R = 0.2$ and 0.3, $P<0.05$, respectively) than differences between freshwater and mangrove units (mean $R = 0.4$, $P<0.01$), and the fringing mangrove forest was highly distinguishable from all other units (mean $R = 0.8$, $P<0.001$). A two-dimensional NMDS ordination (stress = 0.14) of the same data clearly shows this separation of freshwater and marine units (effectuated by the L-31E canal), and the general west-east gradient of composition from the interior to the coast (Fig. 3). Plant species significantly associated with each community type were: (1) in the freshwater swamp forest, *Boehmeria cylindrica* (false nettle), *Casuarina equisetifolia* (Australian pine), *Conocarpus erectus* (buttonwood), *Myrica cerifera* (wax myrtle), *Proserpinaca palustris* (marsh mermaidweed), *Psilotum nudum* (whisk fern), *Rhabdadenia biflora* (mangrovevine), *Schinus terebinthifolius* (Brazilian pepper) and *Thelypteris kunthii* (southern shield fern), (2) in the freshwater marsh, *Cladium jamaicense* (sawgrass), *Juncus rhomerianus* (black rush) and *Typha domingensis* (cattail), (3) in the dwarf mangrove forest, *Laguncularia racemosa* (white mangrove), *Rhizophora mangle* (red mangrove) and *Rhynchospora microcarpa* (southern beaksedge), and (4) in the transitional forest, *Acrostichum aureum* (leather fern) and *Avicennia germinans* (black mangrove). Unit 5 (fringing mangrove forest) had no species that alone defined the community but the three mangrove species (*Rhizophora mangle, Laguncularia racemosa* and *Avicennia germinans*) together defined this unit. Though the coastward sequence of vegetation zones was consistent among sub-basins, there was variation in the breadth of each zone along the 7 km study area (Fig 4a). Further, we acknowledge that vegetation units are defined here very broadly to simplify linkages to mollusk community patterns. Additional distinct community types occur within these units, most notably including a densely vegetated, heavily canopied mangrove forest growing in historic drainages that meander through adjoining units and forests occupying tree islands that punctuate all units of the landscape. Vegetation canopy height was significantly higher in the freshwater swamp forest and transitional and fringing mangroves than in the freshwater marsh and dwarf mangrove community ($P<0.0001$; Fig. 4b).

Soils – Soil depth varied within the BBCW, being significantly deeper in the fringing mangrove forest than other units (126 vs. mean 104 cm, respectively). Areas of shallow soil coincided with areas of freshwater graminiod marsh, while deeper soils coincided with areas of coastal

mangrove fringe forest. All of the sediment cores contained an upper heavily rooted peat underlain by a compact marl. The contact between these layers was consistently abrupt and clearly defined. A basal layer of organic soil occurred beneath the marl layer in several cores taken from the fringing forest along the coastline. The upper peat layer was deepest in the fringing mangroves and gradually became shallower to the interior freshwater marsh (66 vs 12 cm, respectively; Table 1, Figs. 5 a, b).

Salinity – Porewater salinity throughout the BBCW was in the freshwater to brackish range at the time of sampling (1.6 – 27.6; mean 11.3 ppt). A strong west-east increase was observed in most of the sub-basins, with the L-31E clearly separating freshwater (salinity < 5 ppt) from marine (5-20 ppt) conditions throughout the system (Fig. 5c). Pockets of higher salinity were observed in the interior of basins 2, 4, 6, 8 and 9, west of the fringing mangrove forest.

Mollusks – Mollusk shells were found in surface sediments of 74% of the survey sites. At these sites, shell density ranged from 1 to 93 per sample (mean = 10.6). At a mean soil bulk density of 0.2 g cm^{-3} and a mean sampling volume of 113 cm^3, 0.46 shells g^{-1} or an aerial density of 938 shells m^{-2}. Twenty mollusk taxa representing 19 genera were collected and identified from the surface material (Table 2; Fig. 6). Four taxa were identified at the generic level because of limitations restricting more precise identification, e.g. lack of soft anatomy. Within these four cases there appeared to be at least two to three species of each genus present. Therefore, a total of 24-28 species of 19 genera were present within the samples. Of the 20 mollusk species identified, three were bivalves, 17 were gastropods and three were terrestrial (Table 2). The dominant taxa found throughout the modern surface samples, represented by the highest number of occurrences, were *Littoridinops* spp., *Melanoides tuberculata*, *Cyrenoida floridana*, *Cerithidea costata,* and *Polymesoda maritima* (Table 2; Fig. 6).

The weighted averaging (WA) salinity and vegetation type optima and tolerances (ppt) of 15 of the 20 species found in the 13 sub-basins showed a range of preferences (Table 2, Fig. 6). Five of the 20 species were not included in the inference models and calculations due to their lack of representation in either the modern samples or sediments. Four mollusk species preferred freshwater to slightly brackish conditions: *Planorbella duryi, Physella cubensis, Planorbella scalaris, and Littoridinops spp*, having salinity optima ranging from 1.94 (ppt) – 8.29 (ppt) (Table 2, Fig. 6). The remaining 11 species had higher salinity optima (11.0 – 20.7 ppt) indicative of intertidal to marine conditions, including *Melanoides tuberculata*, *Polugira cereolus, Succinea barberi*, *Cyrenoida floridana*, *Daedalochila uvulifera*, unknown sp.1, *Melampus* spp., *Anomalocardia auberiana*, *Truncatella* spp., *Cerithidea costata*, and *Polymesoda maritima*.

The WA vegetation type optima suggested that three of the four freshwater taxa (*Planorbella duryi, Physella cubensis,* and *Planorbella scalaris*) prefer the freshwater swamp forest, while *Littirodinops spp*. preferred the freshwater graminoid marsh. Of the taxa preferring higher salinities, *Melanoides tuberculata*, *Cyrenoida floridana*, *Daedalochila uvulifera*, *Melampus* spp., *Anomalocardia auberiana*, and *Cerithidea costata* preferred the dwarf mangrove forest. The vegetation type optima of the five remaining species were, transitional mangrove forest (*Polygyra cereolus*, uknown sp.1, and *Polymesoda maritima)* and coastal mangrove forest (*Succinea barberi* and *Truncatella* spp.; Table 2, Fig. 6).

Weighted averaging regression models were used to test the strength of the relationship of mollusk species composition to salinity and vegetation type (Fig. 7a,b). Mollusk species composition was found to provide reliable predictions of salinity and vegetation type (R^2 = 0.79 and 0.67, respectively). Predictions for salinity were within 3.8 ppt and vegetation type within 1 unit, according to the predicted RMSE. We found no pattern in the relationship of model residuals with observed values for either parameter.

Core descriptions and chronology

Descriptions – The 10 dated cores had similar profiles to those obtained in the larger soil auger survey, having three or more stratigraphically distinct layers (Fig. 8). With the exception of core 7B, each had an upper dark brown/black, heavily rooted detrital mud surface layer (Munsell color 10YR 2/2, 5/2, 3/2) with a bulk density ranging from 0.03-0.1 g cm^{-3}, containing 50-85 % organic peat (mean 68 +/- 12 %). This layer was shallow (0-4 cm) in the freshwater forest and marsh, deeper in the dwarf mangrove forest (4-12 cm) and deepest in the transitional and fringing forest (18-42 cm). A sharp contact was observed between this layer and a subsurface compact dark gray muck (Munsell color 10YR 4/1, 4/2) that also contained medium-sized roots and occasional darker colored compact organic masses. The lighter material was mostly marl with a bulk density of 0.09-0.45 g $cm^{-3}$and ranged from 8-41 % organic (mean 14 +/- 9 %) with a mean carbonate content of 51-86 %. This base of this layer was less sharply defined as the upper contact and, in most cores, graded into a hard, compact light gray/tan marl containing very fine roots occasional small clumps of compact dark brown/black organic material (Munsell color 10YR 8/1, 8/2 with clumps of 10YR 2/1,). This basal layer had a bulk density of 0.3-0.9 g cm^{-3}, an organic content of 8-14 % (10 +/- 2 %) and carbonate content ranging from 70-90 %. Cores were driven to bedrock so this layer often contained chunks of limestone at the base, which were removed prior to analysis.

Chronology – The five cores from the transitional and fringing mangrove forest (9F, 7D, 7G, 7F and 2F) all had smooth ^{210}Pb activity profiles, with unsupported ^{210}Pb extending to a depth of 25 – 50 cm. Age-depth models (Fig. 9b) show similar accumulation rates among sites between ~ 1960 and the present, averaging 0.06 +/- 0.03 g cm^{-2} yr^{-1} (giving a mean vertical peat accretion rate of 0.3 cm yr^{-1}). Prior to 1960, the average accumulation rate in these cores averaged 0.04 +/- 0.03 g cm^{-2} yr^{-1}, significantly less than the modern period ($P<0.01$). Three cores from the freshwater marsh (10B, 1B and 1C) show an abrupt drop in unsupported ^{210}Pb within the upper 10 cm of sediment and the dating did not extend past the 1900's. Core 1C from the dwarf mangrove forest was intermediated between the two above categories; the profile for unsupported ^{210}Pb was relatively short (ending at 12 cm) but less abrupt, and the resulting chronology extends further back in time. The average accumulation rate from ^{210}Pb in these five cores was 0.03 +/- 0.02 g cm^{-2} yr^{-1}. Core 7B did not appear to reach supported (background) values, and was truncated below 27 cm by bedrock; the chronology therefore, was unreliable chronology and not incorporated in analyses. In the remaining cores, the ^{210}Pb estimated age of the base of the upper peat layer ranged from 1946 to 1985 (mean = 1967) while that of the upper boundary of the underlying marl ranged from 1930 to 1966 (mean = 1944; Fig. 8). Extending the marl accumulation rates (0.03 – 0.04 g cm^{-2} yr^{-1}) beyond the period of measure provides an

indication of the timing of the deeper transition in the cores, which ranges from 1705 to 1860 A.D.

The age of basal materials from the 5 cores analyzed for ^{14}C show that soil accumulation began earlier in the coastal fringe (900-2990 YBP) compared to the dwarf mangrove swamp (820 YBP) and freshwater marsh (310 YBP). Vertical accretion rates for these marl-dominated soils were calculated based on the amount of material accumulated between the ^{210}Pb date of the upper horizon of zone 2 and the depth of the ^{14}C dated basal soil. Accretion rates range from 0.02 cm yr^{-1} in the coastal fringe to 0.2 cm yr^{-1} in the freshwater marsh and averaged 0.08 cm yr^{-1} among sites.

Mollusk-based Paleoecological Inferences

Mollusk shells were found in all of the core samples, with densities ranging from 1-505 per sample (mean = 17.6) and 0.02-8.1 shells g^{-1} dry weight. Sediments contained 17 of the 20 taxa identified in the surface samples (*Melongena corona, Neritina virginea* and *Geukensia demissa granosissima* were not found in the sediments*)* and two taxa*, Pomaceae palundosa* and *Haminoea elegans,* that were not represented by individuals in the surface samples. The dominant taxa found in the sediments, represented by the highest number of occurences, were *Littoridinops* spp. and *Physella cubensis*.

Relative abundances of mollusk taxa differed among the three soil zones (Table 2). Zone 1 was dominated by *Littoridinops* spp. with subdominants *Physella cubensis* and *Cyrenoida floridana*. Zone 1 was also the only layer to contain *Melanoides tuberculata*, *Anomalocardia auberiana*, *Pomaceae palundosa* and *Haminoea elegans*. Zone 2 contained greater abundances of *Littoridinops* spp. and *P. cubensis* than zone 1 and also contained *Planorbella duryi* and P. *scalaris* which were not found in the upper zone. Zone 3 was also dominated by *Littoridinops* spp. and had greater abundances of *P. cubensis*, *P. duryi* and *P. scalaris* than the upper 2 zones. *Melampus* spp., *C. floridana* and *A. auberiana* were conspicuously absent from zone 3 (Table 2).

Mollusk-Predicted Salinity -- Contour maps of mollusk-inferred salinity for the coastal wetland system show significant changes through the period of record (Fig. 10). Salinity inferences for the surface mollusk dataset used for calibration were mapped ("present", Fig. 10a) to visualize correspondence of the mollusk-based inferences with actual measured values (mapped in Fig. 5c). Patterns are generally similar with salinity decreasing shoreward with several small higher excursions to the interior. Average predicted salinity across the entire basin from the current mollusk assemblage was 13.2, while the sediment zones were significantly different with means of 6.9, 2.3 and 0.2 for zones 1, 2 and 3, respectively ($P<0.0001$; Fig. 12). Sediment zone 1, representing the last ~30-70 years shows a more abrupt interior-ward gradient of decreasing salinity with higher values isolated to the coastal fringe and small interior pockets in subunits 1, 7 and 9 (Fig. 10 a). Zone 2, representing the preceeding 100-250 years of accumulation, shows mollusk-predicted salinity values ranged from 0-10 ppt, with one small pocket of higher values in the interior of subunit 1 (Fig. 10 b). Most of the coastal wetland unit could be classified as freshwater to slightly brackish (<5 ppt). All predictions for zone 3 were below 5 ppt (Fig. 10 c), indicating freshwater conditions persisted throughout the entire Biscayne Coastal Wetlands between the time that soils began accumulating and the 17-1800's.

Mollusk-Predicted Vegetation type – Mollusk-based vegetation type predictions mapped for the surface community and sediment zones 1, 2 and 3 also show large magnitude changes over the period of record (Fig. 11). Contour maps show the high degree of correspondence between mollusk-based vegetation type predictions for surface assemblages (Fig 11a, "present") and actual measured vegetation types (Fig 4 a). Average predicted vegetation type was significantly different among the three sediment zones, with means of 3.1 (dwarf mangrove forest), 1.4 (freshwater marsh) and 1.1 (freshwater swamp forest) for zones 1, 2 and 3, respectively ($P<0.0001$). Zone 1 shows a similar east-west zonation of vegetation types as depicted in the modern vegetation maps, with fringing and transitional mangrove forest lining the coastline, dwarf mangrove to the interior and freshwater marsh and swamp forests along the western boundary. There is notably less fringing mangrove forest predicted for zone 1 than measured in the vegetation survey (Fig. 11 a) or predicted from the modern mollusk community. The distribution of vegetation types during the time period encapsulated by zone 2 indicates a lack of distinct zonation with most of the BBCW being occupied by freshwater marsh and swamp forest (Fig. 11 b). A few small areas of subunits 1 and 2 appear to have been colonized by mangroves during this time. By the time interval represented by zone 1, the transitional mangrove forest had expanded 52 times its size in zone 2, and the dwarf and fringing forests had increased in area by a factor of 6 and 21, respectively. During the same interval, 85 and 59 percent of the freshwater swamp forest and marsh were lost. Inferences for Zone 3 suggest that the entire BBCW was freshwater marsh or forest, with forests occupying the majority of the unit and freshwater marshes being confined to the southernmost subunits (Fig. 11 c). Only 0.01 % of the area was occupied by mangroves (all dwarf forest).

Salt-water Encroachment Rates - Although fine-scale resolution of the temporal sequence of change was precluded due to the shallowness of the sediments and the need for bulk material to extract enough mollusks for analysis, we interpolated migration rates on a coarse scale by first determining the average longitude of the location of the freshwater swamp forest and marsh (the only two vegetation types present for the entire duration of record) for zones 1, 2, 3 and the present system. We then calculated the mean distance these communities shifted over the time interval elapsed between each sediment zone. The freshwater ecotones shifted interior-ward an average of 53 meters between zones 3 and 2, representing the long (300-3000 year) pre-development period of deposition in this basin. The average pre-development encroachment rate was 0.14 m yr^{-1} (range, 0.02 to 0.27 m yr^{-1}). Between zones 2 (1700-1960) and 1 (1960-present), freshwater ecotones moved westward by an average of 450 meters, representing an encroachment rate of 3.1 m yr^{-1} (range 1.7 to 4.1 m yr^{-1}). While Zone 1 represents the past ~50 years and includes modern material, comparisons to surface assemblages show that encroachment continues in the contemporary community.

DISCUSSION

The rate of interior-ward migration of coastal ecotones along coastal South Florida has accelerated substantially in the past century. Rates of encroachment calculated by this study (2-4 m yr^{-1}) are one to two orders of magnitude faster in the past 60 years of record than in the previous history of the wetland unit. This rate is lower than that documented by Ross et al. (2000) who, by comparing community composition from a 1940 vegetation survey and aerial

photographs with present data, found the boundary of mixed graminoid-mangrove and sawgrass communities in southeast Florida to have shifted inland by as much as 3.3 km, giving an encroachment rate of 55 m yr^{-1}. The difference may be due to the proximity of boundary canals in the two wetland units; in this study the L-31E canal is only ~4-500 m from the coast and prevents further westward encroachment while area studied by Ross et al. (2000) is bounded 4 km to the west by the same canal. In the present study, the freshwater ecotone migrated 450 meters westward in the past 60 years and the <10% of original freshwater gramminoid marsh remaining is confined from further westward migration by agriculture and urban developments immediately adjacent to the study area. Also impacting westward movement of freshwater marsh and forest components is the rapid invasion and expansion of exotic woody vegetation, including *Casuarina equisetifolia* and *Schinus terebinthifolius*, into areas that were formerly wetter.

The rapid loss rate of freshwater ecosystems from South Florida estuaries is due to a combination of rising sea-level and coastal water management practices. Rates of sea-level rise in South Florida, compiled for the Holocene by Wanless et al (1994) from numerous stratigraphic studies, show relatively constant rates of approximately 0.4 mm yr^{-1} for the past 3000 years until beginning of industrialization in the late 19th Century. The shallow and anastomosing geomorphology of the coastline in this region allowed for the development of mangroves, creating a sedimentary environment unique to North America, but similar to those of Caribbean island and continental coastlines. Unlike gramminoid-dominated salt marshes that line much of the rest of the Atlantic coastline, mangrove communities have higher sedimentation rates that are commensurate with the moderate rates of sea-level rise characterizing the late Holocene. Accretion rates measured in this study of 3.1 and 0.08 mm yr^{-1}, based on ^{210}Pb and ^{14}C, respectively, were similar to the average calculated for mangrove ecosystems of the wider Caribbean region of 3.7 and 1 mm yr^{-1} (the discrepancy between historical and geological rates attributed to organic decomposition and sediment compaction; Parkinson et al. 1994). However, recent rates of sea-level rise calculated from the ~100 year tide gauge monitoring station in Key West show that the rate of sea level has increased an order of magnitude over the period of record to 3-4 mm yr^{-1}, resulting in more than 30 cm increase in the last century (Maul and Martin 1993). Modern peat accretion rates suggest that mangroves in the BBCW are keeping up with the more rapid rate of sea-level rise and continuing to expand into marshland formerly occupied by a freshwater gramminoid/sawgrass community. Ellison and Stoddart (1991) show that mangrove ecosystems can keep pace with rising sea level up to about 9 cm 100 yr^{-1}, which is less than the rate predicted for the next 100 years (10-12 cm 100 yr^{-1}, IPCC 1998). Ellison (1993) further showed that mangrove ecosystems quickly collapse in areas where this rate is greatly exceeded (i.e., Bermuda, where the local rate of sea-level rise exceeds 25 cm 100 yr^{-1}). An additional constraint on the ability of South Florida mangrove communities to sustain increasing rates of salt-water encroachment is the large expanse of dwarf red mangrove whose productivity is much reduced by the combination of susceptibility to intermittent freezes (Ross et. al. In Press), hurricanes and hypersaline soils.

Freshwater marsh vegetation type from the Florida coastline is not only being lost as it is replaced by mangroves advancing with sea-level rise but also by salt-water encroachment exacerbated by water management practices. Prior to construction of the water conveyance system in South Dade in the early 1900's, freshwater flowed from the Everglades into Biscayne

Bay through natural transverse estuaries. Freshwater delivery through these drainages was evidently substantial enough to maintain freshwater salinities throughout the BBCW. Mangroves were restricted to a peripheral fringe which appears on aerial photographs from the 1940's to have occupied a narrow band along the edge of the study unit, as well as along the mouths of the tidal creek outlets (Ross et al. 2000). Freshwater drainage in this basin began with the construction of small ditches (mosquito ditches) to drain water from expanding agricultural land. Major canal construction began in the 1940's when the Princeton, Military and Mowry canals were dug as flood control canals, diverting most freshwater from the Everglades eventually into focused discharges in Biscayne Bay. Finally, the L-31E canal was constructed in 1960 to connect the network of east-west drainage canals. This canal network effectively eliminated the natural eastward flow of freshwater through this system and caused the tidal creeks to fill in with sediment to be later overgrown with woody vegetation (Meeder et al. 2000). Patterns in the distribution of porewater salinity values are now driven by the underlying drainage template; freshwater is completely confined to the west of the L-31E drainage while higher salinities can develop in the interior of each basins where circulation is limited due to higher elevation berms on the east (due to mangroves) and the south and north due to forest vegetation lining former drainages. Sawgrass meadows, once dominant along the coast, are now also confined to freshwater units west of the L-31E canal. It is notable that these sawgrass meadows were likely interspersed with woody vegetation, possibly in tree islands (which are reduced in number today), since the mollusk fauna in basal material contained more terrestrial taxa than modern sawgrass communities.

Mollusks have been reliable indicators of paleoenvironments, particularly of sea-level rise and associated changes, in carbonate-rich, shallow-water coastlines and bays. They are diverse and abundant in estuarine/marine settings and preserve well in the low solute, high pH interstitial environment. Ross et al. (2001) found a similar assemblage of mollusks along a coastal gradient in a nearby wetland, and found strong correspondence of assemblage composition with distance from the coastline. The high degree of variability in salinity in that study, however, precluded the estimation of salinity preferences for collected taxa. However, the placement of these taxa along the coastal gradient was similar to this study, with *Physella cubensis* and *Planorbella* spp. being restricted to freshwater marshes, *Litterindinops* spp, *Polygyra cereolus* and *Cyrenoida floridana* preferring the intermediate dwarf mangrove forest, and *Melampus* spp. and *Cerithidea* spp. being associated more closely with the marine coastline. Brewster-Wingard et al. (2001) collected mollusks from a high density of sites in Florida Bay, and used strong associations with salinity to reliably elucidate increasing environmental variability (particularly in salinity) over the past 100 years in sediment cores. Salinity and temperature preferences are provided for 43 taxa, but only four taxa (*Melampus* spp., *Anomalocardia* auberiana, *Truncatella* spp. and *Melongena corona*) were also found in the present study. The low degree of overlap between the fauna collected by Brewster-Wingard (2001) from a shallow embayment and the coastal wetland studied here is expected; also that the four overlapping taxa had marine salinity optima in both studies. To our knowledge this is the first presentation of quantitative salinity and vegetation type preferences for many of these brackish-water species, and should provide a reliable guide for other mollusk-based ecological research in this region.

CONCLUSIONS

There is clear evidence from the mollusk record that salt-water is rapidly encroaching in the BBCW and this is eliminating the formerly expansive freshwater marsh ecosystem and associated natural tidal drainages. Mangroves are advancing inland at rates similar to that seen in other coastal Caribbean environments, and this pace of migration is only curtailed by artificial impediments such as canals, levees or developing urban and agricultural landscapes. Ross et al. (1991) compared vegetation distributions in aerial photographs from 1935 and 1991 from the lower Florida Keys and also found an increase in mangrove expanse of 33 percent over the 56 yr period. Along the Altantic coastline, sea-level rise and other contributing factors have caused the loss of over 50% of tidal wetlands since the 1800's (Ellison 1993), a process particularly severe in areas of low relief and high erosion (i.e., Louisiana's coastal wetlands, Childers & Day 1990). These problems will only be exacerbated by the combined pressures of development and climate change. Active intervention is necessary which could include massive re-routing of freshwater drainages to re-establishing the natural tidal drainage through coastal wetlands and protecting land behind mangroves to allow areas for inland migration of existing freshwater and estuarine communities.

ACKNOWLEDGEMENTS

This work could not have been possible without the generous assistance of the staff of the Southeast Environmental Research Center (SERC), especially Christine Taylor, Alexander Leon, David Reed, David Jones and Jay Sah in the field and laboratory. We also thank Sarah Bellmund and Biscayne National Park for continued support of this project, Lynn Coultas for assistance in soil sampling and interpretation and Krish Jayachandran for soil characterization and analysis. Radiometric analyses were performed by Beta Analytic, Miami, FL (^{14}C) and Daniel Engstrom (^{210}Pb), who also helped with chronological interpretations. Funding was provided to SERC from the United States Department of the Interior, Everglades National Park. Additional support has been provided by the National Science Foundation through the Florida Coastal Everglades LTER (DEB-9910214) and the Undergraduate Mentoring in Environmental Biology programs (NSF-0102832). This is SERC publication series contribution #xxx.

REFERENCES

Abott, R.T. 1954. American Seashells, 1st Edition. Van Norstrand Reinhold, New York, NY.

Appleby, P.G. and F. Oldfield. 1978. The calculation of lead-210 dates assuming a constant rate of supply of unsupported ^{210}Pb to the sediment. Catena 5: 1-8.

Binford, M. W. 1990. Calculation and uncertainty analysis of ^{210}Pb dates for PIRLA project lake sediment cores. J. Paleolimnology 3: 253-267.

Birks, H.J.B., J.M. Line, S.Juggins, A.C. Stevenson, and C.J.F. Ter Braak. 1990. Diatoms and pH reconstruction. Philosophical Transactions of the Royal Society of London B. 327: 263-278.

Boyer, J. N., J. W. Fourqurean, and R. D. Jones. 1999. Seasonal and long-term trends in water quality of Florida Bay (1989-97). Estuaries 22: 417-430.

Brewster-Wingard, G. L., J. R. Stone and C. W. Holmes. 2001. Molluscan faunal distribution in Florida Bay, past and present: An integration of down-core and modern data. In B. R. Wardlaw (ed.) Paleoecological Studies of South Florida. Bulletins of American Paleontology 361: 199-232.

Childers, D. L. and J. W. Day. 1990. The dilution and loss of wetland function with conversion to open water. Wetlands Ecology and Management. 1: 1-9.

Church, J.A., J.M. Gregory, P. Huybrechts, M. Kuhn, K. Lambeck, M.T. Nhuan, D. Qin, and P.L. Woodworth. 2001. Changes in sea level. Chapter 11 of the Intergovernmental Panel on Climate Change Third Assessment Report, Science Report, Cambridge University Press, 638-689

Dufrene, M. and P. Legendre. 1997. Species assemblages and indicator species: the need for a flexible asymmetrical approach. Ecol. Monogr., 67: 345-366.

Eakins, J.D. and R.T. Morrison. 1978. A new procedure for the determination of lead-210 in lake and marine sediments. International Journal of Applied Radiation and Isotopes 29: 531-536.

Egler, F. E. 1952. Southeast saline Everglades vegetation, Florida, and its management. *Veg.* Acta Geobot. 3: 213-265.

Ellison, J. and D. R. Stoddart. 1991. Mangrove ecosystem collapse during predicted sea-level rise: Holocene analogues and implications. J. Coastal Research 7: 151-165.

Gaiser, E. E., A. Wachnicka, P. Ruiz, F. Tobias and M. S. Ross. 2004. Diatom indicators of ecosystem change in coastal wetlands. In S. Bortone (Ed.) Estuarine Indicators. CRC Press, Boca Raton, FL. pp. 127-144.

Intergovernmental Panel on Climate Change, 1998: The Regional Impacts of Climate Change: An Assessment of Vulnerability. Special Report of IPCC Working Group II. In Watson, R.T., M.C. Zinyowera, and R.H. Moss (eds.). Intergovernmental Panel on Climate Change, Cambridge University Press, Cambridge, United Kingdom and New York, NY, USA, 517 pp.

Juggins, S. 2003. C2 User guide: Software for ecological and palaeoecological data analysis and visualization. University of Newcastle, Newcastle upon Tyne, UK.

Leatherman, S.P., K. Zhang, and B.C. Douglas. 2000. Sea level rise shown to drive coastal erosion. Eos (Transactions American Geophysical Union) 81: 55-57.

Maul, G. A. and D. M. Martin. 1993. Sea level rise at Key West, Florida, 1846-1992: America's longest instrument record? Geophysical Research Letters 20: 1955-1958.

McCune, B. and M. J. Mefford. 1999. Multivariate analysis of ecological data. Version 4.17. MJM Software. Gleneden Beach, OR.

Meeder, J. F., P. W. Harlem, M. S. Ross, E. E. Gaiser and R. Jaffe. 2000. Southern Biscayne Bay Watershed Historic Creek Characterization. Final Report to the South Florida Water Management District.

National Research Council 1993. Managing wastewater in coastal urban areas. Washington DC: National Academy Press.

Nicholls, R.J., F.M.J. Hoozemans and M. Marchand. 1999. Increasing flood risk and wetland losses due to sea-level rise: regional and global analyses. Global Environmental Change, 9: S69-S87.

Park, R.A., M. S. Trehan, P. W. Mausel and R. C. Howe. 1989. Coastal wetlands in the twenty-first century: Profound alterations due to rising sea level. In D.W.Fisk (Ed). Wetlands: Concerns and Successes, pp.71-800. Proceedings of the American Water Resources Association, Tampa, FL.

Parkinson, R. W., R. D. DeLaune and J. R. White. 1994. Holocene sea-level rise and the fate of mangrove forests within the wider Caribbean region. J. Coastal Research. 10: 1077-1086.

Ross, M. S., L. J. Flynn and J. J. O'Brien. 1991. Has 20th Century sea level rise caused the migration of Florida Keys plant communities? American Journal of Botany (Suppl.). 78: 46.

Ross, M. S., J. F. Meeder, J. P. Sah, P. L. Ruiz and G. J. Telesnicki. 2000. The Southeast Saline Everglades revisited: a half-century of coastal vegetation change. Journal of Vegetation Science 11:101-112.

Ross, M. S., E. E. Gaiser, J. F. Meeder and M. T. Lewin. 2001. Multi-taxon analysis of the "white zone", a common ecotonal feature of South Florida coastal wetlands. In Porter, J. and Porter, K. (eds). The Everglades, Florida Bay, and Coral Reefs of the Florida Keys. CRC Press, Boca Raton, FL, USA. pp. 205-238.

Ross, M. S., P. L. Ruiz, J. P. Sah, D. L. Reed, J. Walters and J. F. Meeder. In Press. The influence of proximity to the coast on early stand development in fringe mangrove forests following hurricane. Plant Ecology.

Thompson, F.G. An Identification Manual for the Freshwater Snails of Florida. Curator of Malacology, Florida Museum of Natural History, University of Florida, Gainseville, Florida. Available at: http://www.flmnh.ufl.edu/natsci/malacology/fl-snail/snails1.htm. Accessed August. 20, 2002.

Wanless, H. R., R. W. Parkinson and L. P. Tedesco. 1994. Sea level control on stability of Everglades Wetlands. In S. M. Davis and J. C. Ogden (eds.) Everglades: the Ecosystem and Its Restoration. St. Lucie Press, p. 199-222.

Fig. legends:

Fig. 1. Satellite image of Florida with inset aerial images showing the Biscayne Bay Coastal Wetlands in (a) 1940 before construction of the north-south L-31E canal and in (b) 1990, also showing the numerical designation of wetland subunits separated by east-west drainage ditches.

Fig. 2. Aerial image (1990) of the Biscayne Bay Coastal Wetlands showing the location of (a) sites used to survey vegetation, mollusks, salinity and soil characteristics and (b) coring sites used for the paleoecological survey.

Fig. 3. Non-metric multidimensional scaling ordination biplot of suvery sites based on compositional dissimilarity of vegetation communities, showing differentiation of the five vegetation type categories.

Fig. 4. Contour maps generated from the vegetation survey showing the distribution of (a) community types and (b) mean canopy height across the Biscayne Bay Coastal Wetlands. Sampling locations are indicated on the corresponding aerial image (Fig. 2 a).

Fig. 5. Contour maps generated from the soil survey showing the distribution of (a) soil depth, (b) depth of the upper peat layer in soil cores and (c) porewater salinity across the Biscayne Bay Coastal Wetlands. Sampling locations are indicated on the corresponding aerial image (Fig. 2 a).

Fig. 6. Digital Photographs of mollusk species. These numbers correspond to the numbers and data in Table 1. Freshwater taxa: (1) *Planorbella duryi*, (2) *Physella cubensis*, (3) *Planorbella scalaris*, and (4) *Littoridinops* spp. Saltwater taxa: (5) *Melanoides tuberculata*, (6) *Polygyra cereolus*, (7) *Succinea barberi*, (8) *Cyrenoida floridana*, (9) *Daedalochila uvulifera,* (10) Uknown spp., (11) *Melampus* spp., (12) *Anomalocardia auberiana*, (13) *Truncatella* spp., (14) *Cerithidea costata*, (15) *Polymesoda maritima*, (16) *Melongena corona*, and (*17) Geukensia demissa granosissima*.

Fig. 7. Relationships between observed and mollusk-inferred values of (a) salinity and (b) vegetation type using classical weighted-averaging regression with tolerance down-weighting. The root mean squared error of prediction based on bootstrapping with replacement within the survey dataset is provided.

Fig. 8. Characterization of sediments in the chronologically calibrated cores, indicating the estimated ^{210}Pb date of material above and below the upper peat zone. Coring locations are depicted in Fig 2 b.

Fig. 9. Age-depth models for the 10 cores analyzed for ^{210}Pb. The left panel shows accumulation rates for cores collected from the freshwater swamp forest, freshwater marsh and dwarf mangrove forest while the right panel shows results from the transitional and fringing mangrove forest.

Fig. 10. Contour maps of vegetation types based on weighted-averaging regression/calibration inferences from mollusk assemblage composition in surface material (present) and sediment zones 1, 2 and 3. Coring site locations are indicated.

Fig. 11. Contour maps of salinity based on weighted-averaging regression/calibration inferences from mollusk assemblage composition in surface material (present) and sediment zones 1, 2 and 3. Coring site locations are indicated.

Fig. 12. Area occupied by each vegetation type type and porewater salinity concentrations (with standard error bars) predicted by mollusk communities in surface soils (present) and sediment zones 1, 2 and 3.

Table 1. Means and standard errors () of soil depth, peat depth, vegetation canopy cover and salinity for each vegetation community type (with designated numeric reference categories).

Vegetation Type (Category)	Soil Depth (cm)	Peat Depth (cm)	Canopy Height (m)	Salinity (ppt)
Freshwater Swamp Forest (1)	93 (20)	24 (10)	5 (2)	2.2 (0.9)
Freshwater Marsh (2)	118 (13)	12 (2)	2 (1)	4.9 (4.3)
Dwarf Mangrove Forest (3)	97 (21)	26 (18)	2 (1)	9.0 (8.0)
Transitional Mangrove Forest (4)	108 (19)	41 (16)	5 (2)	16.0 (6.7)
Fringing Mangrove Forest (5)	126 (14)	66 (27)	9 (2)	17.6 (2.0)

Table 2. Number of occurrences, maximum relative abundances, and weighted-averaging (WA) salinity (ppt) and vegetation type optima and tolerances () of mollusks collected from surface sediments in the Biscayne Bay Coastal Wetlands. Relative abundances in zones 1, 2 and 3 of the sediment cores are also provided. Species are listed in increasing order of estimated WA salinity optima.

Fig. no.	Taxon	No. Occ. Surface	Max Rel. Abd. Surface	WA Salinity Opt. (Tol.)	WA Veg. Opt. (Tol.)	Rel. Abd. Zone 1	Rel. Abd. Zone 2	Rel. Abd. Zone 3
1	*Planorbella duryi* (Wetherby)	3	0.14	1.94 (0.42)	1.00 (1.11)	0	0.01	0.01
2	*Physella cubensis* (Pfeiffer)	15	0.67	2.09 (0.46)	1.39 (0.58)	0.09	0.15	0.2
3	*Planorbella scalaris* (Jay)	2	0.14	2.33 (0.12)	1.35 (0.71)	0	0.01	0.03
4	*Littoridinops* spp.	41	1	8.29 (7.96)	2.35 (1.29)	0.57	0.73	0.6
5	*Melanoides tuberculata* (Müller)	32	1	11.01 (8.45)	3.15 (1.02)	0.01	0	0
6	*Polygyra cereolus* (Mühlfeld)	2	0.37	12.82 (8.14)	4.71 (2.83)	0.01	0.01	0.02
7	*Succinea barberi* (Marshall)	2	0.11	13.65 (4.84)	5.00 (1.11)	0	0.01	0.02
8	*Cyrenoida floridana* (Dall)	35	0.93	15.60 (7.78)	3.60 (1.02)	0.09	0.01	0
9	*Daedalochila uvulifera* (Shuttleworth)	2	0.17	16.17 (4.84)	3.00 (1.11)	0	0.01	0.01
10	Unknown sp. 1	9	0.57	16.26 (5.30)	4.27 (0.87)	0.04	0	0
11	*Melampus* spp.	13	0.88	16.54 (6.52)	3.63 (0.84)	0.04	0.01	0
12	*Anomalocardia auberiana* (d'Orbigny)	4	0.05	18.55 (5.69)	3.87 (1.19)	0.01	0	0
13	*Truncatella* spp.	4	0.58	18.77 (3.29)	5.00 (1.11)	0.06	0.1	0.08
14	*Cerithidea costata* (da Costa)	23	0.77	20.36 (5.08)	3.79 (0.88)	0.05	0.02	0.01
15	*Polymesoda maritima* (d'Orbigny)	23	0.85	20.73 (3.64)	4.09 (0.95)	0.01	0.1	0.01
16	*Melongena corona* (Gmelin)	1	0.03			0	0	0
17	*Geukensia demissa granosissima* (Sowerby)	4	0.01			0	0	0
18	*Pomaceae palundosa* (Say)	0	0			0.01	0	0
19	*Haminoea elegans* (Gray)	0	0			0.01	0	0
20	*Neritina virginea* (Linné)	1	0.01			0	0	0

Table 3. Depth and identity of samples from the Biscayne Coastal Wetlands analyzed for radiocarbon by Beta Analytic, Miami, FL. Samples were analyzed by Accelerated Mass Spectrometry (AMS) or by extended counting on a scintillation spectrometer.

Core	Depth below surface (cm)	Conventional ^{14}C age *	Analysis/Sample type	Beta ID
7D	50-54	1750 +/- 40	AMS/bulk organic	Beta-194070
1B	60-64	310 +/- 40	AMS/plant fragments	Beta-194071
1C	42-44	820 +/- 40	AMS/plant fragments	Beta-194072
7F	96-98	900 +/- 40	AMS/plant fragments	Beta-194073
2F	88-90	2990 +/- 60	Extended/peat	Beta-194074

*Dates are reported in RCYBP (radiocarbon years before present, 'present' = 1950 A.D.).

Figure 1

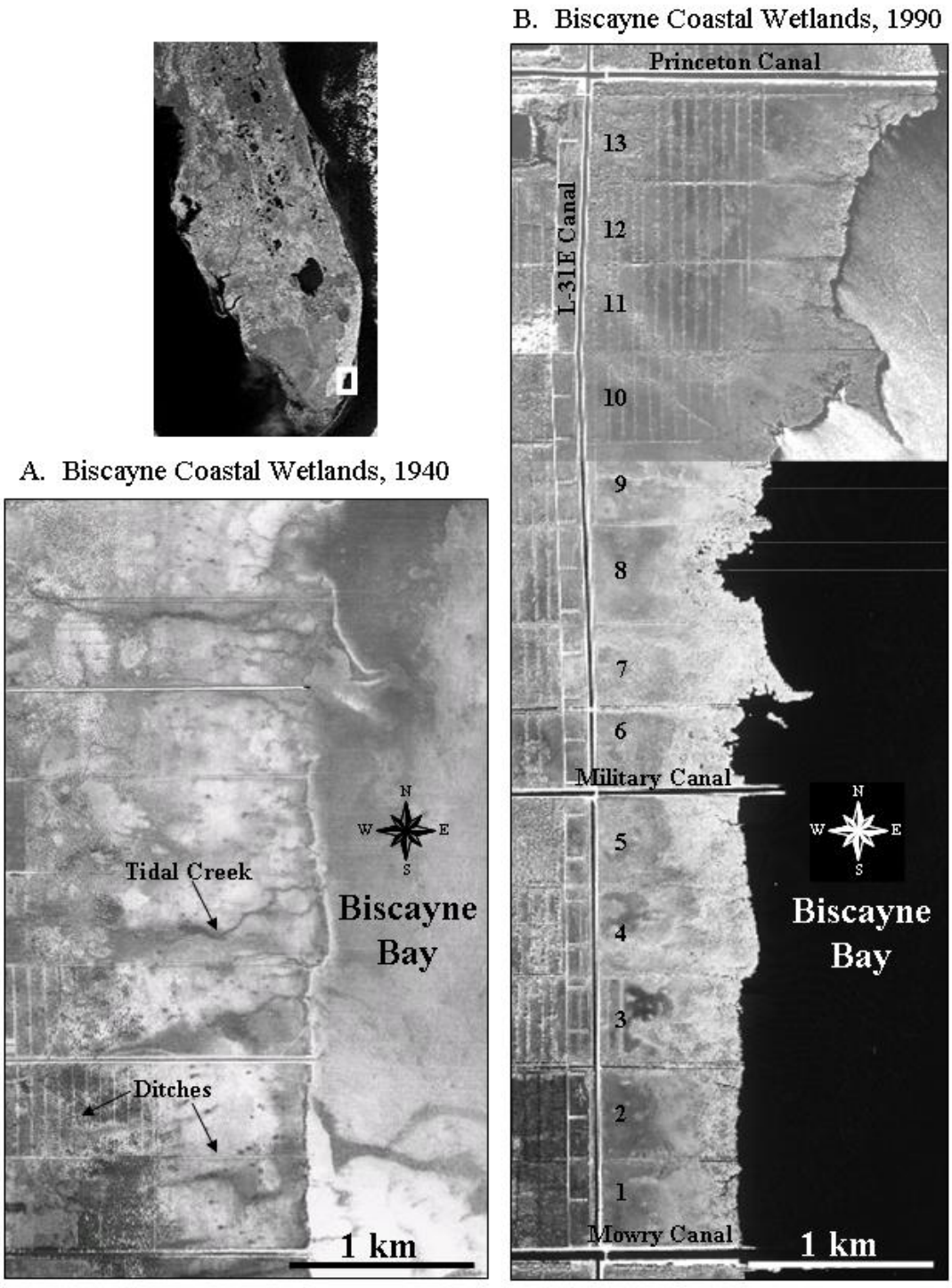
B. Biscayne Coastal Wetlands, 1990
Princeton Canal
13
12
11
10
9
8
7
6
L-31E Canal
Military Canal
5
4
3
2
1
Mowry Canal
N
W
E
S
Biscayne Bay
1 km
A. Biscayne Coastal Wetlands, 1940
Tidal Creek
Ditches
N
W
E
S
Biscayne Bay
1 km

Figure 2

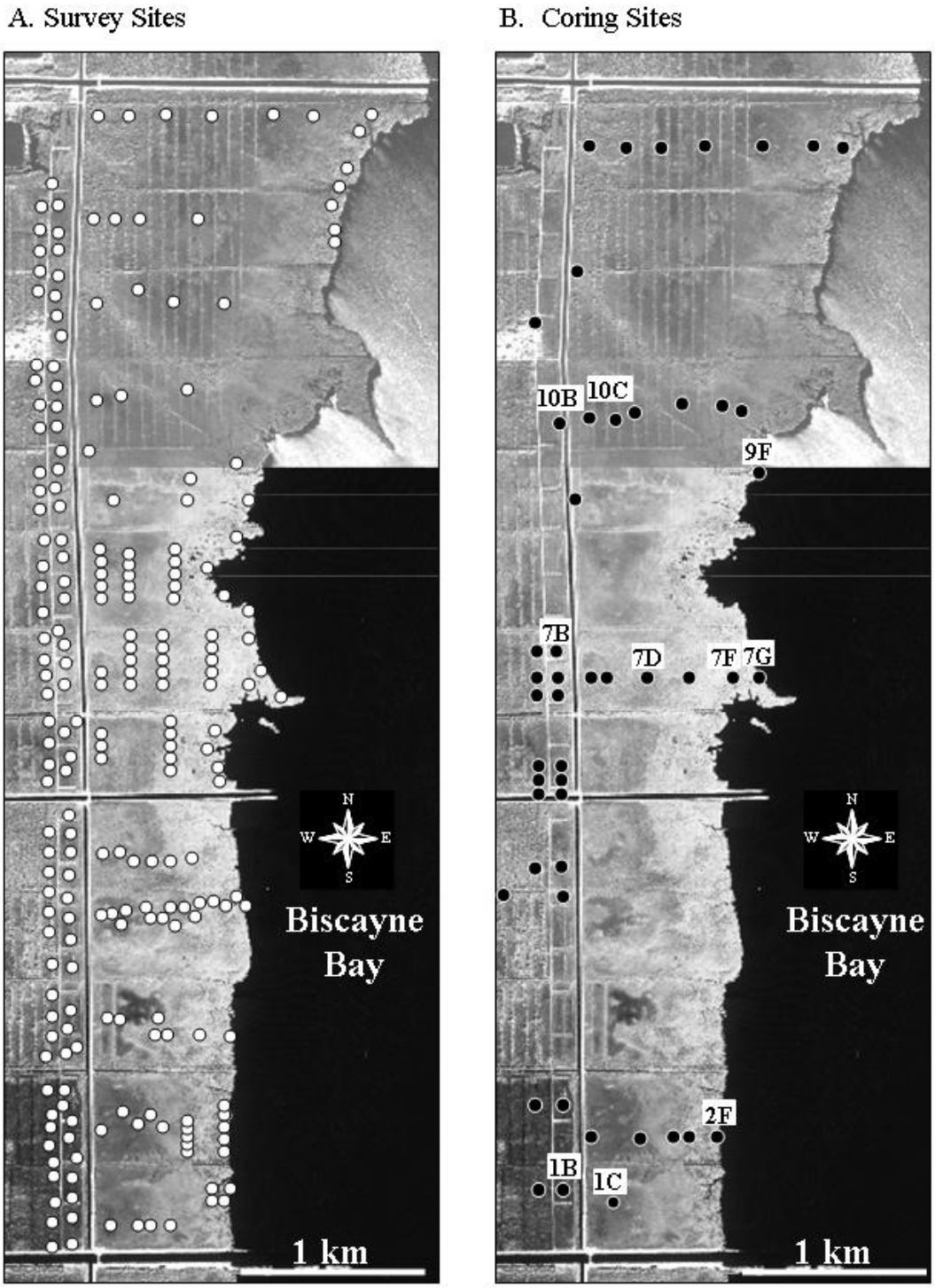
A. Survey Sites
B. Coring Sites
10B
10C
9F
7B
7D
7F
7G
2F
1B
1C
N
W
E
S
Biscayne Bay
1 km

Figure 3

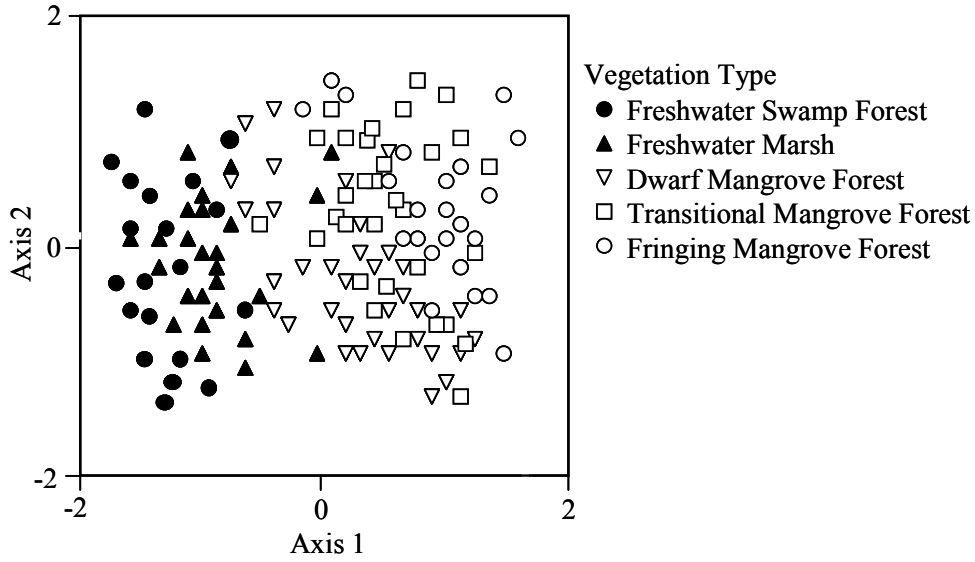
2
0
-2
Axis 2
-2
0
2
Axis 1
Vegetation Type
Freshwater Swamp Forest
Freshwater Marsh
Dwarf Mangrove Forest
Transitional Mangrove Forest
Fringing Mangrove Forest

Figure 4

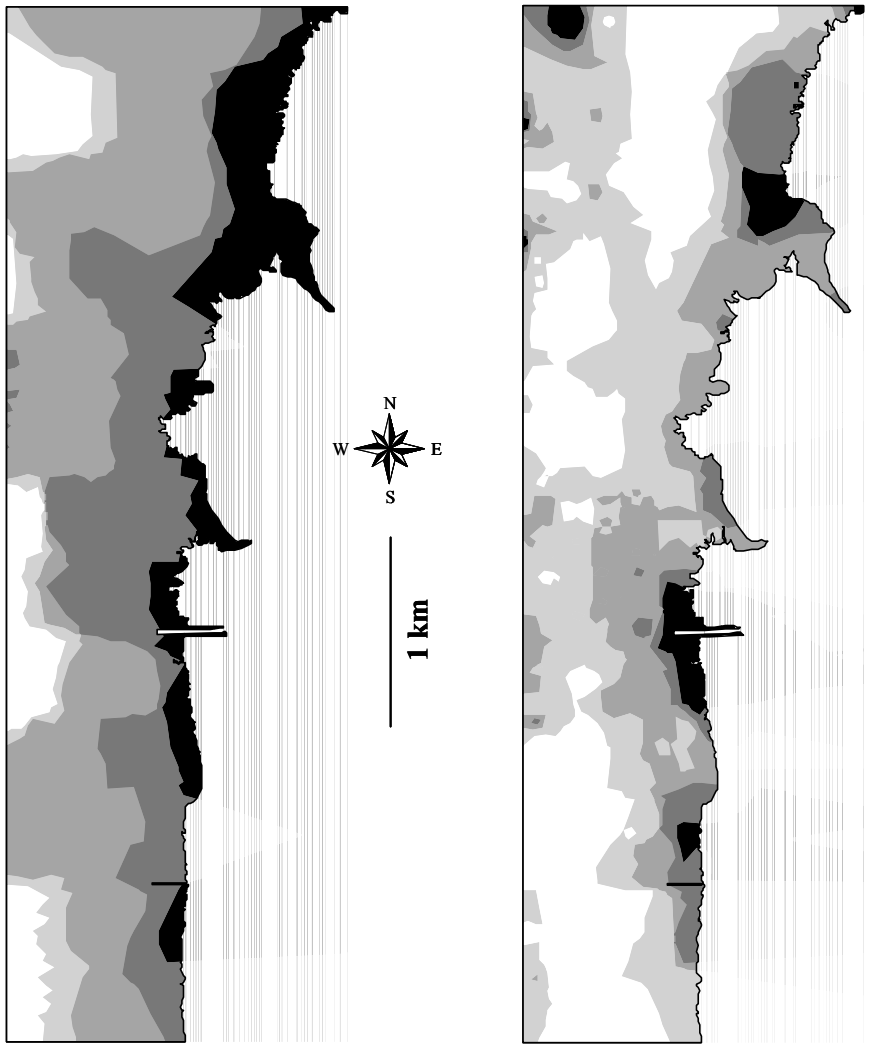

A. Vegetation type

- Freshwater Swamp Forest
- Freshwater Marsh
- Dwarf Mangrove Forest
- Transitional Mangrove Forest
- Fringing Mangrove Forest

B. Mean canopy height (m)

- 0-2
- 3-5
- 6-8
- 9-11
- 12-15

Figure 5

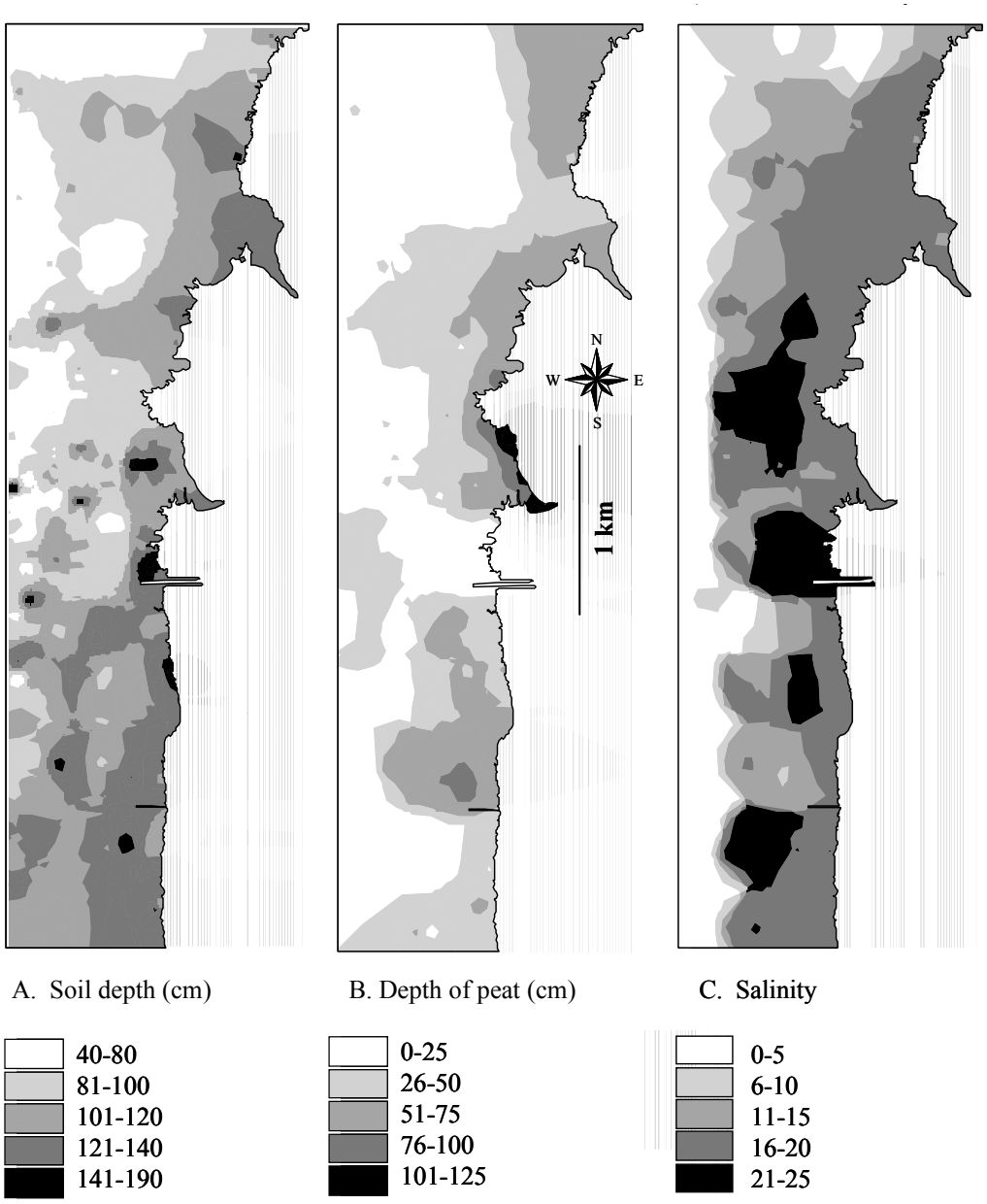
N
W
E
S
1 km
A. Soil depth (cm)
40-80
81-100
101-120
121-140
141-190
B. Depth of peat (cm)
0-25
26-50
51-75
76-100
101-125
C. Salinity
0-5
6-10
11-15
16-20
21-25

Figure 6

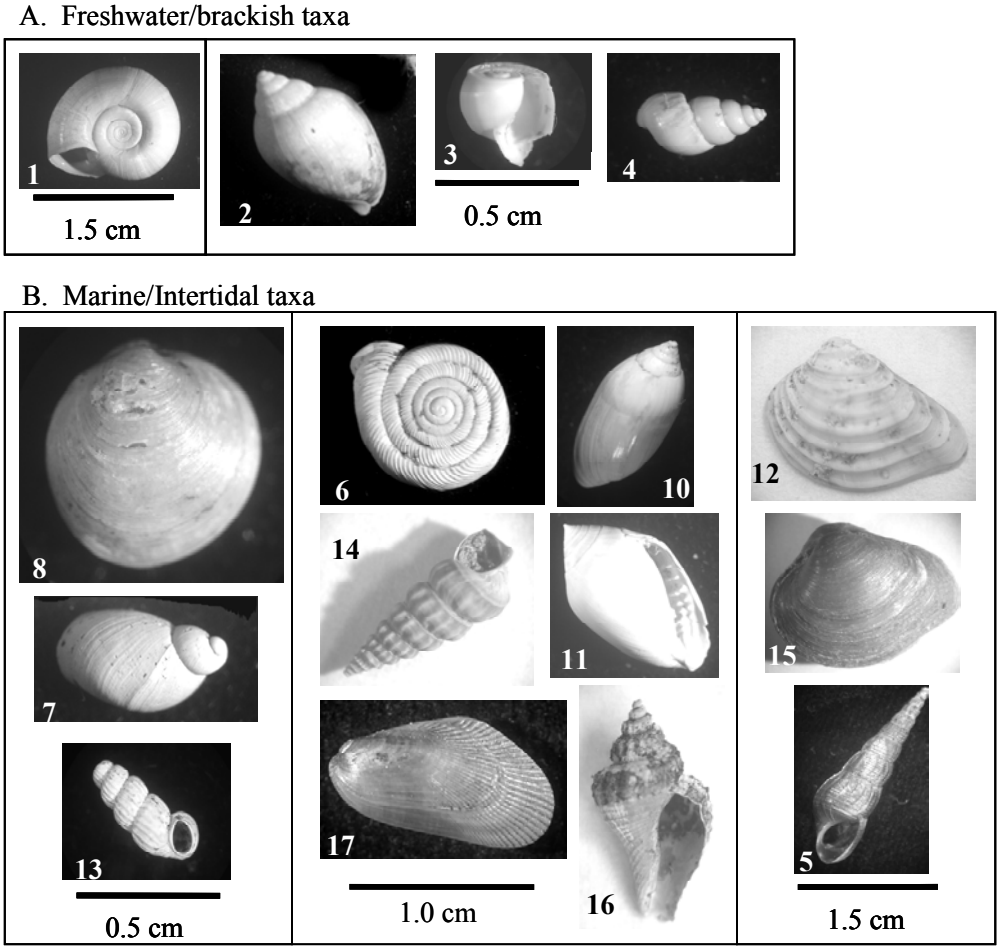
A. Freshwater/brackish taxa
1
1.5 cm
2
3
4
0.5 cm
B. Marine/Intertidal taxa
8
7
13
0.5 cm
6
10
14
11
17
16
1.0 cm
12
15
5
1.5 cm

Figure 7

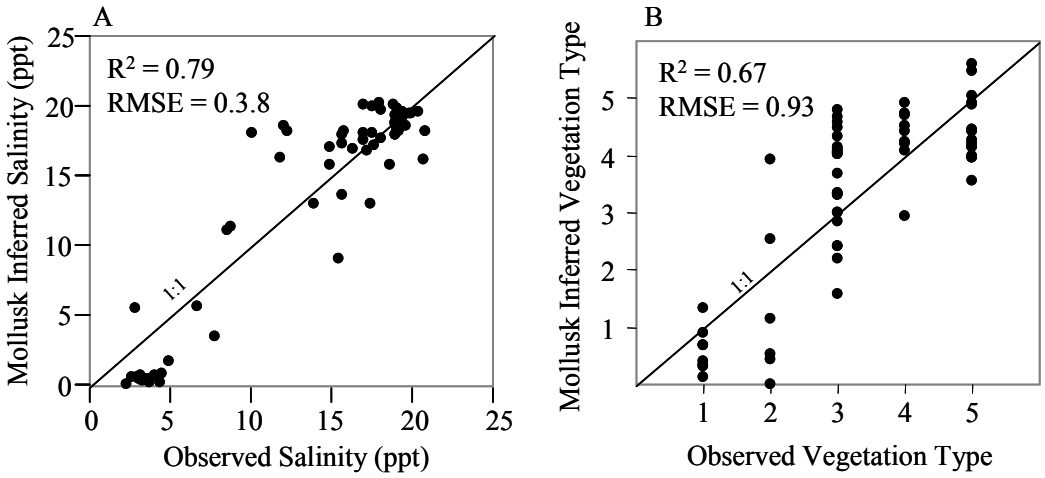
A
$R^2 = 0.79$
RMSE = 0.3.8
1:1
Mollusk Inferred Salinity (ppt)
Observed Salinity (ppt)
0
5
10
15
20
25
B
$R^2 = 0.67$
RMSE = 0.93
1:1
Mollusk Inferred Vegetation Type
Observed Vegetation Type
1
2
3
4
5

Figure 8

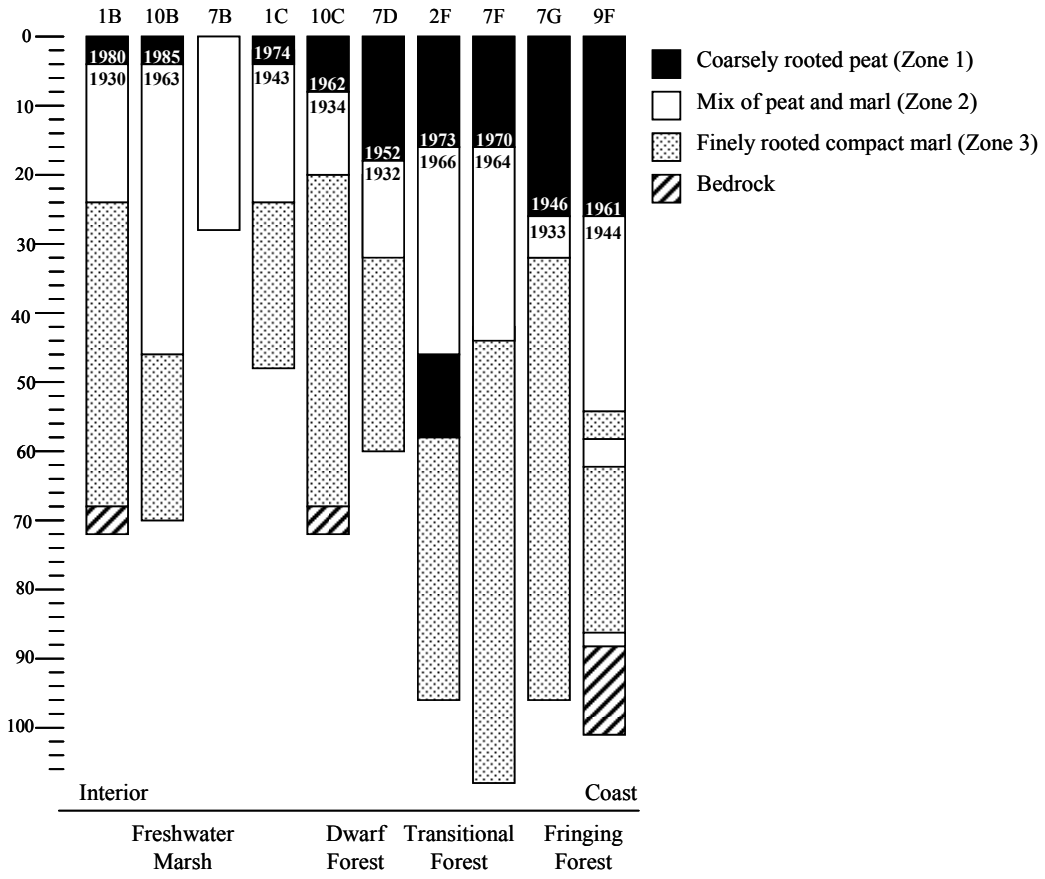
1B
10B
7B
1C
10C
7D
2F
7F
7G
9F
0
10
20
30
40
50
60
70
80
90
100
1980
1930
1985
1963
1974
1943
1962
1934
1952
1932
1973
1966
1970
1964
1946
1933
1961
1944
Interior
Coast
Freshwater Marsh
Dwarf Forest
Transitional Forest
Fringing Forest
Coarsely rooted peat (Zone 1)
Mix of peat and marl (Zone 2)
Finely rooted compact marl (Zone 3)
Bedrock

Figure 9

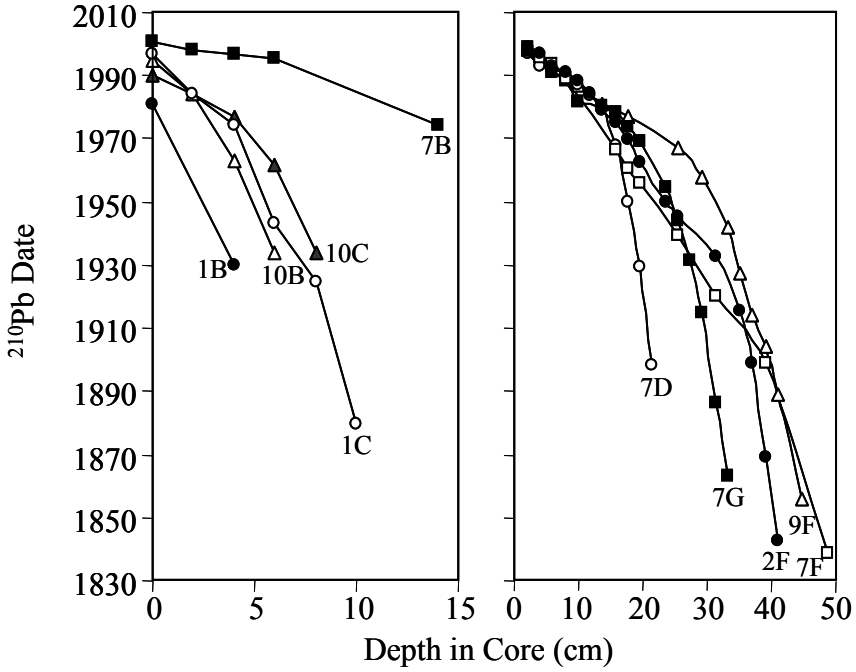
2010
1990
1970
1950
1930
1910
1890
1870
1850
1830
^{210}Pb Date
0
5
10
15
0
10
20
30
40
50
Depth in Core (cm)
7B
1B
10B
10C
1C
7D
7G
9F
2F
7F

Figure 10

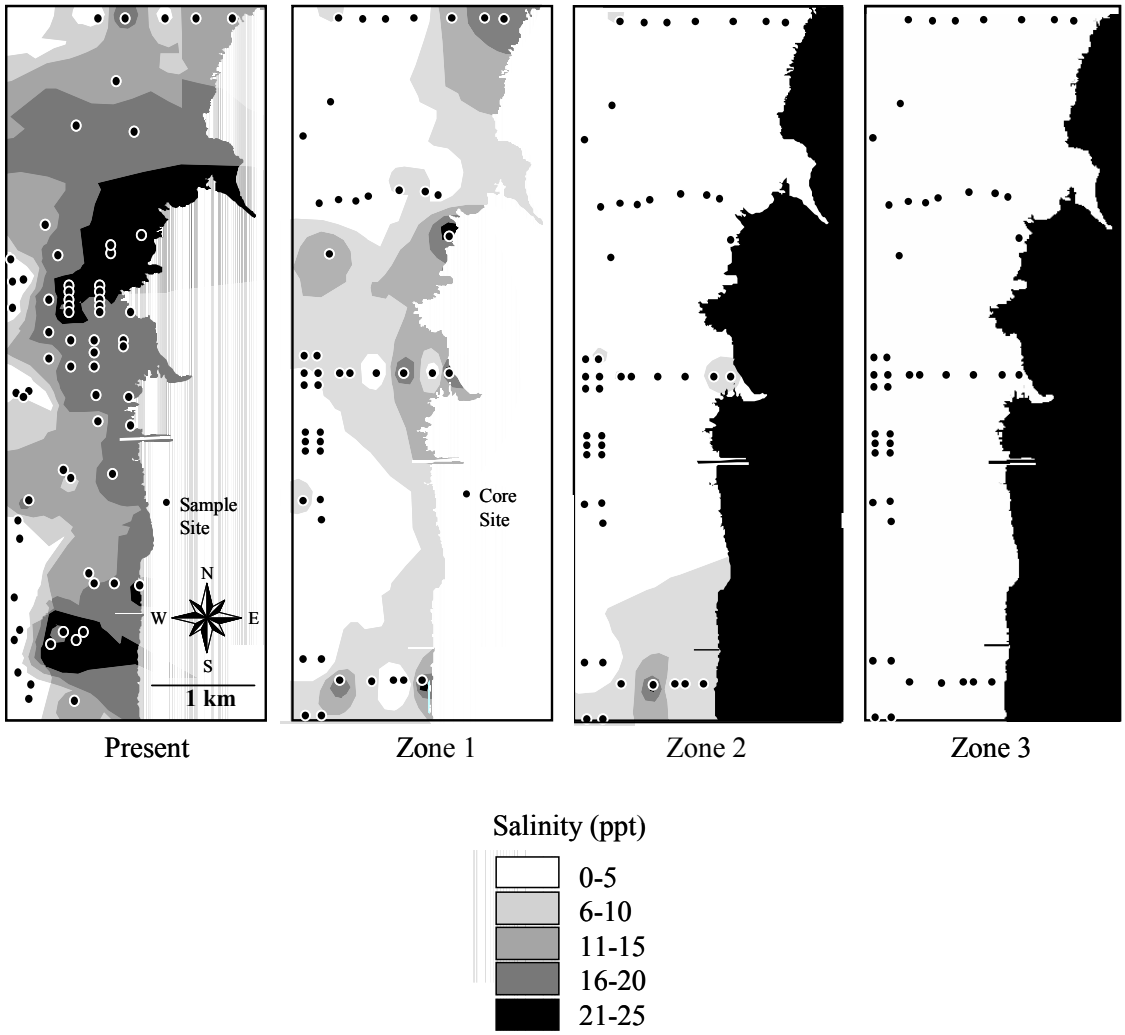
Sample Site
Core Site
N
W
E
S
1 km
Present
Zone 1
Zone 2
Zone 3
Salinity (ppt)
0-5
6-10
11-15
16-20
21-25

Figure 11

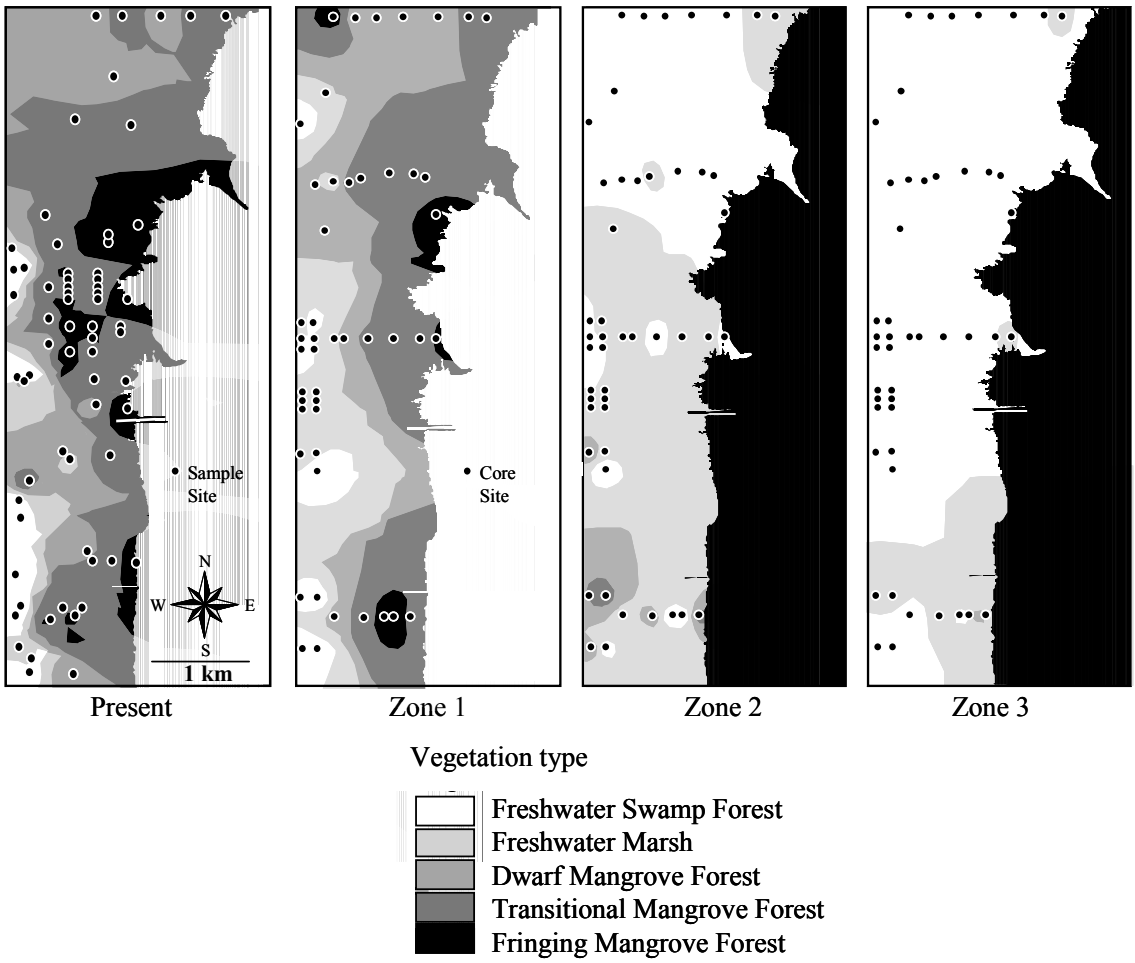
Sample Site
Core Site
N
W
E
S
1 km
Present
Zone 1
Zone 2
Zone 3
Vegetation type
Freshwater Swamp Forest
Freshwater Marsh
Dwarf Mangrove Forest
Transitional Mangrove Forest
Fringing Mangrove Forest

Figure 12

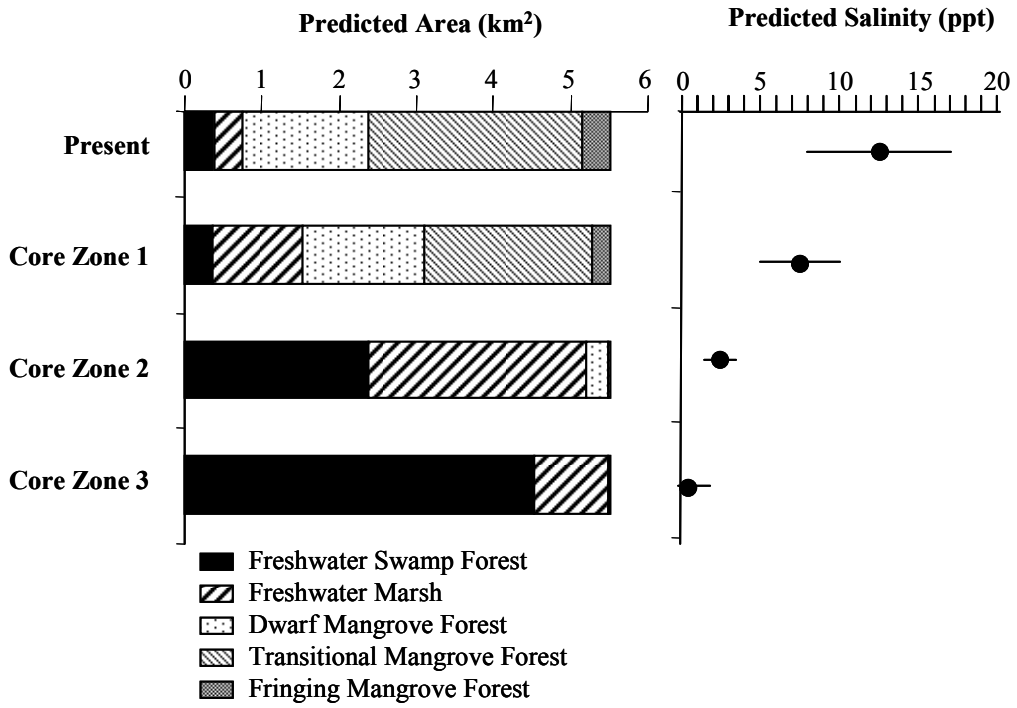
Predicted Area (km²)
Predicted Salinity (ppt)
0
1
2
3
4
5
6
0
5
10
15
20
Present
Core Zone 1
Core Zone 2
Core Zone 3
Freshwater Swamp Forest
Freshwater Marsh
Dwarf Mangrove Forest
Transitional Mangrove Forest
Fringing Mangrove Forest